AMMONIA OXIDATION PROCESS OF ENTRAPPED AND SUSPENDED CELL INHIBITED BY SILVER NANOPARTICLES

Mr. Nguyen Thanh Giao

A Dissertation Submitted in Partial Fulfillment of the Requirements
for the Degree of Doctor of Philosophy Program in Environmental Management
(Interdisciplinary Program)
Graduate School
Chulalongkorn University
Academic Year 2016

กระบวนการออกซิเดชันของแอมโมเนียโดยเซลล์ดักติดและเซลล์แขวนลอยที่ถูกยับยั้งด้วยซิลเวอร์อนุภาคขนาดนาโน

นายเหงวียน ทานห์ ยาว

วิทยานิพนธ์นี้เป็นส่วนหนึ่งของการศึกษาตามหลักสูตรปริญญาวิทยาศาสตรดุษฎีบัณฑิต
สาขาวิชาการจัดการสิ่งแวดล้อม (สหสาขาวิชา)
บัณฑิตวิทยาลัย จุฬาลงกรณ์มหาวิทยาลัย
ปีการศึกษา 2559

Thesis Title	AMMONIA OXIDATION PROCESS OF ENTRAPPED AND SUSPENDED CELL INHIBITED BY SILVER NANOPARTICLES
By	Mr. Nguyen Thanh Giao
Field of Study	Environmental Management
Thesis Advisor	Associate Professor Sumana Ratpukdi, Ph.D.
Thesis Co-Advisor	Associate Professor Tawan Limpiyakorn, Ph.D.

Accepted by the Graduate School, Chulalongkorn University in Partial Fulfillment of the Requirements for the Doctoral Degree

.....Dean of the Graduate School
(Associate Professor Sunait Chutintaranond, Ph.D.)

THESIS COMMITTEE

.....Chairman
(Assistant Professor Chantra Tongcumpou, Ph.D.)
.....Thesis Advisor
(Associate Professor Sumana Ratpukdi, Ph.D.)
.....Thesis Co-Advisor
(Associate Professor Tawan Limpiyakorn, Ph.D.)
.....Examiner
(Prinpida Sonthiphand, Ph.D.)
.....Examiner
(Assistant Professor Benjaporn Suwannasilp, Ph.D.)
.....Examiner
(Associate Professor Ekawan Luepromchai, Ph.D.)
.....External Examiner
(Suwat Soonglerdsongpha, Ph.D.)

เหงวียน ทานห์ ยาว : กระบวนการออกซิเดชันของแอมโมเนียโดยเซลล์ดักติดและเซลล์แขวนลอยที่ถูกยับยั้งด้วยซิลเวอร์อนุภาคขนาดนาโน (AMMONIA OXIDATION PROCESS OF ENTRAPPED AND SUSPENDED CELL INHIBITED BY SILVER NANOPARTICLES) อ.ที่ปรึกษาวิทยานิพนธ์หลัก: สุมนา ราษฎร์ภักดี, อ.ที่ปรึกษาวิทยานิพนธ์ร่วม: ตะวัน ลิมปิยากร, 188 หน้า.

ซิลเวอร์อนุภาคขนาดนาโน (AgNPs) มีการใช้งานในผลิตภัณฑ์ทางการค้าอย่างแพร่หลายเนื่องจากคุณสมบัติทางด้านการฆ่าเชื้อจุลินทรีย์ส่งผลให้มี AgNPs และ ซิลเวอร์ไอออน (Ag+) ปนเปื้อนเข้าสู่โรงบำบัดน้ำเสียและอาจมีผลร้ายต่อกระบวนการแอมโมเนียออกซิเดชัน (AO) และสิ่งแวดล้อม การศึกษานี้มีเป้าหมายเพื่อหาการยับยั้งของ AgNPs และ Ag+ ซึ่งแตกตัวจาก AgNPs ต่อกระบวนการ AO โดยจุลินทรีย์แอมโมเนียออกซิไดซิงแขวนลอยที่ขยายภายใต้สภาวะที่มีความเข้มข้นแอมโมเนียเริ่มต้น 0.5 and 30.0 mM (เรียกชื่อว่า NAS 0.5 mM and NAS 30 mM ตามลำดับ) และศึกษามาตรการลดผลกระทบดังกล่าวด้วยเทคนิคการดักติดเซลล์ ผลการทดลองชี้ให้เห็นว่า AgNPs และ Ag+ มีความเป็นพิษต่อ NAS 0.5 mM สูงกว่า NAS 30 mM เนื่องจากความแตกต่างของสัดส่วนประชากรจุลินทรีย์และแอมโมเนียออกซิไดเซอร์ AgNPs ที่ความเข้มข้น 1-100 mg/L ยับยั้งกิจกรรม AO 90.6 ± 8.6% ถึง 94.8 ± 4.3% และ 44.9 ± 2.4% ถึง 73.8 ± 1.5% ในขณะที่ Ag+ ที่ความเข้มข้น 0.05- 0.50 mg/L ยับยั้งกิจกรรม AO 86.3 ± 0.8% ถึง 93.4 ± 1.24% และ 52.7 ± 2.14% ถึง 93.9 ± 1.89% สำหรับ NAS 0.5 mM และ NAS 30 mM ตามลำดับ ผลการยับยั้งบ่งชี้ว่าความเป็นพิษของ AgNPs เกิดจาก Ag+ เป็นสำคัญ โดยกลไกความเป็นพิษหลักของ AgNPs และ Ag+ ได้แก่ การทำให้เซลล์จุลินทรีย์ตาย สำหรับการลดอิทธิพลของ AgNPs และ Ag+ จุลินทรีย์ถูกดักติดด้วยวัสดุแบเรียมแอลจิเนต (BA) พอลีไวนิลแอลกอฮอล์ (PVA) และส่วนผสมระหว่าง PVA-BA (PVA-BA) ผลการทดลองพบว่าเซลล์จุลินทรีย์ดักติดด้วย BA PVA และ PVA-BA คงกิจกรรม AO ได้ 81-100% 57-97% และ 75-100% สำหรับ AgNPs 1-100 mg/L ในขณะที่เซลล์จุลินทรีย์ดักติดคงกิจกรรม AO ได้ 98-100% 61-99% และ 79-100% สำหรับ Ag+ 0.05-0.50 mg/L ตามลำดับ นอกจากนี้ยังพบว่าการทำลายเยื่อหุ้มเซลล์ของจุลินทรีย์ดักติดจาก AgNPs และ Ag+ ลดลง ซึ่งสามารถบ่งชี้ได้ว่าเซลล์ดักติดมีโอกาสรับสัมผัสซิลเวอร์น้อยกว่าเพราะวัสดุดักติดจำกัดการเคลื่อนผ่านมวลของซิลเวอร์เข้าสู่เม็ดเจล วัสดุ BA และ PVA-BA มีความเหมาะสมสำหรับการลดผลความเป็นพิษของ AgNPs และ Ag+ เนื่องจากวัสดุดังกล่าวคงสภาพความมีชีวิตของจุลินทรีย์ได้สูงและความความคงทนในน้ำเสียสังเคราะห์

สาขาวิชา การจัดการสิ่งแวดล้อม ลายมือชื่อนิสิต .....

ปีการศึกษา 2559 ลายมือชื่อ อ.ที่ปรึกษาหลัก .....

ลายมือชื่อ อ.ที่ปรึกษาร่วม .....

5687848220 : MAJOR ENVIRONMENTAL MANAGEMENT
KEYWORDS: AGNPS, AMMONIA OXIDATION, INHIBITORY KINETICS, NANOSILVER, NITRIFYING SLUDGE, SILVER IONS

NGUYEN THANH GIAO: AMMONIA OXIDATION PROCESS OF ENTRAPPED AND SUSPENDED CELL INHIBITED BY SILVER NANOPARTICLES. ADVISOR: ASSOC. PROF. SUMANA RATPUKDI, Ph.D., CO-ADVISOR: ASSOC. PROF. TAWAN LIMPIYAKORN, Ph.D., 188 pp.

Silver nanoparticles (AgNPs) are widely used in commercial products because of their excellent antimicrobial activity. Entrance of AgNPs and its released Ag ions (Ag^+) into wastewater treatment plants could harm ammonia oxidation (AO) process resulting in environmental problems. This study aimed to study inhibitory effect of AgNPs and Ag^+ on AO process in suspended cells of ammonia oxidizing cultures enriched at initial ammonia concentrations of 0.5 and 30 mM (called NAS 0.5 mM and NAS 30 mM, respectively) and then mitigation measures using entrapment technique were tested. The results indicated that AgNPs and Ag^+ were higher toxic to NAS 0.5 mM than NAS 30 mM due to different proportion of active ammonia oxidizers and communities. Silver nanoparticles of 1-100 mg/L inhibited AO activity by 90.6 ± 8.6% to 94.8 ± 4.3% and 44.9 ± 2.4% to 73.8 ± 1.5%, whereas Ag^+ concentration of 0.05- 0.50 mg/L inhibited by 86.3 ± 0.8% to 93.4 ± 1.24% and 52.7 ± 2.14% to 93.9 ± 1.89% for NAS 0.5 mM and NAS 30 mM, respectively. The inhibition result suggested that the AgNP toxicity mainly derived from the liberated Ag^+. The primary mechanism for toxicity of AgNPs and Ag^+ caused microbial cell death. Cell entrapped in barium alginate (BA), polyvinyl alcohol (PVA), and the mixture of PVA-BA used to mitigate negative influence of AgNPs and Ag^+. The results showed that BA, PVA, and PVA-BA- entrapped cells remained AO 81-100%, 57-97%, and 75-100% at AgNPs 1-100 mg/L whereas the entrapped cells remained AO 98-100%, 61-99%, and 79-100% under Ag^+ 0.05-0.50 mg/L, respectively. Less damage of membrane integrity in the entrapped cells experiments with AgNPs and Ag^+ indicated that the entrapped cells were less exposed to silver since the entrapment matrices could limit mass transfer of silver into the gel beads. BA and PVA-BA were highly recommended for further study in the mitigating toxicity of AgNPs and Ag^+ since they remained high cell viability and more stable in synthetic wastewater.

Field of Study: Environmental Management Student's Signature .....
Academic Year: 2016 Advisor's Signature .....
Co-Advisor's Signature .....

ACKNOWLEDGEMENTS

I would like to thank everyone who have helped me in completing this thesis.

I would like to express my sincere appreciation to my advisor Assoc. Prof. Dr. Sumana Ratpukdi and co-advisor Assoc. Prof. Dr. Tawan Limpiyakorn for their patient advice, encouragement, and support.

My special thanks are also expressed to the chair of the committee Asst. Prof. Dr. Chantra Tongcumpou and the committee members including Assoc. Prof. Dr. Ekawan Luepromchai, Dr. Prinpida Sonthiphand, Assist. Prof. Dr. Benjaporn Suwannasilp and Dr. Suwat Soonglerdsongpha for their insightful comments and suggestions to improve this thesis.

I would like to greatly thank to laboratory managers and staffs at the program for their great supports. I greatly thank to Ms Chutima Ploychankul, Ms Papitchaya Srithep, Ms Preeyakorn Pornkulwat, and Ms Pattaraporn Kunapongkiti for their kind helps. I would like to thank to Dr. Pumis Thuptimdang for helping in obtaining and characterizing of silver nanoparticles. I am very appreciate Dr. Chaiwat Rongsayamanont for further helping with FISH methods and explanation of the results.

This thesis would not be possible without financial support from Scholarship Program for Neighboring/ASEAN Countries, International Program in Hazardous Substance and Environmental Management, Graduate School, Center of Excellence on Hazardous Substance Management and the 90th Anniversary of Chulalongkorn University Fund. Thank you very much for all the supports.

Last but not least, I would like to thank my family for their understanding and support.

CONTENTS

Page

Page

Page

Page

Page

LIST OF FIGURES

LIST OF TABLES

Chapter 1 Introduction

1.1 Rationale

Silver nanoparticles (AgNPs) have been increasing in production and use in many applications such as medical, biomedical, food industry, household appliances, textiles and environmental fields due to their great antimicrobial role [1, 2]. At low level (mg/L) silver could cause toxicity to biological organisms [3-5]. Exposure to AgNPs resulted in oxidative stress, inhibition of enzymes, gene expression and damage of bacterial cell integrity [6, 7]. With increasing production and use, AgNPs were expected to be washed out from consumer products and unavoidably occurred in WWTPs [8, 9] where AgNPs could release Ag^+ and increase toxicity of AgNPs [10].

Nitrification plays significant role in removal of ammonia in wastewater treatment plants (WWTPs). It comprises of two steps that take place in aerobic condition. The first step is the microbial conversion of ammonia to nitrite, while the second step is the oxidation of nitrite to nitrate. The first and rate-limiting step of nitrification is the ammonia oxidation process which is performed by ammonia oxidizing bacteria (AOB) and ammonia-oxidizing archaea (AOA) [11-13]. Ammonia oxidation is considered as a rate-limiting step because it is done by autotrophic microbes owning very slow growth rates and sensitive to environmental conditions including ammonia, pH, oxygen, light and toxic substances such as silver nanoparticles (AgNPs) and silver ions (Ag^+) [6, 14, 15]. Occurrence of AgNPs and Ag^+ release might adversely inhibit this process and consequently reduce discharged water quality resulting in environmental pollution. Several studies have placed focuses on toxicity of AgNPs on nitrifying sludge [3, 7], but there was no study to examine influence of

AgNPs and Ag^+ on AO from nitrifying sludges enriched with different levels of ammonium (NH_4^+–N). Low and high NH_4^+–N levels (NAS 0.5 mM and NAS 30 mM) could represent for different NH_4^+–N loads received by various WWTPs such as municipal and industrial. Also, possible predictions can be made to measure negative effects of AgNPs and Ag^+ on AO in these systems. To fulfil the gap, this study investigated inhibitory effect of AgNPs and Ag^+ on AO from low and high NH_4^+–N enriched nitrifying sludges.

Prior studies discovered that both AgNPs and Ag^+ clearly affected a wide range of organisms including nitrifying microbes [3, 16]. Among previous works, roles of AgNPs or the released Ag^+ to overall toxicity of AgNPs suspension were found differently due to varying experimental conditions including tested conditions, types of AgNPs, and nitrifying cultures. This inconclusive phenomenon was inadequate to finalize environmental treatment technology and management. More study in this area is needed to support the conclusion.

Cell entrapment technique appears to be a good method to mitigate impact of AgNPs and Ag^+ on ammonia oxidation process. Basically, cell entrapment technique or immobilized cells is the technique to immobilize certain microorganisms in a porous material to prevent microorganisms from directly contacting to toxic substances [15, 17]. In addition, high amount of cells can be loaded and the prepared entrapped cells can be recycled. Moreover, the materials such as polyvinyl alcohol (PVA), sodium alginate (SA) can be massively produced and they are not toxic to cells that entrapped in these polymeric materials. Currently, only one study reported using calcium alginate (CA) and PVA to reduce toxicity effect of AgNPs on nitrification [15]. The roles of

barium alginate (BA), polyvinyl alcohol (PVA), and the mixture of polyvinyl alcohol and barium alginate (PVA-BA) entrapped cells in mitigation of inhibition of AgNPs and Ag^+ on AO ammonia oxidation process is still a research gap.

1.2 Research objectives

The overall objective of this study is to investigate inhibitory kinetics of AO influenced by silver nanoparticles (AgNPs) and silver ions (Ag^+) and then mitigate the inhibitory effect by using cell entrapment technique. The specific objectives are as follows:

a) to compare inhibitory kinetics of ammonia oxidation process from nitrifying cultures enriched at different ammonium concentrations influenced by AgNPs and Ag^+,
b) to investigate role of Ag^+ in toxicity of AgNPs suspension influencing on ammonia oxidation process, and
c) to mitigate toxic impact of AgNPs and Ag^+ on ammonia oxidation process using entrapped cells.

1.3 Research hypotheses

a) Silver nanoparticles (AgNPs) caused inhibition of ammonia oxidation process via releasing silver ions (Ag^+) and both AgNPs and Ag^+ damaged membrane integrity resulting in inhibition of ammonia oxidation.
b) Ammonia oxidation process of entrapped cells using barium alginate (BA), polyvinyl alcohol (PVA) and the mixture of PVA and BA (PVA-BA) perform better than suspended cells on ammonia oxidation with silver nanoparticles (AgNPs) and silver ions (Ag^+) since these entrapment matrices reduce contact

between nitrifying cells and AgNPs and Ag^+. As a result, membrane integrity of entrapped cells was less damaged compared to suspended cells.

1.4 Scope of study

- Nitrifying sludges were enriched using activated sludges collected from 2 municipal WWTPs in Bangkok, Thailand.
- The experiments were conducted in batch modes, aerobic condition, and room temperature by using fresh inorganic synthetic wastewater
- Concentrations of AgNPs (average size of 2-12 nm, in spherical shape) of 1, 10 and 100 mg/L were used in this study, whereas concentrations of Ag^+ were from 0.05 – 0.5 mg/L. The AgNPs were obtained from PrimeNANO (Chulalongkorn University, Thailand).
- Initial NH_4^+-N concentrations were in the range between 0 and 400 mg/L
- Barium alginate, polyvinyl alcohol, and the mixture between them were used as entrapment materials for entrapping nitrifying cells from NAS 30 mM for inhibition tests, SEM, live and dead assays.

1.5 Thesis organization

The dissertation was presented from Chapter 1 to Chapter 7.

Chapter 1 was the introductory chapter which presents rationale, research objectives, research hypotheses, and scopes of this entire study.

Chapter 2 summarized the previous works which provided the background understanding relating to this current study including understanding of silver nanoparticles, ammonia oxidation process, entrapment techniques, calculation of kinetics and the principal use of some laboratory equipment.

Chapter 3 was materials and methods in which brief explanation of the experiments was described.

Chapter 4 compared inhibitory kinetics of AO in suspended cells using NAS 0.5 mM and NAS 30 mM influenced by AgNPs and Ag^+.

Chapter 5 presented inhibitory kinetics and mechanism of AO from NAS at initial ammonia concentration of 30 mM influenced by AgNPs and Ag^+. The findings demonstrated that AgNPs and Ag^+ adversely influenced on AO. Inhibitory data from AgNPs and Ag^+ experiments and the amounts of Ag^+ released from AgNPs experiment was investigated. Scanning electron microscopy, transmission electron microscopy, and fluorescent microscopy (with live/dead assay) techniques were used to determined toxicity mechanism of silver species (AgNPs and Ag^+).

Chapter 6 presented the results and discussion of inhibitory kinetics of AO in entrapped cells using NAS 30 mM influenced by AgNPs and Ag^+. The AO entrapped in BA, PVA, and PVA-BA entrapment matrices was tested. Scanning electron microscopy, transmission electron microscopy, and fluorescent microscopy (with live/dead assay) techniques were used to determined toxicity mechanism of silver species.

Chapter 7 summarized the key findings and recommended for the future study. Possible application of the outcomes in this study was also suggested in this chapter.

Chapter 2 Literature review

2.1 Silver nanoparticles

2.1.1 Synthesis and characterization of silver nanoparticles

Nanoparticle has the size between 1 nm and 100 nm and silver nanoparticles (AgNPs) whose particles made from silver. Silver nanoparticles exhibit much better physical, chemical and biological characteristics than metal silver because AgNPs have extremely small sizes and high surface to volume ratio and these characteristics make AgNPs become a highly effective antimicrobial agent [1]. Currently, there are several ways of AgNPs synthesis. Silver nanoparticles can be produced by physical approach such as evaporation-condensation. In this physical method, AgNPs was produced by evaporating silver ions (Ag^+) solution into a carrier gas followed by a cooling process for the formation of AgNPs. By using this method, there was no or less chemical residues in the produced AgNPs, however, this method is time and energy consuming [1]. Silver nanoparticles can also be chemically synthesized by making reactions take place between silver nitrate and reducing agents such as citrate, ascorbate, and sodium borohydride. Among the chemical methods, AgNPs were frequently synthesized by reducing silver nitrate in combination with utilizing capping agents to control particle size and enhance stabilization of AgNP suspension. Sodium borohydride and citrate were the two most commonly used reductant and stabilizing agent in production of spherical AgNPs with the size less than 20 nm [18].

Silver nanoparticles after synthesis is often characterized for size, shape, zeta potential and liberation of Ag^+ because these characteristics potentially influence on

toxicity of AgNPs. Size of AgNPs is scanned by using spectrophotometry in the range of wavelength of 250 to 700 nm. The peaks obtained from the spectra of absorption between 400 nm and 425 nm indicate the synthesized AgNPs are in nano sizes (1-100 nm). The peak appears because of surface plasmon resonance. The surface plasmon resonance is the collective oscillation of conductive electrons around the silver nanoparticles when exposing to radiation (light). The surface plasmon resonance absorbs specific wavelengths of light which is known as the surface plasmon band. Different sizes of AgNPs peak at different wavelengths, for example, AgNPs with a size of 15 nm was peaked at the wavelength of 440 nm [19], whereas a size of 25 nm peaked at 420 nm [20]. Furthermore, more accurate sizes, distribution of sizes and shapes of the synthesized AgNPs can also be confirmed by using transmission electron microscopy or TEM [21]. Zeta potential is measured by using Zetasizer NanoZS [19]. Zeta potential provides information regarding surface charge of synthesized AgNPs. The surface charge would be zero when no oxide layer is found on the surface of AgNPs. The surface charge should be negative value (negative zeta potential) when there is presence of oxidized layer on the AgNPs. The zeta potential also provides information regarding chance of AgNPs would form aggregates or being well-dispersed in suspension. Higher value of zeta potential, AgNPs would be likely to remain in suspension, whereas lower value of zeta potential, AgNPs would be likely to aggregate to each other [22].

The silver ions associated with AgNPs are also measured because ionic silver is one of the most toxic cationic metals to bacteria [23]. In order to measure dissolved silver from AgNPs, the suspension of AgNPs is centrifuged using ultracentrifuge machine at very high speed at 165,000 x g for 1-2h at 4^{o}C. The AgNPs pellet is removed

and the supernatant is collected. Then, the supernatant is dissolved in 5% HNO_3 before using atomic absorption spectroscopy (AAS) for determination of liberated silver [21]. In other study, Ag^+ could be also determined using inductively coupled plasma-mass spectrometry (ICP-MS) after suspension of AgNPs were filtered through Amicon centrifugal ultrafilter devices using porous cellulose membranes limiting AgNPs sizes from 1-2 nm [24].

2.1.2 Production and use of AgNPs

The production of products containing AgNPs have been yearly increasing. For the time period from 2006 to 2013, the products that contain AgNPs have been increased 15 times (from 25 products increased to 383 products) and AgNPs accounted for 23.5% of the total products containing nanomaterials [25]. Healthcare was the largest sector that contributed to 30% of worldwide market revenue in 2014. It is expected that AgNPs market around the world will reach 2.45 billion by 2022 [25]. In the US, an estimator reported that AgNPs were produced from 2.8-20 tons per year [26]. Other study estimated that there were approximate 0.6-55 tons of AgNPs annually produced in European countries [27]. In the same study, it was also calculated that approximate 5.5-550 tons of AgNPs were globally produced. The literature revealed that the production of AgNPs rapidly increase over years due to demand of use.

Silver nanoparticles are broad-spectrum antibacterial and are very powerful against Gram negative and Gram positive as well as drug-resistant bacteria [28]. It could be also an effective antifungal, antiviral and anti-inflammatory activity [29, 30]. Silver nanoparticles show low toxicity to humans and other animals at low concentration [4]. Therefore, AgNPs have been used in many applications such as

medical, biomedical, food industry, household appliances, textiles and environmental fields [1, 2]. In medical applications, AgNPs are embedded into wound dressings, bandages, topical ointments and creams, and coated on medical devices to prevent attachment of harmful organisms [31]. Nano silvers are used in biomedical fields such cancer therapy, diagnosis, drug delivery, biosensors, biological labels and cell imaging [32]. Food processing sectors also utilize AgNPs for food packaging, and food contact materials [33]. Household appliances such as washing machines, computers, wall painters, tables and kitchen wares are also related to the use of AgNPs. Textiles including clothes, towels, socks, jackets, shoes, beddings and so on also use a large amount of AgNPs to kill bacteria and to protect users [34, 35]. Silver nanoparticles are applied in environmental fields such as water purification, wastewater treatment, and water disinfection [36, 37]. In addition, AgNPs have been also used widely in catalysis. It is used as fuel cell catalyst, fuel additive catalyst and hydrogen production photocatalyst to enhance the reactions of producing final desired products [38]. With increasing use, discharge of wastewater containing AgNPs into environments are unavoidably.

2.1.3 Occurrence, fate and transport of AgNPs in environment

Silver nanoparticles have been proved to release during consumption due to intensive uses. For example, washing process using washing machine released approximate 0.05 mg/L silver, and roughly 45 μg Ag g per gram of consumer's product was liberated [39]. It was also reported that 1 gram of sock could release 0.3-377 μg Ag into the environment. There were 322 mg silver per kg fabrics were released silver coated fabrics into synthetic sweat [40]. Former studies presented that silver was detected

ranging from 4 µg/L to 1 mg/L and 2 to 195 mg/L in influent concentration and biosolid concentration of WWTP, respectively [41-43]. Previous studies also estimated that approximately 300 tons of silver annually leached and ended up in worldwide environment [44]. The other study estimated that silver from textile and plastic production would end up in wastewater treatment systems (WWTS) with an amount of 190-410 tons per year. From WWTSs, silver would be transported to other environmental compartments with different proportions, for instance treated wastewater containing 20-130 tons of silver per year would move to natural receiving waters, while 80-190 tons of silver annually end up in soil from wastewater treatment sludge. Approximate 8-17 tons of silver per year would be emitted into the atmosphere due to solid waste incineration [5]. It is clearly indicated that AgNPs after discharge to the environment, it could be further transported to media such as water, soil and air. Silver nanoparticles after release will first move into WWTS. In reality, silver has been globally detected in WWTPs [45-47]. In WWTPs, AgNPs would interact with microbes and cause concerns for microbial activity in WWTPs since AgNPs are well known as an excellent biocide [48] leading to reducing efficiency of WWTP performance [8]. In environment, AgNPs fate and transport would be governed by presence of sulfide (S^{2-}), pH, dissolved oxygen (DO) and organic matter [8]. Silver nanoparticles would be likely to dissolve in the conditions of high DO and low pH (pH < 6), whereas AgNPs tended to precipitate in form of silver sulfide (Ag_2S) in absence of dissolved oxygen [5]. In WWTPs where DO, S^{2-} and organic matters are abundant, forms of silver could be Ag^+, Ag_2S and aggregated AgNPs. These forms of silver could contribute to reducing or enhancing toxicity of AgNPs in WWTPs depending on environmental conditions. In short, AgNPs occurred in WWTPs where they may have

a variety of fates in wastewaters, including being converted into ionic form, forming a complex with other ions, molecules, or molecular groups, agglomerating or remaining in nanoparticle form [49, 50] which could influence on toxicity of AgNPs.

2.1.4 Factors effect on toxicity of AgNPs

Prior studies pointed out that several factors have influence on toxicity of AgNPs including size and shape of the nanoparticles (NPs) [10, 51, 52]. Size relates to surface areas, smaller size has more surface areas and better contact and interact with bacterial cells compared to bigger size [51, 53, 54]. Silver nanoparticles with the size smaller than 10 nm interact with bacteria and produce electronic effects which enhance the reactivity of AgNPs. For instance, the former study reported that AgNPs of 7 nm showed the best antibacterial effect against *Escherichia coli* and *Staphylococcus aureus* compared to AgNPs of 29 and 89 nm [53]. Silver nanoparticles with smaller size could release more Ag^+ thus exhibiting more toxicity than AgNPs with larger size [55]. It is clearly indicated that bactericidal effect of AgNPs is size-dependent.

Shape also shows influence on toxicity of AgNPs [52]. Prior findings indicated that truncated triangular shape showed inhibition on bacteria at silver content of 1 µg, whereas the silver contents were much higher to show the inhibitory effect on bacteria for spherical shape (12.5 µg) and rod shaped particles (50 to 100 µg).

Forms of silver speciation also influence on the toxicity. In WWTPs, silver may be present in forms of nanoparticles or ions [5]. Silver ions could produce additional toxicity effect on microorganisms because AgNPs have been considered as continuing source of Ag^+ [10]. Five milligram per liter of AgNPs (average size of 7 ± 3 nm) released 7.8 ± 0.7 µg/L dissolved silver in the effluent [56]. In other study, AgNP

(averaged size of 50 nm) concentration of 10 mg/L liberated 1.2, 0.7, and 0.7 mg Ag^+ per liter for flocculent sludge, granular and the biomass free control, respectively [7]. It was clearly showed that size of AgNPs effects on its dissolution, AgNPs with smaller size released more Ag^+ than larger size [55].

Types of AgNPs also influence on dissociation of Ag^+ from AgNPs. Lee et al. (2012) reported that sol-type and powder-type AgNPs (0.05-1.00 mg/L) released Ag^+ in oxidation condition by 36% and 49% respectively [24]. In addition, types of coated AgNPs also influence on dissolution of Ag ions. The dissolved silver concentrations increased after 4 h exposing to biomass. At 2 mg/L of initial AgNPs, the dissolved silver concentrations were 21.6 ± 8.3, 16.1 ± 9.5, and 63.5 ± 2.2 µg/L, respectively, whereas the ionic silver concentrations were found at 160.9 ± 10.3, 37.9 ± 1.3, and 150.0 ± 3.2 µg/L in the treatments amended with 20 mg/L AgNPs of the PVP, GA, and citrate coated AgNPs, respectively [6].

Dissolved oxygen is another factor that has strong effect on toxicity of AgNPs because under presence of oxygen, AgNPs release Ag^+ and reactive oxidative species (ROS) which could enhance toxicity of AgNPs [8]. However, under absence of oxygen, AgNPs could be agglomerated with sulfide to form silver sulfide particles (Ag_2S) [57]. In reality, it is very hard to differentiate toxicity between AgNPs and liberated Ag^+ because the quantification result is often addressed in terms of total silver which is both come from the nano form and from the ionic form [58]. Thus, separation of toxicity of Ag^+ from AgNPs is an interesting research area.

pH is an important factor that could effect on AgNPs speciation. There are more AgNP dissolution at acidic pH than at neutral pH [59]. Prior research found that there

was only 2% of commercial AgNPs transformed to Ag^+ at pH 6-9. However, increasing pH could raise level of Ag^+ dissociation from AgNPs [60].

Coatings (capping agents) influence on toxicity of silver nanoparticles. Coatings can be done using inorganics (metal oxide), organics (starch, citrate), and polymers (polyvinyl alcohol). In this study, starch coated AgNPs was used. Uncoated AgNPs are easy to agglomerate, thus coating can help to reduce matter of agglomeration and to form stable suspension. It was previously reported that AgNPs in well-dispersed form was more toxic than in aggregated form [57]. Coating also effects on toxicity of AgNPs through influencing on dissolution of AgNPs. There were less Ag^+ liberated from coated AgNPs than the uncoated ones [6]. Experiments have been conducted to prove this point. Toxicity of three types of coatings materials on AgNPs including citrate, gum arabic, and polyvinylpyrrolidone against *Nitrosomonas europaea* has been tested. The experimental results indicated that different coating AgNPs influenced differently on ammonia oxidation of *N. europaea*. At 2 mg/L, citrate, gum arabic, and polyvinylpyrrolidone AgNPs inhibited ammonia oxidation (AO) by 91.4 ± 0.2, 67.9 ± 3.6, and 29.5 ± 9.4%, respectively [6]. Coating also has changed zeta potential values of AgNPs which also related to toxicity of AgNPs. Zeta potentials of -23.0 ± 1.1, -21.0 ± 1.3, and 11.6 ± 1.8 mV were recorded for citrate, gum arabic, and polyvinylpyrrolidone AgNPs, respectively [6]. Higher zeta potential resulted in less inhibitory effect of AgNPs on AO of *N. europaea*.

Silver nanoparticles may have a variety of fates in wastewaters, including being converted into ionic form, forming a complex with other ions, molecules, or molecular groups, agglomerating or remaining in nanoparticles form [49].

Sludge characteristics also show effect on toxicity of AgNPs. For example, flocculent sludge was able to remove AgNPs from 30-58%, whereas granular sludge could only remove 2.5-9.4% [7]. Flocculent sludge could be more effectively in removal of AgNPs, but short-term exposure to AgNPs showed that AO rate was reduced by 21-25%, while no inhibitory effect was observed for the granular sludge at AgNPs of 1, 10, 50, and 100 mg/L [7]. Toxicity of AgNPs and Ag^+ in WWTSs was reduced due to adsorption or precipitation [61].

2.1.5 Toxicity of AgNPs on microorganisms

Toxicity of AgNPs has been intensively studied in recent years. Silver nanoparticles exhibited negative impact on nitrifying cultures in short-term experimenting. Toxicity of different silver species including AgNPs, Ag^+, and colloid $AgCl_2$ on ammonia oxidizing cultures was investigated [62]. The findings reported that the silver species inhibited differently on activity of microorganisms including heterotrophic and autotrophic activities. Autotrophic activity of nitrifying bacteria was seriously inhibited by AgNPs, whereas Ag^+ and colloid $AgCl_2$ showed less inhibitive effects compared to AgNPs. Heterotrophic activity was more sensitive to toxicity of Ag^+ than AgNPs and colloid $AgCl_2$. The less inhibitory effect of AgNPs on heterotrophic activity was also reported in the other study [63].

The above studies clearly showed that ammonia oxidizing culture was more sensitive to AgNPs. However, AgNPs inhibited differently on nitrification potential rates and abundance of AOB members such as *Nitrosomonas europaea*, *Nitrosospira multiformis* and *Nitrosococcus oceani* due to due to dissimilarities in physiochemical characteristics of each species [64]. This study pointed out that AgNPs could influence

distinctively on ammonia oxidizing cultures enriched at different NH_4^+-N and SRT since these factors have significant effect on community, abundance, and activity of nitrifying cultures. However, no study was conducted to investigate impact of AgNPs on different ammonia oxidizing cultures.

Study on long-term effect (60 days) of AgNPs (0.1 mg/L) on membrane bioreactor (MBR) activated sludge indicated that the quality of influent and effluent water as well as nitrifying bacterial community structure were not significantly different before and after exposed to AgNPs. However, silver resistance gene *silE* and extracellular polymeric substances (EPS) increased in response to AgNPs addition [61].

Long-term effect of AgNPs (5 mg/L and 50 mg/L) on aerobic granular sludge was studied [65]. The results indicated that AgNP did not show any significant impact on microbial activities of the sludge from day 0 to day 35. However, AgNPs partially inhibited the ammonia oxidizing rate (33.0%), respiration rate (17.7% and 45.6%) and denitrification rate (6.8%) at day 69. It was showed that ammonia oxidation activity was more sensitive to AgNPs than denitrification. The more sensitive of nitrifying activity than denitrifying activity on exposure to AgNPs was also previously reported [66]. In addition, microbial functional enzymes such as the *ammonia mono-oxygenase* and *nitrate reductase* activities were decreased under presence of AgNPs. However, community of microorganisms in the aerobic granular just slightly changed [65].

Silver nanoparticles were more toxic on ammonia removal than other nanoparticles such as copper nanoparticles (CuNPs), zinc oxide nanoparticles (ZnO NPs), titanium oxide nanparticles (TiO_2 NPs), alumina particles (Al_2O_3 NPs), and gold nanoparticles (AuNPs). Addition of CuNPs (0.1-10 mg/L, 220 ± 25 nm) into

wastewater biological nutrient removal did not show any impact on ammonia oxidation [67]. Exposure of ZnO and TiO_2 nanoparticles (<100 nm) of 1-100 mg/L inhibited only 3.6-12.5% of sludge's oxygen uptake rate and did not cause change in microbial community in short term test (24 h). The study found that ZnO and TiO_2 at 10 mg/L resulted in insignificant community change in activated sludge in long-term (13 days) operation [68]. Alumina nanoparticles (Al_2O_3 NPs, 20 ± 5 nm) from 1 to 50 mg/L produced marginal effect on nitrification, denitrification and phosphorus removal in biological wastewater treatment plant. This was supported by the fact that Al_2O_3 NPs were mostly absorbed onto activated sludge where these NPs did not show serious impact on viability and integrity of surface of activated sludge [67]. It was reported that ammonia oxidation rates of AOB cultures were not influenced due to addition of AuNPs [69]. The insignificant effect of AuNPs was indicated by indifference in the ammonia oxidation rates between the control and the AuNPs treatments. In contrast, AgNPs did partially influence on ammonia oxidation rate of AOB culture and the level of impact of AgNPs was increased when AgNPs concentration increased.

Long-term studies also indicated that ammonia oxidation activity was higher sensitivity than other microbial activity to AgNPs and AgNPs were more toxic than other nanoparticles. This is one of the reason AgNPs was selected in this study.

Silver nanoparticles not only show toxic impact on microorganism but also exhibit negative influence on animals and even human organs. Prior studies indicated that AgNPs influenced on *Oryzias latipes* by damaging chromosomes [70] and rat by causing negative effect on liver and kidney [71]. Silver nanoparticles showed several inhibitory effects for human cells such as HepAD38 [72], Cytochrome P450 [19], and

skin cells [73] by inhibiting DNA or RNA formation, interrupting oxidation-based biological process and damaging skin through penetration process.

2.1.6 Mechanisms of AgNPs toxicity on microorganisms

Several mechanisms have been proposed for toxicity effect of AgNPs on microorganisms in the previous studies. Silver nanoparticles, with its large surface area, will easily contact with microbes. After that AgNPs attach to the membrane of the cells and penetrate into the cells. Silver nanoparticles or silver ions interrupt the respiratory chain of bacteria resulting in death of cells [74].

The other study proposed that AgNPs toxicity closely related to the release of Ag^+ [75]. Therefore, the toxicity of AgNPs comprise of toxicity impact of AgNPs itself and its dissociated Ag^+. There were three possible toxicity mechanisms with AgNPs and released Ag^+ [75]. Firstly, AgNPs could directly contact with cell membrane and destroy the membrane of the cells. Secondly, Ag^+ was taken up by bacteria then Ag^+ inside the bacteria would disrupt production of ATP and replication of DNA. Thirdly, AgNPs and Ag^+ could generate reactive oxygen species and these generated species would cause cell death.

A novel mechanism was proposed for the effect of AgNPs on a model bacteria *Escherichia coli*. AgNPs induced apoptosis-like response including early and late apoptosis for *E. coli.* Early apoptosis involved accumulating ROS, increasing levels of intracellular calcium, and exposing phosphatidylserine in the outer membrane, whereas late apoptosis made up by disrupting membrane potential, activating caspase-like protein, and degrading DNA [76].

Relating to toxicity effect of AgNPs on nitrifying bacteria, prior studies found that AgNPs could bind to cell membrane, destroy function of membrane, and generation of ROS species [10, 77, 78]. Pure culture study indicated that AgNPs damage cell wall of *N. europaea* and make the nucleoids disintegrated and condensed next to cell membrane [10]. Silver nanoparticles were found to negatively influence on the expression of adenosine triphosphate (ATP) synthase, ammonia monooxygenase (AMO) and hydroxylamine oxidoreductase (HAO) which are functional genes of the ammonia oxidizer *N. europaea* [10]. It was also found that AgNPs released Ag^+ and then both of them caused oxidative stress via enhancing production of ROS species [7]. Silver ions was released because of oxidation of metal silver by peroxide intermediates (H_2O_2) [79]. Prior study indicated that Ag^+ produced more ROS species than AgNPs, thus resulting in more toxicity of AgNPs [7]. Silver ion is susceptible to uptake by ion transporters because it shares properties with Na^+ and Cu^+ [4]. Silver ions at low concentration resulted in a post-transcriptional interruption on membrane-bound nitrifying enzyme function [7]. Further increased in Ag^+ caused heavy metal stress response led to membrane disruption [6]. Ag ions caused cell death due to leakage of significant amounts of proton through the membrane of *Vibrio cholera* [80]. Moreover, Ag^+ are able to combine strongly with thiol groups then inactivating electron-transport chain causing cellular oxidation and DNA replication [51, 81].

Mixed culture study of nitrifying culture also showed that AgNPs formed pits and damaged bacterial cell walls and caused cell death [15]. Bacterial cell damage was indicated by the release of extracellular lactate dehydrogenase [7].

2.2 Ammonia oxidation process

In most WWTPs, nitrification is applied to remove aerobically ammonia which is one of the main waste products released from daily activities from humans and animals. Autotrophic nitrification is a two-step process with the first step is the aerobic conversion of ammonia to nitrite and then nitrite is oxidized to nitrate due to microbial activity. Both steps occurred in aerobic conditions and the involved microorganisms use inorganic nitrogen and carbon dioxide as their energy and carbon source. The first step, aerobic ammonia oxidation (AO), is the sensitive step because ammonia is oxidized by autotrophic microorganisms. For very long time, researchers of AO have surely confirmed that ammonia oxidizing bacteria (AOB) are the sole microorganisms who oxidize ammonia to nitrite. Until recently, several studies have indicated that with the diverse and abundant occurrence of AOA in WWTPs through detection of archaeal *amoA* genes [11, 82-84] leading to a suggestion that AOA potentially involved in AO.

Anaerobic ammonia oxidation (anammox) process is the process in which ammonium is converted to dinitrogen gas (N_2) in anoxic condition using nitrite as electron acceptor [85]. This process could be found in wastewater [86]. However, it is important to keep DO lower than 0.2 mg/L to ensure anaerobic ammonia oxidation process to take place because anammox bacteria are very sensitive to DO [87].

2.2.1 Microorganisms involved in ammonia oxidation

Now, two distinct groups of ammonia oxidizing bacteria (AOB) and ammonia oxidizing archaea (AOA) belonging to the phylum Proteobacteria and Crenarchaeota/Thaumarchaeota, respectively, have been recognizing and potentially involving in AO [11, 13, 88, 89].

2.2.1.1 Ammonia oxidizing bacteria

Ammonia oxidizing bacteria have been intensively studied. Deep knowledge in this group of microorganisms has been achieved. Phylogenetic relationships within AOB have been established based on 16S rRNA and *amoA* genes sequences. All AOB are classified as the members of the β- and γ-subclass of Proteobacteria based on comparative 16S rRNA sequence analysis. The β- subclass of Proteobacteria comprise of the genera *Nitrosomonas-Nitrosococcus mobilis*, *Nitrosospira*, *Nitrosolobus* and *Nitrosovibrio*, whereas the genus *Nitrosococcus* fall within the γ-subclass of Proteobacteria [90]. Many ideas suggested that *Nitrosospira*, *Nitrosolobus* and *Nitrosovibrio* should be reclassified into the single genus *Nitrosospira*, while the nitrosomonads can be further subdivided into the *Nitrosomonas europaea/Nitrocuccus mobilis* cluster, the *Nitrosomonas marina* cluster, the *Nitrosomonas oligotropha* cluster and the *Nitrosomonas communis* cluster [91]. Comparative analysis of *amoA* sequences suggested that *N. europaea/Nc.mobilis* cluster, the *N. marina* cluster, the *Nitrosospira*-cluster are retained, while the members of the *N. oligotropha* cluster and the *N. communis* cluster form no monophyletic assemblages [91].

Ammonia oxidizing bacteria in industrial WWTP

Ammonia oxidizing bacteria are found in industrial WWTPs and they fall in 4 clusters which are *N. europaea*/*Nc. mobilis* cluster, *N. communis* cluster, *N. oligotropha* cluster and unknown *Nitrosomonas* cluster [11]. Different clusters inhabit in various ammonia concentrations indicated through affinity constant for ammonia. Affinity constant for ammonia of 50 -100 μM can be considered high and representatives for this environment are members of *N. europaea*/*Nc. mobilis*. This explains why *N.*

europaea/*Nc. mobilis* are commonly found in WWTPs receiving high NH_4^+-N loads. *N. communis* cluster have been classified as AOB with moderate affinity constants for ammonia (14 - 43 µM). The member of *N. oligotropha* cluster, and *N. oligotropha* cluster are low in affinity constants for ammonia (1.9 – 4.2 µM) was found in WWTP with low NH_4^+-N load (10 mg N/ L) [11, 92]. In industrial wastewater systems, AOB are often the main players in nitrification process [12].

Ammonia oxidizing bacteria in municipal WWTPs

Municipal WWTPs often receive low NH_4^+-N strength wastewater (5 – 13 mg N/L), only members of *N. communis* cluster and *N. oligotropha* cluster were frequently found in all 7 municipal WWTPs in Bangkok, Thailand [11]. Similarly, previous study proved that *N. communis* cluster and *N. oligotropha* clusters frequently occurred in various environments, but *N. europaea* cluster just appeared in some systems [93]. In eight municipal WWTPs in China, majority of AOB belonged to *Nitrosomonas* genus, with the species of *N. ureae*, *N. oligotropha*, *N. marina*, and *N. aestuarii* were predominant [94]. It has been generalized that *N. oligotropha* cluster were common AOB in municipal WWTPs.

2.2.1.2 Ammonia oxidizing archaea

Recently, scientists pay their attention to the third domain of life which is the domain Archaea. They find that archaea are relatively highly abundant in various environments. Having widely distributed, it potentially plays role in biogeochemical cycles for example nitrogen and carbon cycles on earth.

Ammonia oxidizing archaea are continuously discovered from WWTPs. In Bangkok, Thailand, sludge samples from three industrial and four municipal WWTPs

were collected for investigation of ammonia oxidizing communities. The study showed that AOA and AOB *amoA* genes were approximately equal in some municipal WWTPs and AOA *amoA* gene copies in municipal WWTPs outnumbered those industrial WWTPs [11]. The author and coworkers reasoned for more abundance of AOA *amoA* genes in municipal WWTPs that was because NH_4^+-N concentration is generally low compared to that in industrial plants leading to a conclusion that the occurrence of AOA was negatively correlated with effluent NH_4^+-N concentration. It was found that most of the sequences (80 *amoA* sequences) retrieved fell into a soil lineage (Group I.1b) and some sequences belonged to marine lineage (Group I.1a). The AOA found in this study were formerly found to be widely distributed in moderately thermal and marine environments. With abundance of AOA in WWTPs, the study suggested that AOA should potentially involve in nitrogen removal in WWTPs. Some estimation of activity of AOA in AO was performed in this study with certain assumptions. In this regard, AOA was predicted to contribute from 27 to 97% of AO in two out of four full-scale municipal WWTPs. However, AOA sometimes found in industrial wastewater but at lower abundance than AOB. And these AOA sequences belong to soil lineage group [94]. Laboratory scale study showed that high NH_4^+-N enriching reactors with NH_4^+-N of 10 mM (140 mg N/L) and 30 mM (420 mg N/L), AOA amoA genes decreased significantly, and after 360 days of operation AOA amoA genes were less than detection limit (1.7×10^2 copies mg $sludge^{-1}$), whereas AOB amoA genes abundance significantly increased. However, AOA could be detected in those reactors by PCR technique implying that AOA was still there but at low level of abundance [95]. This study supported evidence that AOA favored low ammonium condition and therefore they often occurred in a less abundant than their counterpart AOB.

2.2.2 Metabolism of AOB and AOA

All AOB share a common pathway that AOB possess an ammonia monooxygenase (AMO), which derives electrons from the ubiquinone pool to oxidize ammonia to hydroxylamine. Right after that hydroxylamine is oxidized to nitrite by a hydroxylamine oxidoreductase (HAO), which delivers electrons back (via iron-based electron transfer system-cytochrome c proteins) into the ubiquinone pool for respiration and further activation of AMO [96].

In AOA, AMO is consistently found in AOA metagenomes, but a putative HAO has not been identified [96]. It is hypothesized that archaeal AMO either produce hydroxylamine or doesn't produce hydroxylamine. If the archaeal AMO oxidizes ammonia to hydroxylamine similar to the bacterial pathway then hydroxylamine would subsequently be oxidized to nitrite by one or multiple novel enzymes, for example, putative *multicopper oxidases*, which could function similarly to the bacterial HAO. The four electrons would then be transferred to a quinone reductase (QRED) via small blue copper-containing plastocyanin-like electron carriers [96].

Alternatively, the archaeal AMO may act as dioxygenase and insert two oxygen atoms into ammonia, producing nitroxyl (HNO) from the spontaneous decay of HNOHOH. The nitroxyl may be then oxidized to nitrite by one of the multicopper oxidases-like proteins (MCO-like proteins) acts as nitroxyl oxidoreductase (*NXOR*) with the extraction of two protons and two electrons in the presence of water. The extracted electrons are then transferred to QRED [96].

2.2.3 Targeting AOB and AOA using functional *amoA* genes markers

Molecular techniques are used to study ammonia-oxidizing microbes in the environment. Ammonia-oxidizing bacteria can be identified by targeting 16S rRNA genes or *amo*A genes [91]. Using 16S rRNA genes was better than *amo*A genes in terms of resolution in construction of tree topologies even though the resulting tree topologies using the two genes were highly similar [91]. However, identifying ammonia-oxidizing community using *amo*A genes also has advantages over using 16S rRNA genes. Previous study reported that using *amo*A genes reduce the risk to target taxonomically related organisms since *amo*A genes mainly target ammonia oxidizing microorganisms who can oxidize ammonia in environmental samples [97]. Communities of AOB and AOA in samples can be distinguished using *amo*A genes because this functional gene marker is sufficiently divergent between AOB and AOA [98-100].

2.2.4 Environmental factors affecting ammonia oxidizing process

2.2.4.1 Ammonium concentration

Ammonia, the main substrate in the ammonia oxidation process by AOA and AOB, has the most critical effect on shaping communities and abundance of ammonia oxidizing archaea and bacteria [84]. In culture dependent studies, AOA could survive in various NH_4^+-N concentrations range from low (0.14-0.18 µg/L) [101] to high (0.14-140 mg/L) [102]. In WWTPs, AOA dominated AOB at low NH_4^+-N concentration (5.40-38.6 mg/L) such as in municipal WWTPs but not found in industrial WWTPs. The occurrence of AOA was found to be negatively correlated with effluent NH_4^+-N concentration. Ammonia oxidizing bacteria (AOB) can adapt in various types of environments with a wide range of NH_4^+-N concentrations from low to high [14]. Thus,

AOB can be found in both municipal and industrial WWTPs. However, AOA was commonly found in low NH_4^+-N condition and rarely found in industrial WWTPs [12].

2.2.4.2 Dissolved Oxygen

Ammonia oxidation process is the process to convert ammonia to nitrite under aerobic condition. Therefore, dissolved oxygen (DO) is required for this process. The concentration of DO has crucial effect on the rates of ammonia oxidation in WWTS [103]. The growth rate of nitrifying bacteria was at minimum rate at DO of 0.5 mg/L. These microbes required DO at 1 mg/L to normally function. Dissolved oxygen at 2 mg/L, specific oxygen uptake rate was maximum and remained stable [104]. Theoretically, the amount of oxygen consumed per one milligram NH_4^+-N were 4.57 mg O_2 [103].

However, requirement of DO for AOA and AOB may be different. From the enrichment cultures AOA exhibited low half saturation constant for oxygen (Ks), for example culture AR, *N. maritimus* and Ca. N. *koreensis* have Ks values of 0.064 mg/L (2.01 µM), 0.125 mg/L (3.91µM), and 0.332 mg/L (10.38 µM), respectively [101, 105, 106] while the values for *N. europaea* range from 0.219 – 0.555 mg/L (6.9 to 17.4 µM) [107]. At the sediment-water interface where low oxygen was found in estuarine wetlands, nitrification rate was observed positively correlated with diversity and abundance of AOA but not AOB [108]. In pond sediments, DO is suggested to be the key factor determining the predominance of AOA [89]. These studies implied that AOA were less impacted by DO than AOB thus playing primarily role in AO in estuarine wetland sediments. Interestingly, AOA had also been found coexistence with anaerobic

ammonia oxidation (Anammox) bacteria in three anammox WWTPs with relatively higher abundance [89].

Different from ammonia oxidation process which always requires DO, denitrification process and anammox process use nitrate and nitrite as terminal electron acceptor therefore the presence of DO above 0.2 mg/L could seriously negatively influence on these process [87, 109]. However, it should be noted the anoxic processes will be replaced by aerobic processes when oxygen is present since oxygen is a better electron accepter for metabolism than nitrite and nitrate. The concentration of oxygen at the surface of the cells may be more significant for the anaerobic processes than the bulk concentration [109].

2.2.4.3 pH and alkalinity

pH has strong effect on nitrification process in sediment of streams. The study found that nitrification rate reached maximum value at pH 7.5, and at this pH value nitrification rates were two times higher than the other values. pH has only inhibitory effect and non-toxic [103].

Nitrifying activity in activated sludge is heavily dependent on pH. A study showed that the activity was good at pH range of 7.5-8.5 and the pH below 6.5 or above 10, there was limited or no activity. However, microorganisms depend on pH differently. Each species may exhibit its ability to tolerate with certain pH. For instance, AOA can survive in low [110, 111], neutral [101, 105, 110], and slightly alkaline pH [105]. It was reported that pH plays an important role in growth and activity of AOA. For instance, *N. maritimus* has optimum pH in the range of 7.4-7.6. Below this range,

for example, at pH 6.7, *N. maritimus* had no activity, and at pH 7.0 there was no growth [101].

Alkalinity is important factor in ammonia oxidation process because this process is carried out by chemoautotrophic microorganisms which use inorganic carbon as carbon source. It was reported that 7.1 mg alkalinity (as $CaCO_3$) are consumed for every mg NH_4^+-N oxidized. In the nitrification process, majority of alkalinity is consumed to neutralize acidic environment generated during oxidation of ammonia to nitrite and nitrate. However, due to slow growth rates of ammonia oxidizers, small amount of alkalinity is utilized [103].

2.2.4.4 Temperature

Temperature at which nitrification activity could be observed was 4 to 45°C [103] and optimum for growth of nitrifying bacteria 28-36°C, specifically optimum temperature for *Nitrosomonas sp.* is 35°C and at the temperature between 54 and 58°C will cause dead.

Ammonia oxidizing archaea could sustain in different profiles of temperatures ranging from cold (5°C) [112] to hot (72 °C) [113]. AOA could also tolerate a wide range of temperature in which the temperature may fluctuate from 5 to 17°C. For instance, the growth range temperatures of *Ca*. N. *viennensis*, culture EN123, *Ca.* N. *devanaterra*, and *Ca*. N. *koreensis* in 20-47 °C, 32-37 °C, 20-30 °C, and 15-30 °C, respectively [101, 105, 110].

2.2.4.5 Organic compounds

Nitrification rates were affected by additions of dissolved organic carbon acetate at the concentration of 30 mg C/L, but lower than that value there was no effect [114]. Pyruvate addition up to 0.1-10 mM has showed positive effect on growth of archaeon *Candidatus* Nitrososphaera *viennensis* while addition of other organic compounds such as peptone, yeast, extract, glucose, lactose, arabinose, malate, sucrose, galactose, acetate, trimethyline, ethanolamine, and methanolamine showed no growth activation [110]. In contrast, Konneke et al. (2005) found that the addition of organic compounds in very low concentrations appeared to inhibit the growth of the strain SCM1 [101].

In the environment, organic load from paper and pulp mill effluent in sediment has showed effect on abundance of AOB and AOA. Observation of gene abundance of total AOB and AOA found that total gene abundance of AOB was reduced, whereas there was an increase in that of AOA in paper and pulp mill impacted effluent. This leads to a conclusion that organic load could play important role in niche differentiation between AOA and AOB [115]. Relating to effect of organic matter on AOA, it was reported that both acetate and leaf litter did not have effect on AOA communities structures, but stimulated their growth. However, addition of leaf litter and acetate did have effect on communities of AOB and promoted their growth in early stage of incubation. Supplement of leaf litter had more obvious effect on growth of AOB than acetate [116].

In agriculture, the availability of nitrogen and organic carbon were found to positively correlate with diversity indexes of archaeal *amoA* genes [117, 118]. Strauss (2000) found that nitrogen availability is one of the most important factor influencing

nitrification and carbon may be an important factor when it is in form of relatively labile and under high C:N ratio environmental conditions [114].

2.2.4.6 Light intensity

High light intensity of 500 μmol photons m^{-2} s^{-1} completely inhibited AOA and AOB, and at lower light intensity of 60 and 15 μmol photons m^{-2} s^{-1} inhibited AOA, with no evidence of recovery, but less or not inhibited AOB [119]. White light of 30 μmol photons m^{-2} s^{-1} strongly inhibited the growth of AOA, no effect on AOB [120]. The less density of AOA compared to AOB over years and the AOA reached highest density in winter suggested that AOA abundance was potentially related to sunlight [89].

2.3 Nitrification inhibitor - Allylthiourea

Allylthiourea (ATU) is a metal chelating agent that has been successfully used in AO research. It was previously found that ATU at 86 μM completely inhibited activity of nitrifying sludge containing mainly AOB [121] and ATU at 0.2 μM could inhibit 50% ammonia oxidizing activity of *Nitrosospira multiformis*, a member of AOB [86]. Most recently, a study revealed that AOB activity was totally suppressed at ATU of 100 μM [122]. Allylthiourea exhibits less negative effect on activity of AOA. In enriched cultures, ATU at 172 μM partially inhibited growth and activity of archaeon Candidatus *Nitrosoarchaeum limnia* strain SFB1 [123]. Shen and his colleagues (2013) found that the AO activity of pure culture of *Nitrososphaera viennensis* was inhibited by 50% at ATU 193 μM [124]. In addition, ATU 50 and 100 μM was found to stimulate growth of AOA by 32% and 34% in terms of *amoA* gene abundance [102]. The literature revealed that ATU exhibits more effective inhibitory effect on AOB rather than AOA.

Therefore, it is assumed that ATU can be used to roughly observe AO activity of AOA. In this study, ATU is sometimes used to confirm the ammonia oxidation activity.

2.4 Solid retention time

Solid retention time (SRT) is the average amount of time that microbes present within a reactor calculated by dividing total mass of biomass in the treatment system for total mass of biomass lost or wasted daily. Thus, removing a measured amount of biomass from the reactor contents can change SRT. Solid retention time represents basic relationship to bacterial growth rate [125], so it is important operational parameter to study for design calculations and for the control of biological treatment systems. Solid retention time has influenced on nitrification activity. The highest ammonium removal efficiency (84%) was obtained at the SRT of 10 days while increasing SRT to more than 15 days lowered the removal of NH_4^+-N [126]. Long SRT resulted in reducing nitrification activity due to partial inactivation of biomass [127] although long SRT generally resulted in greater biomass concentration. However, short SRT resulted in washing out of biomass especially slow growth rates as ammonia oxidizers thus causing stress for AO process.

2.5 Cell entrapment technique

Cell entrapment technique, immobilization of microorganism in a porous polymeric matrix, is a potential method to use for bioremediation using microorganism. Previously, immobilized cell method has been applied to efficiently treat non-toxic substance such as organic carbon [128], hazardous substances such as atrazine and lindane in contaminated agricultural soils [17, 129]. In addition, cell entrapment technique could be used to reduce toxicity effect of AgNPs on nitrifying activated

sludge, for example, the entrapment matrices successfully reduced the adverse effects of AgNPs on nitrification activity [15] or mitigated toxicity effect of disinfectants on chemical oxygen demand (COD) removal [130]. Immobilized cells showed better removal performance and toxicity reduction than suspended cells because it provides high cell loading, the cells are less exposed to toxins and it can be recycled [129, 130]. However, there is limitation when applying cell entrapment technique. One major limitation with cell entrapment is that mass transfer could be limited activity of the entrapped cells [131]. Crosslink structures and small pore-size are the main cause of limitation of mass transfer and permeability.

2.5.1 Cell entrapment using alginic acid sodium salt

Brown sea-weed is a biological source of alginic acid extraction. Alginate is a series of linear copolymers containing blocks of (1,4)-linked β-D-mannuronate (M) and α-L-guluronate (G) residues in which G residues (GGGGGG), M residues (MMMMMM) are arranged consecutively and one after another (GMGMGM). It is found that only G-blocks of alginate involve in cross-linking with divalent cations such as calcium ions to form hydrogels [132]. For this reason, the mechanical characteristics of alginate gels could be enhanced by increasing the length of G-block and molecular weight. Molecular weight of alginate is increased to improve the physical nature of hydrogels, however, an alginate solution from high molecular weight exhibits high viscosity which could harm to microorganisms due to high shear forces [132].

The interaction between divalent cations and alginate forms a gel structure by ionic cross-linking. This type of linking is generated because divalent cations bind solely to G-blocks of the alginate chains, the G-blocks of one polymer then form

junctions with the G-blocks of adjacent polymer chains resulting the egg-box model of cross-linking [133].

Sodium alginate (SA) is cheap and it can be massively produced [134]. It was used in various functions such as gelling agents, suspending agents, and emulsion stabilizers [135]. Sodium alginate is a hydrophilic polysaccharide and spherical gel particles were formed when SA was mixed with divalent cations such as calcium ions (Ca^{2+}). The gel of sodium alginate is heat stable up to 150 ^{o}C. The binding of Ca^{2+} by alginate or calcium alginate (CA) was illustrated in **Figure 2-1** [134].

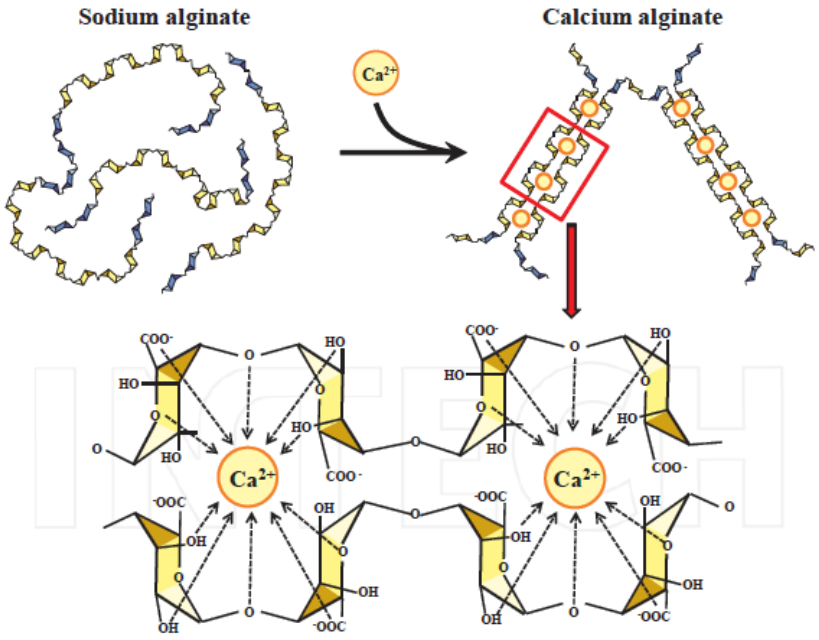

Figure 2-1 Formation of gel network between sodium alginate and calcium ions

Calcium alginate (CA) is the commonly used entrapment matrix because it is a natural polymer and not harmful to entrapped microbes and environment [136]. Calcium alginate prepared by a procedure previously described [15, 136]. Briefly, sodium alginate solution of 2 % (w/v) was mixed with the concentrated nitrifying activated sludge (NAS). The mixture was dropped into a calcium chloride ($CaCl_2$) solution of 3.5 % (w/v) to form CA spherical beads with a diameter of 3 or 6 mm.

Siripattanakul-Ratpukdi et al. (2014) used CA to entrap nitrifying cells to examine toxicity effect of AgNPs on nitrification process in the entrapment matrix using respirometric experiment. In this experiment, oxygen depletion was monitored instead of reduction of ammonium concentration. The results indicated that CA-entrapped cells could mitigate inhibitory effect of AgNPs (0.05-5.00 mg/L) on nitrification activity up to 100%. This is the pioneer study to indicate that entrapped cells could be potentially used for real application for reducing toxicity effect of AgNPs on nitrification activity in wastewater contaminated with AgNPs.

Change from calcium chloride ($CaCl_2$) to barium chloride ($BaCl_2$) could improve the quality of the gel beads produced. For instance, $BaCl_2$ was used instead of $CaCl_2$ in preparation of the gel beads to produce barium alginate (BA) in the previous study [137]. The study found that BA beads proved to have better physic-chemical properties than the more commonly used CA beads. The immobilized cells in BA gel retained a high yield and activity [137]. The result of this study lead to an idea to use BA instead of CA to entrap nitrifying sludge in reducing toxicity impact of AgNPs and Ag^+ since AgNPs is a release source of Ag^+.

Recently, BA entrapped cells technique was used to treat wastewater (COD) better than free cells [138]. For the BA-entrapped cell preparation, sodium alginate 2% (w/v) was dissolved into sterile distilled water and thoroughly mixed with prepared activated sludge. The mixture was manually dropped into a barium chloride solution of 5% (w/v) using a sterile syringe to form spherical beads with a size of 3-5 mm. The beads remained in the solution for 2 h for hardening. Siripattanakul-Ratpukdi and Tongkliang (2012) was one of the first researchers using BA-entrapped cells in treating pollutants in wastewater.

However, the use of BA-entrapped cells in mitigation of inhibitory effect of AgNPs and Ag^{+} on AO is not reported in the previous studies.

2.5.2 Cell entrapment using polyvinyl alcohol

Polyvinyl alcohol (PVA) is produced from polyvinyl acetate through hydrolysis. It is an man-made polymer that has been used in many fields of application such as industrial, commercial, medical, and food sectors because it is non-toxic to humans, and easily biodegradable [139]. PVA is completely dissolved at water temperature approximate 100^{o}C which is maintained for at least 30 min. All PVA grades water solubility, stability to variation of temperature, resistance to chemical and biodegradability [140]. The demonstration of chemical structure of PVA [139] is presented in Figure 2-2.

In environmental aspect, PVA is not harmful to activated sludge microorganisms [15, 141] and it can be abundantly produced at a low cost [137]. Polyvinyl alcohol when mixed with boric acid will form a cross-linked polymer [142]. Sodium borate acts a cross-linking agent to bind PVA chain together (Figure 2-3). PVA

generated a crosslink with boric acid for a period from 10 min to 2 h to form a spherical structure which content water. Then the gel beads were solidified by esterification of PVA with phosphate (sodium phosphate buffer 1 M). The PVA cell entrapment preparation procedure was according to the previous work [143]. A PVA solution of 10 % (w/v) was mixed with the concentrated nitrifying cells homogenously. The mixture was dropped into a saturated boric acid solution to form 3 or 6 mm spherical beads. The formed spherical beads were transferred to 500 mL of 1 M sodium orthophosphate buffer (pH 7.0) and left for 1–2 h to obtain hardened PVA beads. Previously, PVA-immobilized cells were used to effectively remove organic carbon [128], atrazine and lindane [17, 129]. PVA-entrapped cells could be highly effective in removal of ammonia under presence of AgNPs [15]. However, removal of ammonia under presence of Ag^{+} using PVA-entrapped cells is a gap in current research.

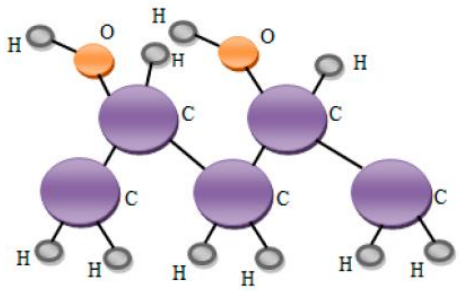

Figure 2-2 Structure of polyvinyl alcohol

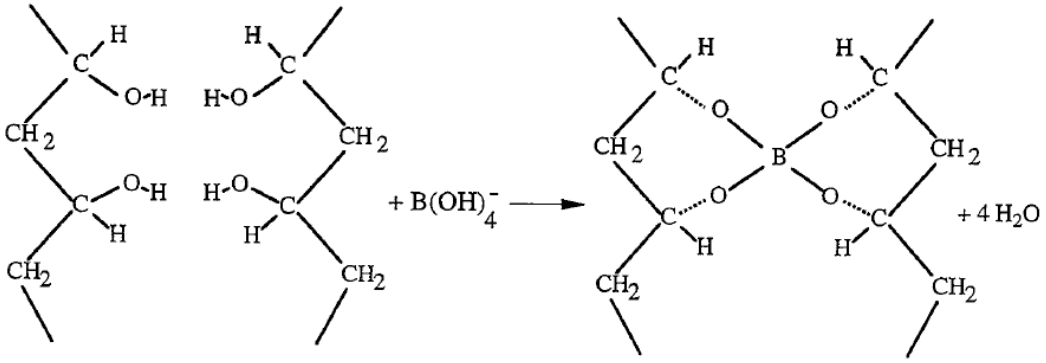

Figure 2-3 Cross-linking of polyvinyl alcohol with boric acid.

The network is formed by borate chelate ions and hydroxyl groups on adjacent polymer strands.

2.5.3 Cell entrapment using mixture of PVA and BA

Successful application of immobilization techniques to biological wastewater treatment must satisfy the requirements of carriers having strong consistency, durability, and high cell viability as well as low cost [144]. A combination between PVA and CA was proposed for entrapping phenol degrading *Pseudomonas* to removal phenol using the fluidized bed reactor [145]. PVA has been widely used because it provides the strength and high crosslinking capacity to the matrix whereas alginate reduces the agglomeration and increases the surface properties [145, 146]. Combination of PVA and SA would result in a compound in which the carboxylate group of SA is reported to form hydrogen bonding with the hydroxyl group of PVA [147]. Combination of SA (1%), PVA (8%), $CaCl_2$ (1%) could maximize the activity of the cells entrapped [148]. This study pointed out that SA from 0.5-3.0% and PVA from 4-12% showed the highest activity of immobilize cells. This could mean that a wide range of concentration of SA and PVA are suitable for selection for entrapping cells. This combination also resulted in more

stability of the produced gel beads and could be stored for a long time [148]. Since BA was better than CA in terms of physical and chemical properties [137], it is suggested to use BA to replace CA in producing gel beads for entrapment of NAS to study inhibitory kinetics of AO influenced by AgNPs and Ag^+. Currently, study of application of cell entrapment using mixture of BA and PVA in protecting ammonia oxidation process from toxicity impact of AgNPs and Ag^+ is not available. Conducting research in this areas is a need to expand understanding in the field of using entrapped cells for treating wastewater containing AgNPs or Ag^+.

2.6 Kinetics calculation

Monod kinetics is often used to model microbial kinetics as showed in Equation 2.1.

$$\mu = \mu_{max} \frac{S}{Ks + S} - b \qquad (2.1)$$

where μ is specific biomass growth rate (gVSS/gVSS.d), μ_{max} is maximum growth rate of biomass (gVSS/gVSS.d), b is the specific biomass decay rate (gVSS/gVSS.d), S is substrate concentration and Ks is the half saturation constant. In short-term experiment (60 h), the term decay rate b could be neglected.

For studying the kinetics of ammonia oxidation, the term μ and μ_{max} could be replaced by q (ammonia oxidation rate in mg N/L/h) and q_{max} (maximum ammonia oxidation rate in mg N/L/h) since activity was more sensitive for quantitative measurement than biomass [149].

2.7 Inhibition models

Competitive, uncompetitive and noncompetitive are the main types of enzyme inhibition. For competitive inhibition, the inhibitor and substrate compete for reactive site on the enzyme. In this type, the reaction rate will not change, while the Ks will increase. The equation 2.2 is given to describe the competitive inhibitor.

$$r_s = r_{\max} \frac{S}{S + K_s(1 + \frac{I}{K_i})} \qquad (2.2)$$

For the type of uncompetitive inhibition, the enzyme-substrate, but not the free enzyme, is bound by the inhibitor. In this model, r_{max} doesn't change but Ks will increase. The model of this type of inhibition is described as in the equation 2.3.

$$r_s = \frac{(r_{\max} /(1 + \frac{1}{Ki}))S}{(Ks /(1 + \frac{I}{K_i})) + S} \qquad (2.3)$$

In non-competitive inhibition type, the inhibitor binds to any sites on the enzyme resulting in changing enzyme composition and stopping forming of products. In this model, r_{max} will decrease but Ks will not change. The equation 2.6 describes kinetics of non-competitive inhibition.

$$r_s = r_{\max} \frac{(r_{\max} /(1 + \frac{I}{K_i}))S}{Ks + S} \qquad (2.4)$$

where r_s is the specific substrate utilization rate (gS/L.h), r_{max} is maximum substrate utilization rate (gS/L.h), S is substrate (g/L), I is the concentration of inhibitor (g/g), K_s is half saturation concentration coefficient, known as equilibrium or affinity coefficient, K_i (g/L) represents the inhibitory coefficient, E is enzyme, ES is enzyme substrate complex.

2.8 Atomic absorption spectroscopy

This research used atomic absorption spectrometry (AAS) to quantify silver concentration in the aqueous sample. This instrument is used for quantitative analysis of chemical elements (more than 70 different elements of metals) using the absorption of optical radiation by free atoms in the gaseous state. The absorption spectrometry is used to assess the concentration of the analyte in the being measured samples by comparing to the known standard concentrations. In this technique, the main principle is that the electrons of the atoms can be excited for a short period of time by taking up a certain amount of quantity of energy from the radiation of a given wavelength. The wavelength is specific to a specific electron transition in a specific element. Each wavelength corresponds to one element and this makes the technique highly selective to an element. A detector is used to measure the radiation flux with a sample and without sample in the atomizer and these two values of absorbance are used to calculate concentration or mass of the analyte.

2.9 Scanning electron microscopy

The scanning electron microscopy (SEM) is used to obtain information such as external morphology, composition of chemicals, crystalline structure and direction of materials of being observed sample. This technique uses focused beam of high-energy electrons to initiate various signals (electron-sample interactions) at the surface of solid specimens. As a result, two-dimensional image is obtained at the areas range from one centimeter to five microns in width (magnification from 20X-30,000X, spatial resolution from 50-100 nm). In principle, source of accelerated electrons in an SEM carry significant amounts of kinetic energy come into contact with the solid sample. After contact with the solid sample the incident electrons are decelerated and the energy is dissipated into different signals such as secondary electrons, backscattered electrons, diffracted backscattered electrons, photons (characteristic X-rays), visible light, and heat. For imaging of samples, secondary electrons and backscattered electrons are used in which secondary electrons are specifically used for displaying morphology and topography on samples whereas backscattered electrons are used for showing contrasts of samples. Photons or characteristic X-rays are utilized for elemental analysis. Therefore, energy-dispersive spectroscopy (EDS) system is often coupled with SEM for quantitative or semi-quantitative determination of composition of elements using a sensitive X-ray detector to separate the characteristic X-rays of different elements into an energy spectrum, and a software is then used to analyze the energy spectrum to determine the amount of particular elements. This study focuses on using SEM and EDS for obtaining information regarding cell morphology, and AgNPs-cells agglomeration, respectively.

2.10 Transmission electron microscopy

Transmission electron microscopy (TEM) works using a beam of electrons transmitted through the specimen and interact with the specimen when it pass through. The interaction between the electrons and the specimen forms a two-dimensional image of the specimen with a maximum magnification of one nanometer. With this resolution, TEM can be utilized to analyze quality, shape, size, density of quantum wells, wires, and dots. In this study, TEM is used to analyse size and shape of AgNPs, and AgNPs-cells interaction.

2.11 Fluorescence in situ hybridization

Fluorescence in situ hybridization (FISH) is a molecular cytogenetic technique that is used for visualization of particular nucleic acid sequences in specific cellular or chromosomal sites by hybridization of complementary fluorescently labeled probe sequences with intact cells. Principally, the complementary DNA sequence will be bound to single-stranded DNA in FISH technique. Therefore, a DNA probe for a specific chromosomal region will recognize and hybridize to its complementary DNA sequence on a metaphase chromosome or within an interphase nucleus. FISH procedure comprises of crucial steps of sample preparation and fixation, denaturation of probe and sample, hybridization of a fluorescently labeled probe to sample (annealing), post-hybridization washing and detection. The probe signal can be seen by using fluorescent microscopy. Commercially synthesized oligonucleotide probes which are fluorescently 5’ labeled by AF and CY3 (ThermoHybaid, Ulm, Germany) were used. In the current study, FISH was applied to analyze spatial distribution of microbial communities in the nitrifying cultures.

Chapter 3 Materials and Methods

3.1 The entire experimental framework

The overall framework for this entire study was indicated in Figure 3-1. There were three main experiments in this research. Experiment 1 was to compare inhibitory kinetics of ammonia oxidation activity from low ammonium reactor (NAS 0.5 mM) and from high ammonium reactor (NAS 30 mM). The experiment 2 was to understand inhibtory kinetics and mechanism of ammonia oxidation from NAS 30 mM. The third experiment was to reduce the toxic impact of silver nanoparticles and silver ions using entrappment tecnique.

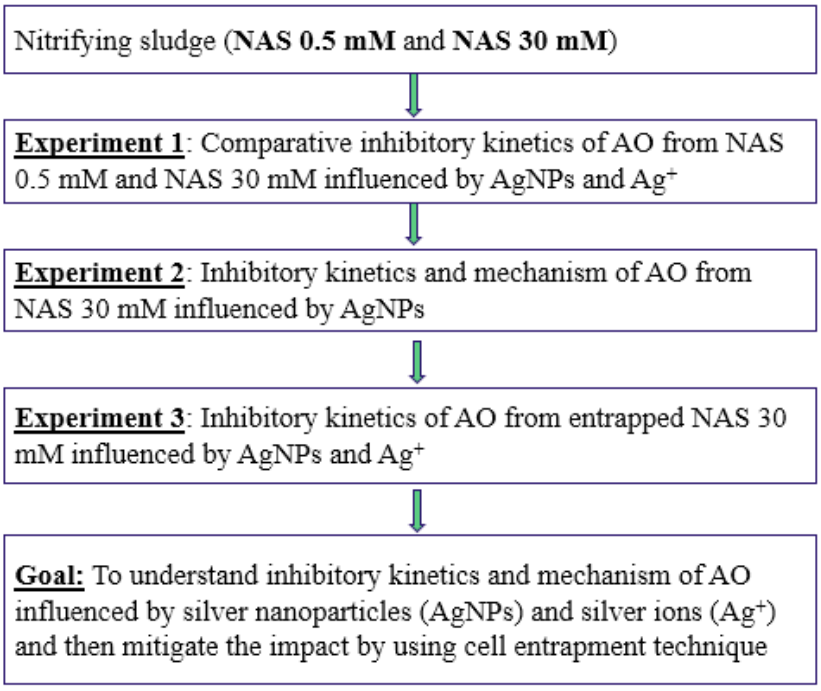

Figure 3-1 The experimental framework of the entire study

3.2 Description of the experiments

3.2.1 Experiment 1

This experiment investigated inhibitory effect of AgNPs and Ag^+ on AO from low and high NH_4^+–N enriched nitrifying sludges.

In this study, the concentrations of AgNPs were 1, 10 and 100 mg/L. The concentration of AgNPs of 1 mg/L was selected because it was relevant to the concentration detected in WWTPs [150], while the concentrations of AgNPs at 10 and 100 mg/L were selected based on a prediction that AgNPs will be increasingly accumulated in the future [63]. The concentration of Ag^+ was selected based on the concentrations of Ag^+ released from the stock AgNPs of 1, 10 and 100 mg/L.

Framework of experiment 1 was presented in Figure 3-2. The ammonia oxidation from NAS 0.5 mM and NAS 30 mM were used to expose to the same initial concentrations of AgNPs and Ag^+ and the reduction of initial NH_4^+–N concentration was monitored as the indicator of the toxic response. Before taking the cultures for the kinetics experiments, live/dead assays were performed to test viability of the enriched microbes to support for explanation of the inhibitory kinetics data. Ammonium consumption and nitrate production were quantified using Salicylate–hypochlorite method [151], and Colorimetric method 4500 [152], respectively. Live and dead assays were performed using staining kit (LIVE/DEAD® BacLight™ Bacterial Viability, Molecular Probes, Invitrogen) and observing under confocal laser scanning microscopy (CLSM) [62]. These analysis methods were used consistently in the entire work. More details of the experimental methodology could be found in Chapter 4.

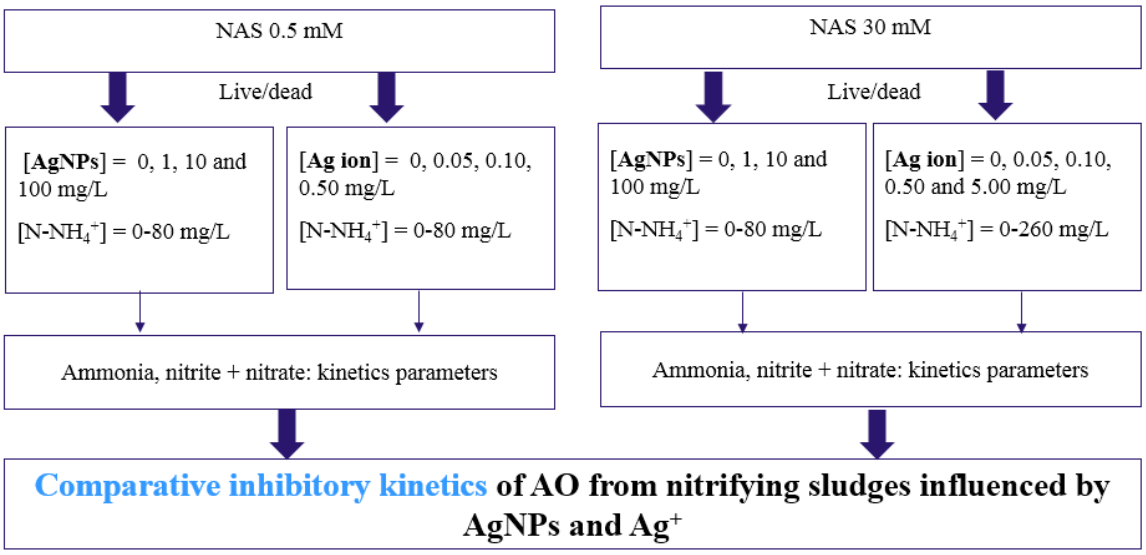

Figure 3-2 Comparative inhibitory kinetics of AO from nitrifying sludge influenced by AgNPs and Ag^+

3.2.2 Experiment 2

This experiment was designed to elaborate inhibitory kinetics and mechanism of AO activity from NAS 30 mM influenced by AgNPs and Ag^+. The experimental steps were presented in Figure 3-3. Firstly, the inhibitory kinetics of ammonia oxidation influenced by AgNPs were conducted. During the experiments with AgNPs, the Ag^+ release was monitored. The experiments with Ag^+ were then performed with the concentrations equal to the release. By comparing toxicity effects of AgNPs and Ag^+, role of Ag^+ in overall toxicity of AgNPs suspension was clarified. Later, the community of microbes in NAS 30 mM was estimated using Fluorescent 16S rRNA targeted oligonucleotide probes and in situ hybridization (FISH). The FISH result confirmed NAS 30 mM was dominated by ammonia oxidizing microbes thus supported for the reduction of ammonia oxidation activity of this culture under presence of silver species (AgNPs and Ag^+). Scanning electron microscopy (SEM) was used to observe morphology of cells

and aggregation of cells and AgNPs. Transmission electron microscopy (TEM) was applied to examine physiology of cells after exposed to silver species. In addition, microbial viability was also observed using confocal laser scanning microscopy (CLSM) to reaffirm the damage of membrane integrity after exposed to AgNPs and Ag^{+}. Additional details of methodology of the experiment 2 could be found in Chapter 5.

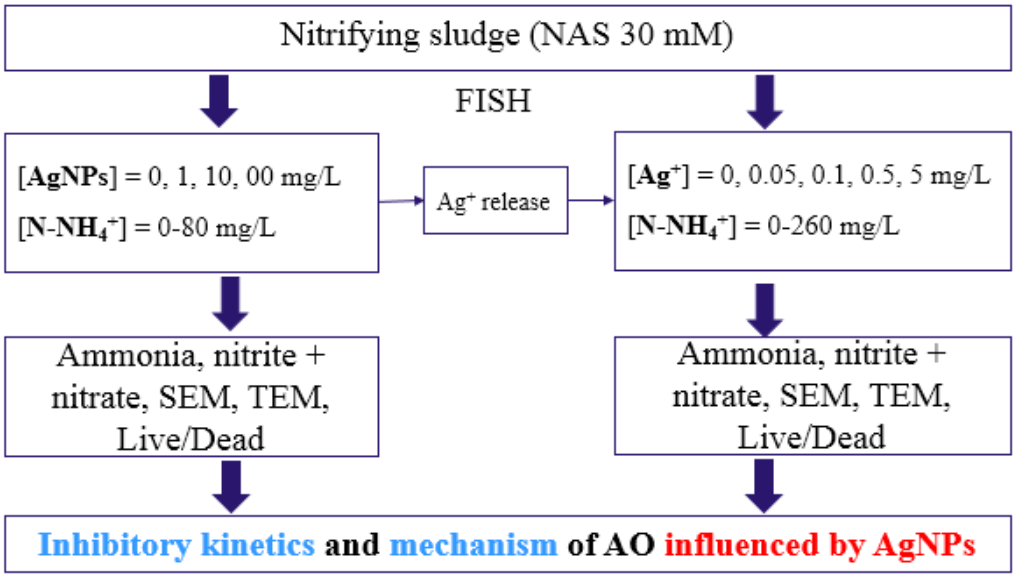

Figure 3-3 Inhibitory kinetics of AO from NAS 30 mM influenced by AgNPs and Ag^{+}

3.2.3 Experiment 3

This experiment was conducted to mitigate harmful impact of AgNPs and Ag^+ on ammonia oxidation activity using cells from NAS 30 mM entrapped in barium alginate (BA), polyvinyl alcohol (PVA) and the mixture of BA and PVA (PVA-BA). The experimental framework was displayed in Figure 3-4. In this experiment, the concentrations of entrappment materials were selected based on published papers. The amounts of AgNPs, Ag^+ and MLSS, sampling intervals were identical to those used in the experiment 2, and thus influence of AgNPs and Ag^+ on entrapped cells could be compared to those in the suspended cells obtained from the experiment 2. Similar to the previous experiments, ammonium reduction, nitrate production were monitored to evaluate reponse of ammonia oxidation activity to AgNPs and Ag^+. SEM was used to observe microbial cells and internal structure in the gel beads. Live/dead assays were also performed for examining viability of microbial cells after exposed to AgNPs and Ag^+. The entrapped cells were shaken on rotary shaker at the speed of 200 rpm for 30 days to examine the stability of the entrapped cells in synthetic wastewater. At the same time with the stability test, concentrations of AgNPs were also quantified using spectrophotometer to examine the amount of AgNPs remaining in well dispersed form. Additional description of methodology of this experiment could be found in Chapter 5.

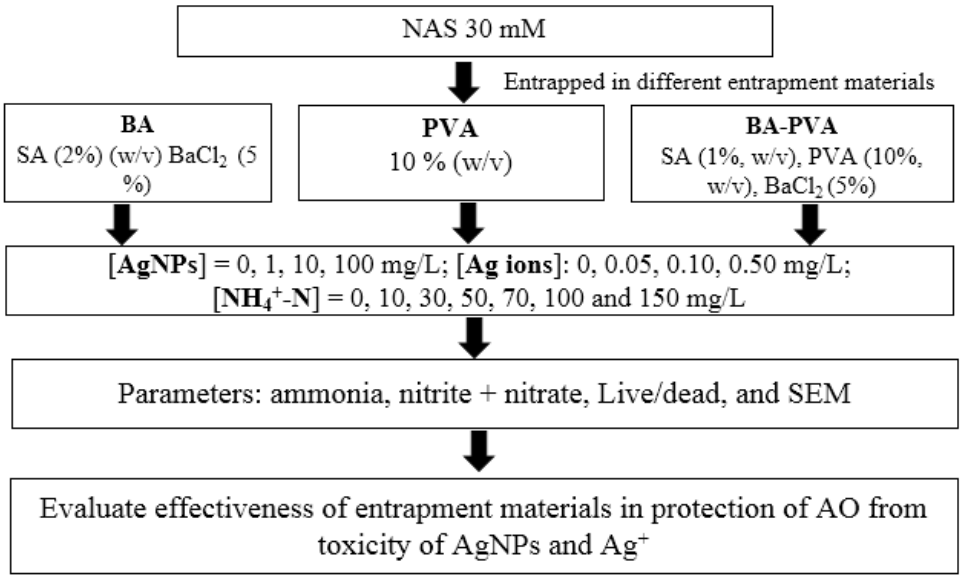

Figure 3-4 Framework of inhibitory kinetics of AO in entrapped cells influenced by AgNPs and Ag^+

3.3 Source of AgNPs and Ag^+

Silver nanoparticles (5,000 mg/L) were provided by PrimeNANO technology (Prime Nanotechnology Co. Ltd., Chulalongkorn University, Thailand). It was chemically synthesized from silver nitrate ($AgNO_3$) using sodium borohydride ($NaBH_4$) and starch as reducing and capping agents, respectively. Silver nitrate ($AgNO_3$, Merck, Darmstadt, Germany) was used as source of Ag^+. The stock solution of Ag^+ (100 mg/L) was prepared by dissolving 0.1573 g of $AgNO_3$ in 1,000 mL sterilized distilled water. The solution was used immediately after preparation.

3.4 Nitrifying cultures

Nitrifying culture can be developed by enriching inoculums containing ammonia oxidizing microbes from environments (for example, activated sludge from municipal WWTPs). The inoculum is enriched using media containing only inorganic synthetic

wastewater (SWW) to limit growth of heterotrophic bacteria which often outcompete autotrophic ammonia oxidizing microbes in natural environments and promote growth of ammonia oxidizing microbes. Ammonium, solid retention time (SRT) and hydraulic retention time (HRT) are three main factors having effects of abundance, ammonia oxidation activity and communities of ammonia oxidizing microbes. Variation of these factors can generate different ammonia oxidizing cultures which could possibly represent for various naturally environmental conditions. The pure culture of ammonia oxidizing microbes only convert ammonia to nitrite, whereas nitrifying culture complete the nitrification process in which ammonia is converted to nitrite and then nitrate. Microorganisms including ammonia oxidizing microbes, nitrite oxidizing microbes and other bacteria (heterotrophs) coexist in nitrifying culture, while only ammonia oxidizing microbes exist in pure ammonia oxidizing culture. Communities of a nitrifying culture are more relevant to environmental conditions than that of pure ammonia oxidizing culture. The cells obtained from nitrifying cultures are called nitrifying cells.

Two mixed ammonia oxidizing cultures were developed in laboratory condition by varying NH_4^+–N and SRT. The low NH_4^+–N enriched nitrifying sludge (NAS 0.5 mM) was enriched at initial NH_4^+–N concentration of 7.2 ± 1.1 mg/L and at an equal of SRT and HRT of 28 days. The high NH_4^+–N enriched nitrifying sludge (NAS 30 mM) was enriched at influent NH_4^+–N of 429 ± 62 mg N/L (NAS 30 mM) at SRT which was equal to HRT of 4 days. Low and high NH_4^+–N levels could represent for different NH_4^+–N loads received by various WWTPs such as municipal and industrial.

3.4.1 Low ammonium enriched nitrifying activated sludge

NAS 0.5 mM: the seed sludge was collected from a municipal WWTP in Bangkok, Thailand. The collected sludge was cultivated in batch reactor with solid and hydraulic retention time of 28 days (SRT = HRT = 28 days) at initial NH_4^+-N concentration of 7.2 ± 1.1 mg/L. The reactor operating conditions (DO and temperature) were similar to those with NAS 30 mM.

3.4.2 High ammonium enriched nitrifying activated sludge

NAS 30 mM: The seed sludge was taken from a continuous flow nitrifying culture-enriching reactor. The reactor has been operating with both hydraulic retention (HRT) and solid retention time (SRT) of 4 days with no sludge return. The collected seed sludge was then cultivated in a batch reactor, with SRT and HRT of 14 days, at initial NH_4^+–N concentration of 429 ± 62 mg N/L. The dissolved oxygen (DO) concentration was maintained above 2 mg/L, and pH was adjusted between 7.0–7.8 using 5 N NaOH by pump. The batch reactor fed with inorganic synthetic wastewater (SWW).

The composition of SWW contained 1.9821 g/L $(NH_4)_2SO_4$, 0.2 g/L NaCl, 0.2 g/L K_2HPO_4, 0.4 g/L $MgCl_2.6H_2O$, 0.1 g/L $CaCl_2.2H_2O$, 0.5 g/L KCl, and 1 g/L $NaHCO_3$ with an addition of inorganic salt solution (1 mL). The inorganic salt solution comprised of 40 g/L $MgSO_4$ $7H_2O$, 40 g/L $CaCl_2$ $2H_2O$, 200 g/L KH_2PO_4, 1 g/L $FeSO_4$ $7H_2O$, 0.1 g/L Na_2MoO_4, 0.2 g/L $MnCl_2$ $4H_2O$, 0.02 g/L $CuSO_4$ $5H_2O$, 0.1 g/L $ZnSO_4$ $7H_2O$, and 0.002 g/L $CoCl_2$ $6H_2O$.

3.4.3 Preparation of cleaned cells for AgNP and Ag^+ experiments

The enriched NAS 0.5 mM and NAS 30 mM cultures in batch reactor were harvested and centrifuged at 5,000 rpm for 20 min and clear supernatant was removed to collect

the settled cells. The collected cells were re–suspended and centrifuged to wash in SWW. The washing process was repeated for five times to obtain cleaned cells, which were used for inhibitory kinetics experiments with AgNPs and Ag^+.

3.5 Synthetic wastewater for AgNP and Ag^+ experiments

The composition of SWW for inhibitory kinetics tests with AgNPs and Ag^+ comprised of $(NH_4)_2SO_4$, 1 g/L $NaHCO_3$, 0.1 g/L K_2HPO_4, and 0.025 g/L $MgSO_4$, and 0.025 g/L NaCl. The media was previously used for studying impact of AgNPs on AO activity (Gu et al., 2014).

3.6 Chemical analysis

3.6.1 Measurement of ammonia

Ammonium was analyzed by using Salicylate-hypochlorite method. In this test, ammonia reacts with salicylate and sodium hypochlorite under presence of sodium nitroprusside to form indophenol blue. The indophenol blue was then determined by spectrophotometer [151]. Firstly, five ml of sample was filtered through 0.45-µm filter paper. Dilution of the sample was appropriately made if estimated concentration of ammonia is greater than 1 mg N/L. Secondly, for color development, the filtrate was then added with 1 ml alkaline-hypochlorite solution, 0.6 ml salicylate-catalyst solution. The prepared samples were then stirred well and put in the dark at least one hour before the measurement of absorbance but not more than 24 hours. The samples then were measured at the absorbance of 640 nm.

3.6.2 Measurement of nitrite

The parameter measurement was followed Colorimetric method [152]. Sample was pre-treated by filtering or diluting into the range of 0-1 mg/L of nitrite. Then, 5 ml of

pretreated sample was used for the measurement. The color development reagents comprise of solution 1 (dissolve sulphanilamide in hydrochloric) and solution 2 (dissolve N-(1-Naphthyl)-Ethylenediamine Dihydrochloride in DI water) were added. Let the color to be developed at least 1 h after chemical addition. Developed color was measured for absorbance at 543 nm with UV visible spectrophotometers (Thermo Electron Corporation, Hexious α, Cambridge, UK).

3.6.3 Measurement of nitrate

Nitrate in the samples was converted to nitrite using vanadium chloride (VCl_3, 0.8 g in 100 ml HCl 1M)[13]. Nitrite was then measured using the method described above.

3.6.4 Measurement of MLSS

The MLSS samples were analyzed according to Standard Method 2540-D (Total Suspended Solids Dried at 103-105ºC) [152]. Briefly, approximate 200 mL of a well-mixed sample was filtered through a weighed standard glass-fiber filter by using vacuum pump. The residue retained on the filter was dried to a constant weight at 103 to 105°C for 1 h. The increase in weight of the filter represents the total suspended solids.

3.6.5 Live/dead assays

For sample preparation, the suspended cells are collected by centrifuge at 10,000 g for 10-15 min. Then the supernatant was discarded. The pellet was re-suspended in NaCl 0.85% and then centrifuged for 10 min at 10,000 g to settle the cells. This washing process was repeated for five times. Then the clean cells were suspended in 1 ml of NaCl 0.85%. A control dead cells was prepared by killing nitrifying cells by autoclaved at least 121°C for 15 min.

For preparation of staining solution, the staining solution was prepared by mixing at the ratio 1:1 of Component A (SYTO 9 dye, 1.67 mM / Propidium iodide, 1.67 mM in DMSO) and Component B (SYTO 9 dye, 1.67 mM / Propidium iodide, 18.3 mM in DMSO). For staining the samples, 3 μL of the dye mixture was added for 1 mL of the bacterial suspension. The stained samples were mixed thoroughly and incubated at room temperature in the dark for 15 min.

For the observation of stained cells, 5 μL of the stained bacterial suspension were trapped between a slide and an 18 mm square coverslip and then placed in the containing chamber of the confocal laser machine. The excitation/emission maxima for these dyes are about 480/500 nm for SYTO 9 stain and 490/635 nm for propidium iodide (PI). The background remains virtually non-fluorescent. Ten microscopic fields were selected for calculation of live and dead proportions using ImageJ software (ImageJ 1.4.3.67, Broken Symmetry Software). The proportions of dead cells were presented by mean ± SD.

3.7 Kinetics calculation

NH_4^+–N oxidation rates were calculated using equation 3.1 which compared change of NH_4^+–N reduction versus time, whereas the Monod kinetics parameters including q_{max} and Ks were calculated from Monod equation as indicated in equation 3.2.

$$q = \frac{dS}{dt} \quad (3.1)$$

$$q = \frac{q_{max} S}{K_s + S} \quad (3.2)$$

where q is NH_4^+–N oxidation rate (in milligrams of N per liter per hour, mg N/L/h); q_{max} is the maximum NH_4^+–N oxidation rate (in milligrams of N per liter per hour, mg N/L/h), S is initial NH_4^+–N concentration (in milligrams of N per liter, mg/L), Ks is the half–saturation constant for ammonia (in milligrams of N per liter, mg/L), t is time (in hour, h). q_{max} and Ks were calculated using SigmaPlot version 11.0 (Sigmaplot, SYSTAT, Inc., USA). Under the presence of AgNPs or Ag^+ equation 3.2 can be modified to equation 3.3

$$q = \frac{(q_{max} /(1 + \frac{I}{K_i}))S}{K_s /(1 + \frac{I}{K_i}) + S} \quad (3.3)$$

Where Ki is inhibitory constant (in the unit of mg AgNPs per liter or mg Ag^+ per liter), i can be AgNPs or Ag^+. Level of toxicity of a substance to a target microorganism can be indicated by a Ki value. A higher toxicity level would have a lower Ki value. Ki was calculated by using Enzyme Kinetic Modules incorporated in the SigmaPlot version 11.0 (Sigmaplot, SYSTAT, Inc., USA).

3.8 Inhibition calculation

The percentage of inhibition of AO activity was calculated based on equation 3.4 which compared rates of AO in the controls and in the AgNPs or Ag^+ treatments.

$$\text{Inhibition } (\%) = \frac{(q_c - q_i)\, x\, 100}{q_c} \qquad (3.4)$$

where q_c is NH_4^+–N oxidation rates in the controls (in milligrams of N per liter per hour, mg N/L/h), q_i is the NH_4^+–N oxidation rate under presence of AgNPs or Ag^+ (in milligrams of N per liter per hour, mg N/L/h).

3.9 Data analysis

For the experiments conducted in triplicate the mean ± standard deviation (SD) values were presented in which mean was calculated by averaging the values from at least three replications of inhibitory kinetic data or from 10 CLSM-images of live/dead assays or 22-FISH-images. One-way analysis of variance (ANOVA) was used to test the significant differences among the treatments. Tests were considered significantly different at $p < 0.05$. Ducan test was further applied to consider the difference among the being tested treatments [153]. Statistical analyses were performed by using IBM SPSS statistics for Windows, Version 19.0 (IBM Corp., Armonk, NY, USA).

Chapter 4 Comparative Inhibition of Silver Nanoparticles and Silver Ions on Ammonia Oxidation of Nitrifying Sludges

4.1 Introduction

Nanoparticle has the size between 1 nm and 100 nm and silver nanoparticles (AgNPs) whose particles made from silver. Silver nanoparticles exhibit much better physical, chemical and biological characteristics than metal silver because of extremely small sizes and high surface area per unit mass. These characteristics make AgNPs a highly effective antimicrobial agent [1]. Therefore, they have been used in many applications such as medical, food industry, household appliances, and textiles to prevent negative impact of harmful microorganisms [2]. In addition, AgNPs could also be used to coat on material to remove bacteria completely from supplied water, hence they are potentially used in water purification [37]. However, AgNPs have been released during consumption process. A study showed that approximately 300 tons of silver annually leached and ended up in worldwide environment [44]. In reality, silver has been globally detected in WWTPs [47] where they could release Ag ions (Ag^+) [6, 7], and interacted with active biomass causing concerns for microbial activity [48].

In WWTPs, ammonia oxidizing microorganisms are known as the most sensitive to environmental conditions and toxic substances including AgNPs and Ag^+ because of its inefficient growth rate and low yield [6]. Ammonia oxidation (AO) process plays a pivotal role in nitrification by aerobically oxidizing ammonia to nitrite. This process is crucial to nitrogen removal in WWTPs [14] and in aquatic environment [154]. Occurrence of AgNPs and Ag^+ in WWTPs might adversely harm to AO and consequently reduce quality of effluent water discharged from wastewater treatment

facilities. Several studies have focused on studying toxicity of AgNPs [7, 64] on AO or nitrification activity. However, no study was conducted to examine influence of AgNPs and Ag^+ on AO from nitrifying sludges enriched with different levels of ammonium (NH_4^+–N). Low and high NH_4^+–N levels could represent for different NH_4^+–N influents received by various WWTPs such as municipal and industrial. Also, possible predictions can be made to measure negative effects of AgNPs and Ag^+ on AO in these systems. To fulfil the gap, this study investigated inhibitory effect of AgNPs and Ag^+ on AO from low and high NH_4^+–N enriched nitrifying sludges.

4.2 Methodology

4.2.1 Experimental setup

The inhibitory kinetics experiments were performed in experimental flasks. The final clean cells concentration in each experimenting flask in all experiments was equal at 50 mg/L as mixed liquored suspended solids (MLSS). The initial AgNPs concentrations of 1, 10 and 100 mg/L and Ag^+ concentrations of 0.05, 0.10 and 0.50 mg/L were used for the inhibitory tests with both nitrifying sludges. All inhibitory kinetics experiments were conducted in batch mode, in aerated condition, at room temperature, and at neutral pH. Five mililiter of aqueous samples were periodically collected for analysis of ammonium and nitrate. Ammonium consumption was quantified using Salicylate–hypochlorite method [151], whereas the nitrite (NO_2^-–N) plus NO_3^-–N addressed by total NO_2^-–N was measured by colorimetric method 4500 [152] after NO_3^-–N in aqueous samples were converted to NO_2^-–N by using vanadium chloride (VCl_3, 0.8 g in 100 ml HCl 1M). In this chapter, only inhibitory kinetics between NAS 0.5 mM and NAS 30 mM was discussed.

4.2.2 Live/dead cells observation of the two nitrifying cultures

The live and dead cells of nitrifying sludge cultures taken from the enriching reactors were determined using a staining kit (LIVE/DEAD® BacLight™ Bacterial Viability, Molecular Probes, Invitrogen) and observed under CLSM (FluoView FV10i, Olympus, Japan). Live and dead cells were investigated by staining cells with an appropriate mixture of the SYTO 9 and propidium iodide (PI) stains according to the manufacturer's protocol as described in Chapter 3. All bacterial cells were stained with fluorescent green from SYTO 9 whereas dead cells (damaged cells) were only stained with fluorescent red from PI. The presence of dead cells would reduce the emission of fluorescent green. The autoclaved nitrifying sludge was used as a positive control for the dead cells. The excitation/emission maxima for SYTO 9 and PI stains were 480/500 nm and 490/635 nm, respectively. Twenty two images from CLSM of each sample were used for calculation of the areas of live and dead cells using the software ImageJ (ImageJ 1.4.3.67, Broken Symmetry Software).

4.3 Results and discussion

4.3.1 Silver nanoparticles characterization

Characterization of AgNPs using transmission electron microscopy indicated that the starch-coated AgNPs had the spherical shapes (Figure 4-1) and the size of AgNPs in the range of 2-12 nm accounted for 91.4%, whereas size from 12-30 nm only took 8.6% (Figure 4-2).

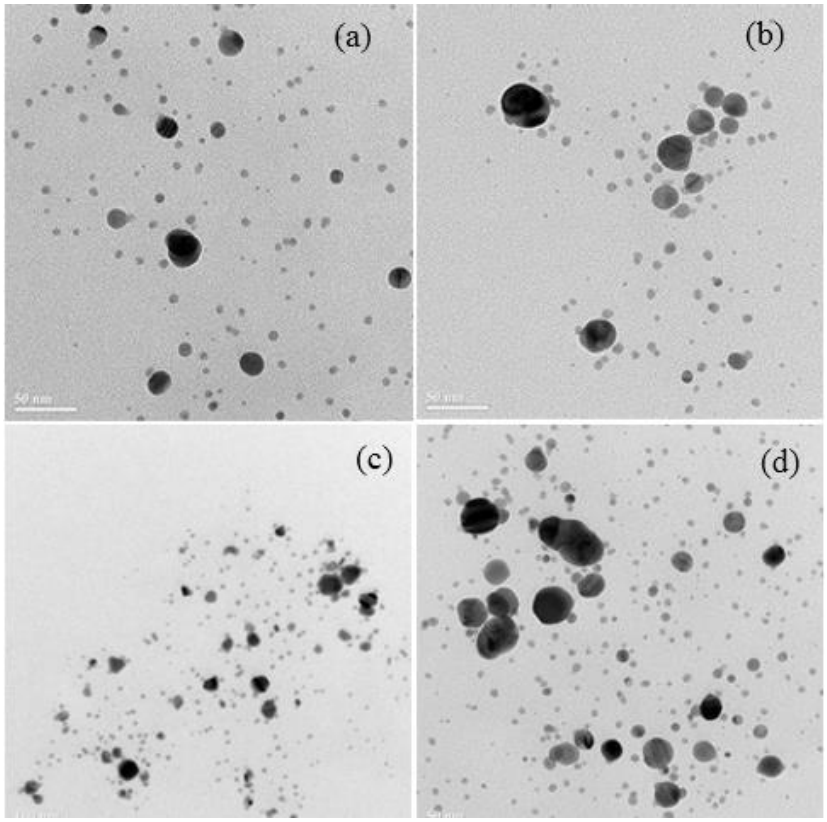

Figure 4-1 TEM images of the AgNPs of 10 mg/L

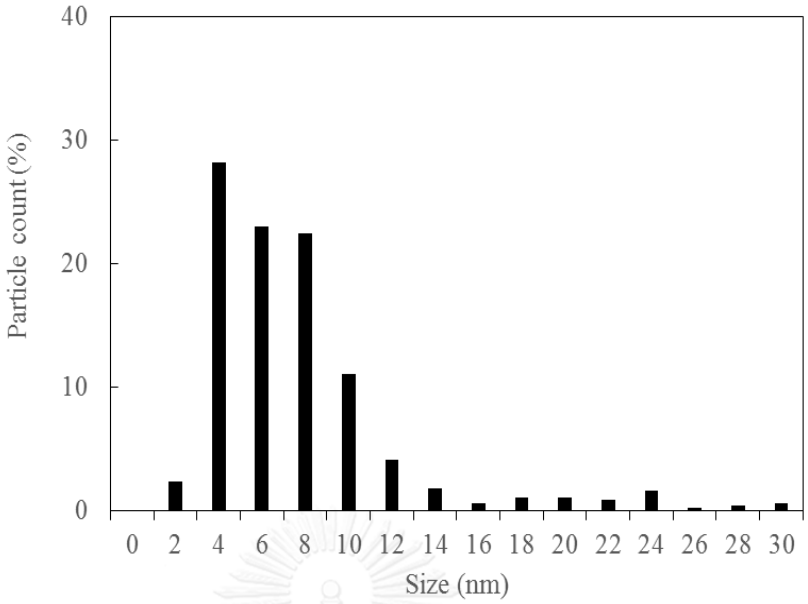

Figure 4-2 Size distribution of AgNPs

Silver nanoparticles have its own localized surface plasmon resonance (LSPR) and size of AgNPs is scanned by using spectrophotometry in the range of wavelength of 250 to 700 nm. Different sizes of AgNPs would have peak at different wavelengths. Sizes of AgNPs ranged from 25-50 nm would have absorption peaks between wavelengths of 390-420 nm [155]. Increasing size of AgNPs leads to increase of the wavelengths of the surface plasmon resonance, for example AgNPs of the sizes from 65-85 nm would have the peak at approximately 440 nm [156]. In this study, AgNPs peaked at wavelength of 400 nm. Silver nanoparticles in the well-dispersed form or non-agglomerated form has a maximum absorbance (λ_{max}) at near 400 nm [157, 158]. Figure 4-3 also indicated that AgNPs used in this study was well dispersed in the SWW. Non-aggregated form of AgNPs could enhance toxicity of AgNPs since they have more chance to contact on microorganisms and release more silver ions [6].

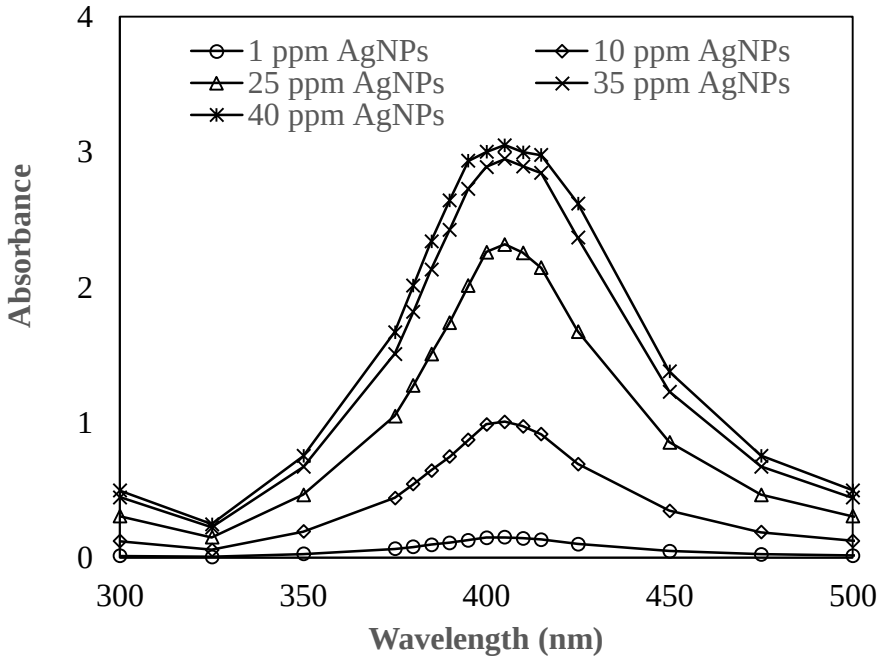

Figure 4-3 Absorbance of AgNPs at 1 – 40 mg/L.

Previous study found that surface plasmon resonance of AgNPs was affected by the shape of AgNPs [159]. A relationship between shape of AgNPs and absorption peaks was established. Silver nanoparticles in triangular would peak at wavelength of about 625 nm whereas AgNPs in spherical shape was peaked at lower wavelength, for example at 450 nm. In this study, the AgNPs has spherical shape showed UV absorption peak at lower wavelength of 400 nm (Figure 4-3). Previous studies found that AgNPs in spherical shape exhibited higher toxicity compared to rod-shaped paricles but exhibited lower toxicity than truncated-shaped [52].

4.3.2 Kinetics of ammonia oxidation in control conditions

The kinetics of AO without silver species were presented in Table 4-1**.**

Table 4-1 Kinetics parameters for inhibitory effect of AgNPs and Ag^+

Types of NAS	Silver (mg/L)	Ks (mg/L)	q_{max} (mg/L/h)	R-squared
	AgNPs			
0.5 mM				
	0	3.13	0.3608	0.92
	1	-	0.1214	0.69
	10	-	0.0475	0.37
	100	-	0.0363	0.46
30 mM				
	0	13.48	0.6982	0.85
	1	5.75	0.2962	0.80
	10	3.72	0.1850	0.85
	100	-	0.1128	0.46
	Ag ions			
0.5 mM				
	0.00	2.27	0.7548	0.98
	0.05	-	0.4842	0.86
	0.10	-	0.2923	0.76
	0.50	-	0.2641	0.76
30 mM				
	0.00	17.83	0.6379	0.93
	0.05	7.28	0.2492	0.67
	0.10	4.98	0.0901	0.29
	0.50	4.76	0.0175	0.25
	5.00	-	0.0176	0.43

The kinetics experiment without addition of AgNPs or Ag^+ showed that ammonia oxidizing microbes (AOM) in NAS 0.5 mM exhibited the characteristic of high affinity to ammonia (Ks= 2.27- 3.13 mg/L). In contrast, AOM in NAS 30 mM showed low affinity to ammonia with a high Ks values (13.49 – 17.83 mg/L). The value of Ks from NAS 30 mM was higher than that from NAS 0.5 mM indicating that community of ammonia oxidizing microbes in the two nitrifying cultures were

different. Lower Ks value means ammonia oxidizers have higher affinity to ammonia, whereas higher Ks value indicates ammonia oxidizers have lower affinity to ammonia.

Nitrifying cultures enriched at low and high NH_4^+–N resulted in different species of ammonia oxidizing bacteria (AOB) with distinct Ks values. For instance, *Nitrosomonas oligotropha* has Ks values of 0.42–1.05 mg/L [160], whereas *Nitrosomonas europaea* has Ks values of 12.3–27.4 mg/L. In low NH_4^+–N environment, the dominant AOB species were *N. oligotropha*, whereas in high NH_4^+–N condition the dominant AOB species were *N. europaea* [14]. The ammonia oxidizing microbes with low Ks values often abundantly occurred in municipal WWTPs, whereas the ones with high Ks values frequently appeared in industrial WWTPs [14]. In this study, it could imply that NAS 0.5 mM containing ammonia oxidizers which were commonly found in municipal WWTPs, whereas NAS 30 mM having ammonia oxidizers which were often detected in industrial WWTPs.

4.3.3 Inhibitory kinetics of ammonia oxidation influenced by AgNPs

The results from Figure 4-4 indicated that addition of AgNPs into NAS 0.5 mM and NAS 30 mM caused adverse inhibition on AO activity. Ammonia oxidation activity in NAS 0.5 mM was almost completely inhibited (Figure 4-4a), whereas it was partially suppressed in NAS 30 mM (Figure 4-4b). Half–saturation constants (Ks) at different AgNPs concentrations in NAS 0.5 mM could not be estimated because AgNPs exhibited highly toxic to this culture. Monod curves turned into linear lines and the Monod equation is not valid to predict Ks values. In the case of NAS 30 mM, AgNPs only partially inhibited AO, Monod kinetics parameters including Ks and q_{max} were

successfully calculated and they were found decrease when AgNPs concentration increased (Table 4-1).

The negative influence of AgNPs on AO from the both nitrifying cultures was concentration dependent. Higher AgNPs resulted in higher inhibitive effect. AgNPs at 1, 10, and 100 mg/L inhibited AO activity in NAS 0.5 mM and NAS 30 mM by 90.6 ± 8.6%, 91.6 ± 7.2%, 94.8 ± 4.3% and 50.5 ± 9.48%, 63.3 ± 7.9%, and 76.8 ± 5.8%, respectively (Figure 4-5). It was clearly showed that toxicity of AgNPs on AO in NAS 0.5 mM was higher than that in NAS 30 mM.

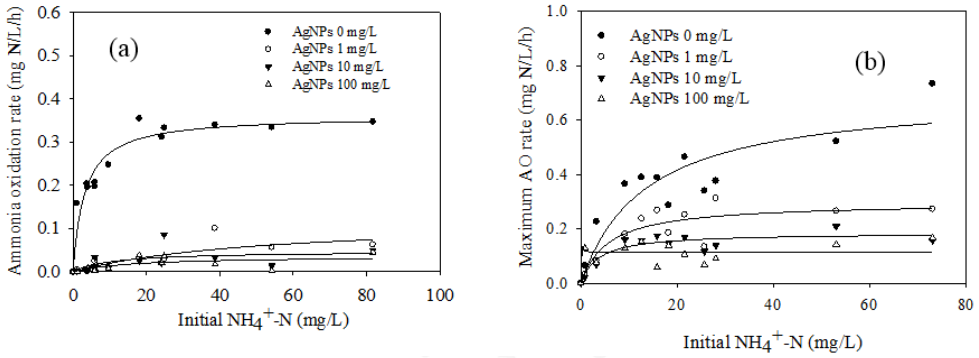

Figure 4-4 Kinetics of AO from NAS 0.5 mM (a) and NAS 30 mM (b) influenced by AgNPs

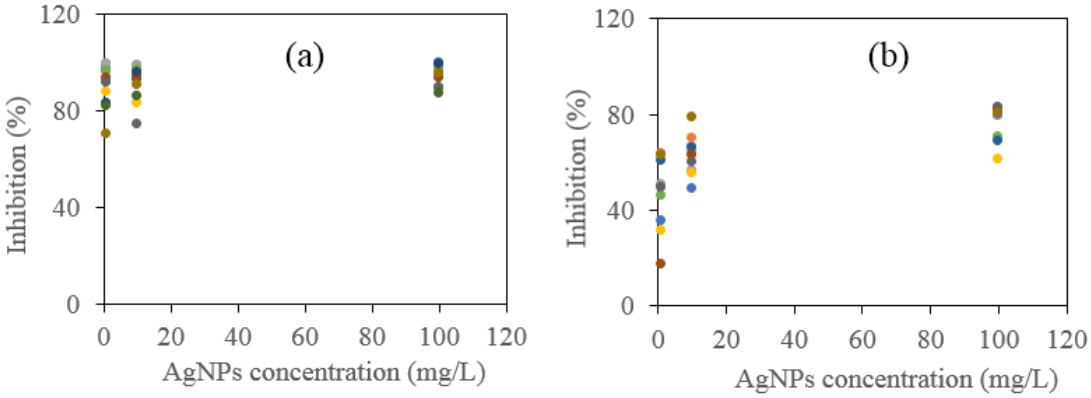

Figure 4-5 Inhibition of AgNPs on AO from NAS 0.5 mM (a) and NAS 30 mM (b) at different initial ammonium concentrations.

4.3.4 Inhibitory kinetics of ammonia oxidation influenced by Ag^+

For NAS 0.5 mM, the amendment of Ag^+ into the nitrifying culture sharply reduced q_{max} (Figure 4-6a). The values of q_{max} were reduced when Ag^+ concentration increased (Table 4-1) indicating that inhibition of Ag^+ on AO from this culture was also concentration-dependent. Figure 4-7a showed that AO in NAS 0.5 mM almost reach full inhibition by 86.3 ± 0.8%, 89.1 ± 0.7% and 93.4 ± 1.2% at Ag^+ concentrations of 0.05, 0.10, and 0.50 mg/L, respectively.

For NAS 30 mM, supplement of Ag^+ drastically reduced AO_{max} but Ag^+ did not completely stop AO (Figure 4-6b). Figure 4-7b presented that AO in NAS 30 mM was suppressed by 52.7 ± 2.1% - 96.2 ± 1.3% at Ag^+ concentration at 0.05–0.50 mg/L. Due to partial inhibition, values of Ks were estimated. The values of Ks and q_{max} decreased when Ag^+ concentration increased (Table 4-1).

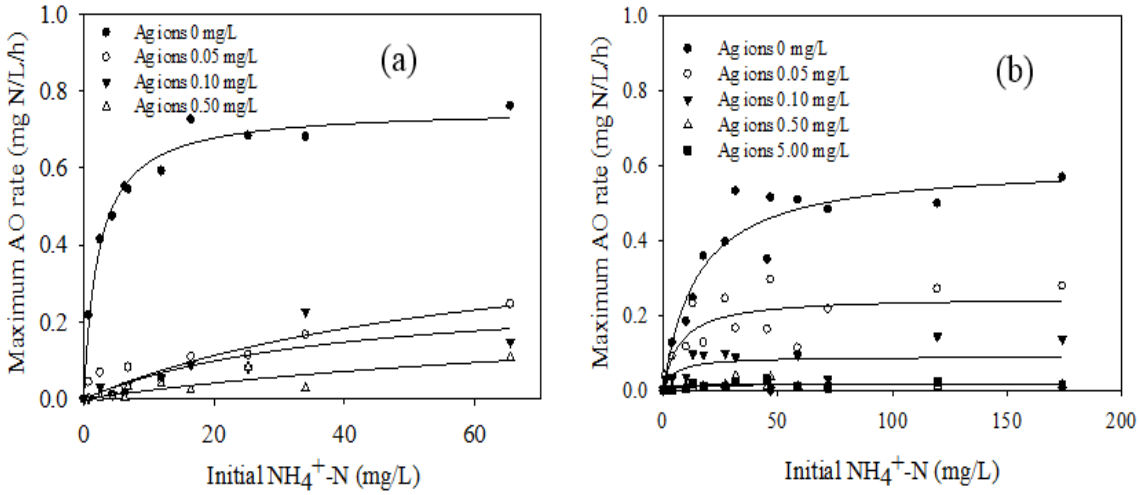

Figure 4-6 Kinetics of AO from NAS 0.5 mM (a) and NAS 30 mM (b) influenced by Ag^+

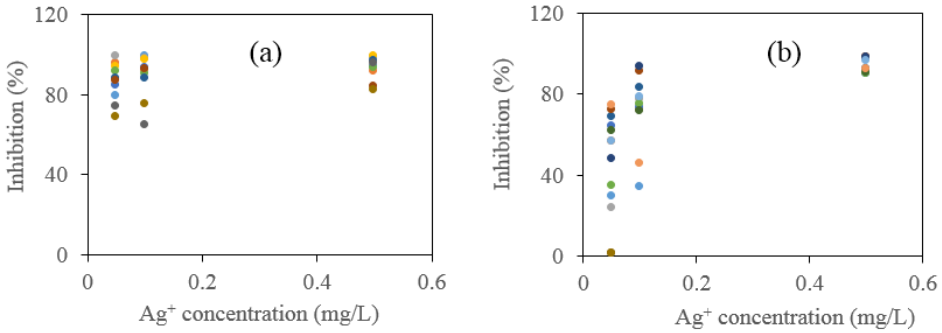

Figure 4-7 Inhibition of Ag^+ on AO from NAS 0.5 mM (a) and NAS 30 mM (b) at different initial ammonium concentrations.

4.3.5 Comparison inhibitory effect of AgNPs and Ag^+

In this study, the inhibitory effects of AgNPs and Ag^+ were examined with two nitrifying cultures including NAS 0.5 mM and NAS 30 mM. Toxicity of Ag^+ on AO activity from NAS 0.5 mM and NAS 30 mM was higher than that of AgNPs. For example, it was found that AgNPs at 1 mg/L inhibited AO activity by 90.6 ± 8.6% and 44.9 ± 2.4%, whereas Ag^+ at 0.05 mg/L (20 times lower than concentration of AgNPs at 1 mg/L) suppressed 86.3 ± 0.80 and 52.7 ± 2.1% from NAS 0.5 mM and NAS 30 mM, respectively.

Both AgNPs and Ag^+ showed more adverse impact on AO activity from NAS 0.5 mM than from NAS 30 mM for several reasons. Firstly, AgNPs and Ag^+ exhibited more negative influence on NAS 0.5 mM due to the level of AO activity. The AO activity in NAS 30 mM was higher than that in NAS 0.5 mM (Table 4-1) because NAS 0.5 mM was enriched with long SRT. This study found that dead cells in NAS 0.5 mM and NAS 30 mM were 41.4 ± 18.1 - 67.9 ± 12.2% and 7.3 ± 5.3% - 10.7 ± 6.9%,

respectively (Figure 4-8). An example of live and dead cells in NAS 0.5 mM and NAS 30 mM was given in Figure 4-9 which clearly indicated higher dead cells (in red color) in NAS 0.5 mM than in NAS 30 mM. The higher dead cells observed from NAS 0.5 mM could be the reason lead to lower AO activity. Former study also found that enrichment using long SRT could reduce nitrification due to partial inactivation of biomass [127].

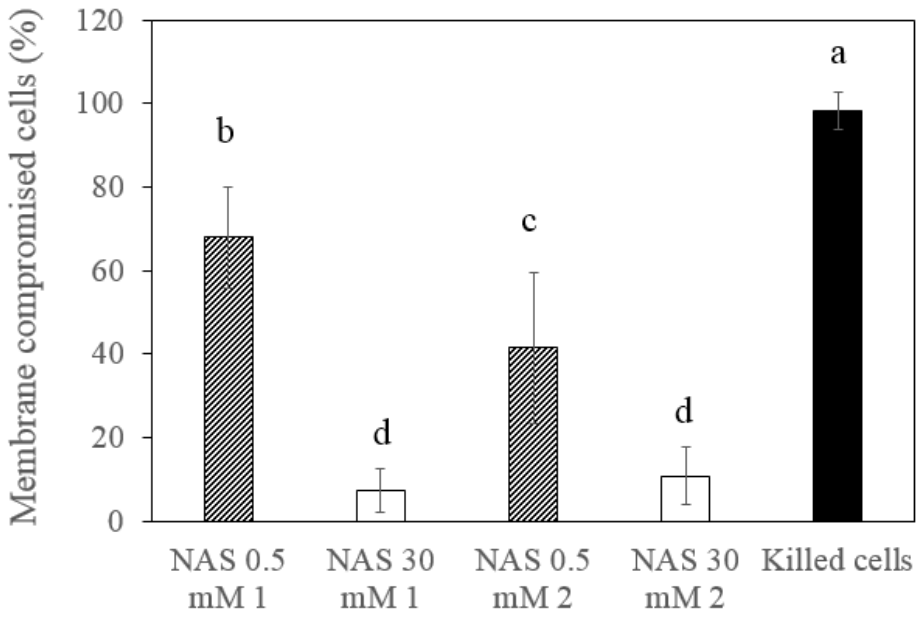

Figure 4-8 Percentage of membrane compromised cells estimated from NAS 0.5 mM and NAS 30 mM.

The samples were collected directly from the reactors. Error bars show standard deviation. Different letters indicate statistically significant ($p < 0.05$). NAS 0.5 mM 1 and NAS 30 mM 1 were collected on 22-9-2016 and NAS 0.5 mM 2 and NAS 30 mM 2 were collected on 7-10-2016. The letter a-d indicates the membrane damaged from the highest level to the lowest one.

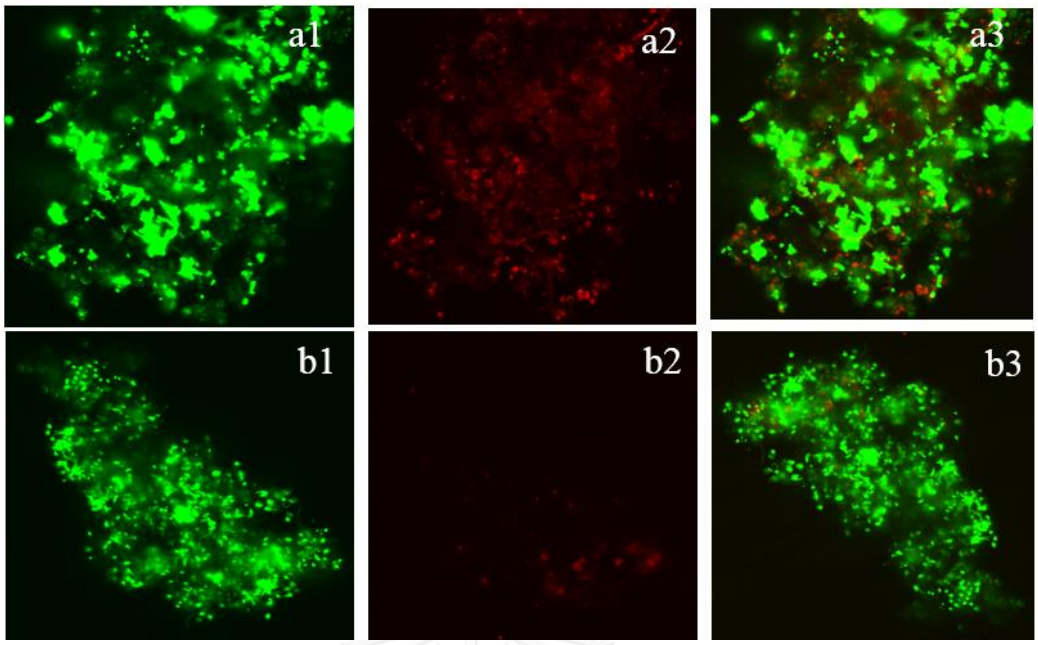

Figure 4-9 CLSM-images of membrane integrity of NAS 0.5 mM and NAS 30 mM.

It was noted that a1, a2 and a3 showing the total cells (comprise of live and dead cells), dead cells and overlay of total and dead cells for NAS 0.5 mM; b1, b2, and b3 showing the total cells, dead cells and overlay of total and dead cells for NAS 30 mM.

Secondly, the physical structure of the sludge containing nitrifying cells collected from NAS 30 mM were in larger size and more in cluster forms while those harvested from NAS 0.5 mM were more in separated forms (Figure 4-9). The aggregated forms of microbes in NAS 30 mM could probably help them more resistant to AgNPs than NAS 0.5 mM. This possibly supported the explanation that why the inhibitory effect of AgNPs on AO from NAS 30 mM was less than those from NAS 0.5 mM because part of nitrifying cells from NAS 30 mM was less exposed to AgNPs and Ag^{+} than from NAS 0.5 mM. Prior study found that *N. europaea* biofilms could tolerate higher concentrations of both Ag^{+} and AgNPs [161]. The protection mechanism may come from mass-transfer limitations as proposed in the prior study [162]. Thirdly,

community of ammonia oxidizers in the two cultures were different thus resulting different tolerance to AgNPs and Ag^+. Former researcher revealed that the toxicity of AgNPs and Ag^+ on target microorganisms are species-specific [64, 163]. It was previously reported that nitrification potential rate was inhibited differently because of difference in species of AOB [64]. More specifically, uncapped AgNPs at concentration of 0.5 mg/L adversely reduced activity of *N. europaea*, whereas uninhibited activity of *N. multiformis*. The difference in inhibitive effect was potentially come from the disparity in physiological characteristics of the two ammonia oxidizers [64]. Communities of ammonia oxidizers in the two nitrifying cultures were different thus resulting in their various tolerance to AgNPs. In this study, the values of Ks could indicate that AOB in the two nitrifying cultures were not the same. Fourthly, the variation of toxicity effect of AgNPs and Ag^+ on ammonia oxidation from the nitrifying cultures could be resulted from difference in duration of enrichment that could subsequently lead to various proportion of ammonia oxidizers in the two cultures.

In addition to the above mentioned reasons, previous study suggested that extracellular polymeric substances (EPS, is made of polysaccharides, proteins, phospholipids, humic substances and nucleic acids.) produced from bacteria could reduce toxicity of AgNPs and Ag^+ via reduction of Ag^+ to AgNPs by the hemiacetal groups of sugars in EPS [164]. The other study reported that EPS could result in increasing size of AgNPs thus reducing toxicity of AgNPs [158]. Removal of EPS could make bacteria more sensitive to AgNPs [158, 165]. In this study, the more cluster of microbes in NAS 30 mM could be due to EPS. EPS could play role in different toxicity impact of AgNPs and Ag^+ on ammonia oxidation activity. Future study should

investigate role of EPS in relation of toxicity of AgNPs and Ag^+ on the nitrifying cultures. In addition, further research should be extended to examine toxicity impact of AgNPs and Ag^+ on individual groups of nitrifying bacteria who complete nitrification process.

The present study found that Ag^+ were much more toxic on AO activity than that of AgNPs. The kinetics experiments using NAS 30 mM and NAS 0.5 mM showed that the obtained K_i values supported the evidence that Ag^+ were more toxic to AO activity. It was found that K_i of Ag^+ was 0.29 mg/L and 0.17 mg/L, whereas K_i for AgNPs was estimated to be high of 73.5 mg/L and 3.37 mg/L, for NAS 30 mM and NAS 0.5 mM, respectively. Silver nanoparticles and Ag^+ were highly toxic to AO activity from NAS 0.5 mM since values of K_i were much lower than those estimated for NAS 30 mM indicating AgNPs and Ag^+ were more toxic to AO activity from NAS 0.5 mM than that from NAS 30 mM. Several literature also found that Ag+ was adversely toxic to ammonia oxidation/nitrification. For example, Ag^+ at 0.05 mg/L inhibited nitrification of *N. europaea* by approximate 20% [161, 166], at 0.10 mg/L inhibited 75% [166] and at 0.25 mg/L inhibited more than 90% [6, 161, 166]. The inhibitory effect of Ag^+ on AO found in the present study was higher or comparative to those in the reported findings. Moreover, several former studies also demonstrated that the toxicity of Ag^+ was higher than AgNPs to several types of microorganisms

Study on inhibitory kinetics of AO activity influenced by AgNPs and Ag^+ is still limited. Only our previous finding found that the K_i value of AgNPs on AO process of the enriched NAS 5 mM was 5.5 mg/L [167]. This estimated value was significantly higher than K_i values of Ag^+ in the two cultures and the K_i value of AgNPs with NAS

0.5 mM. However, it was much lower than K_i value of AgNPs (73.5 mg/L) with NAS 30 mM. The current and former results of K_i values revealed that nitrifying activated sludge enriched using higher NH_4^+-N concentration could better tolerate to toxicity of AgNPs. The better tolerance to toxicity of AgNPs could relate to abundance and community of ammonia oxidizers in each NAS. In addition, the difference in estimated K_i for AgNPs between the previous and the current study could be attributed to disparity in experimental conditions. Firstly, previous study used indirect parameter such as oxygen uptake rate (OUR) in which DO was measured, whereas this study used direct parameter such as NH_4^+-N to estimate K_i value. Secondly, the ammonia oxidizing cultures were not the same resulting in different levels of AO activity due to different in proportion and community of ammonia oxidizers, for example, in the previous study the culture was enriched at 5 mM of NH_4^+-N, whereas in this study the cultures were enriched at 0.5 mM and 30 mM of NH_4^+-N. Furthermore, the difference in characteristics of AgNPs such as size, shape, coating agents also influence on toxicity of AgNPs. Estimated K_i values varied depending on several factors, however, inhibitory constant K_i values of AgNPs and Ag^+ found in the present study clearly indicated that both AgNPs and Ag^+ were very toxic to AO activity and Ag^+ were more toxic to AO activity than that of AgNPs. The toxicity effect of AgNPs and Ag^+ on ammonia oxidation in nitrifying sludge was concentration dependent.

Size of AgNPs contributed to magnitude of toxicity of AgNPs. Previous study found that AgNPs concentration from 1-100 mg/L inhibited AO by 21-25% [7] which was lower compared to the current study. This happened could be because the AgNPs

used in the previous study having larger size (50 nm) than the current study (2-12 nm). The prior study also reported that AgNPs with smaller size could release more Ag^+ [55].

Coating also effects on toxicity of AgNPs through influencing on dissolution of AgNPs. There were less Ag^+ liberated from coated AgNPs than the uncoated ones [6]. Toxicity of AgNPs coated with citrate, gum arabic, and polyvinylpyrrolidone influenced differently on AO of *N. europaea*. At 2 mg/L, citrate, gum arabic, and polyvinylpyrrolidone AgNPs inhibited AO by 91.4 ± 0.2%, 67.9 ± 3.6%, and 29.5 ± 9.4%, respectively [6] while AgNPs (at 1 mg/L, starch coated-AgNPs) suppressed AO by 90.6 ± 8.6% and 44.9 ± 2.4% for NAS 0.5 mM and NAS 30 mM. However, it should be noted that the difference in inhibition of AO could be attributed to variation in experimental conditions such as composition of SWW, types of nitrifying cultures.

This study found that AO was very sensitive to AgNPs which was agreed with the previous study reported that nitrifiers were very susceptible to toxicity of AgNP due to functional enzyme (AMO) located near surface of cell membrane and AgNPs tended to interact with cell membrane [6]. Therefore, it was previously reported that ammonia oxidizers were more sensitive to AgNPs than nitrite oxidizers and heterotrophic microorganism [8]. Due to high sensitivity to toxic chemicals, ammonia oxidation activity was used as indicator of impact of contaminants on nitrification and therefore treatment failure [168].

The toxicity of AgNPs vary according to several factors such as sizes and coatings, the result of this study enhances understanding regarding to toxicity of AgNPs with different characteristics on ammonia oxidation activity.

4.3.6 Inhibition model of AgNPs and Ag^+

The models of inhibition are often used in studying enzymatic activity and Michaelis-Menten equation is used for prediction of the inhibition types. Michaelis-Menten equation is similar to Monod equation but the former is often used for enzymatic activity whereas the later is used for whole cell study. These equations are both described by a rectangular hyperbolic relation between enzyme or whole cell and substrate. The rate of substrate utilization is increased linearly (first-order kinetics) when the substrate concentration is low. In contrast, the rate of substrate consumption will reach maximum and remained unchanged (zero-order kinetics) when substrate concentration is increased to high level. There are three basic types of inhibition models in enzyme kinetics study. They are competitive, uncompetitive, and non–competitive inhibition, which are identified by observing change of half-saturation constant (Ks) and velocity on substrate (V_{max}) values in enzymatic study. This principle was applied in the current study to predict inhibition type because it is well known that ammonia oxidation process is the conversion of ammonia (substrate) to nitrite in aerobic condition. This conversion process involved functional enzymes ammonia monooxygenase (AMO) and hydroxylamine oxidoreductase (HAO) found in most ammonia-oxidizing microbes. Prediction of inhibition models was possible to perform in this study because the ammonia oxidation activity occurred due to the activation of functional enzymes in ammonia-oxidizing microbes under NH_3 presence. Under the presence of toxic substances such as AgNPs and Ag^+, the activity of ammonia oxidation could be partially or fully inhibited due to cell death leading to inactivation of functional enzymes. In addition, this study used whole cells of ammonia oxidizers so Monod equation was used to present the relationship between ammonia oxidation activity and

the substrate (NH_3). In reality, Monod equation was previously used in the study of ammonia oxidation kinetics [149]. In the present study, the inhibition type of AgNPs and Ag^+ was predicted based on the changing of apparent q_{max} (maximum ammonia oxidation rates under presence of AgNPs or Ag^+) and Ks values in AO process.

For NAS 30 mM, supplement of AgNPs and Ag^+ drastically reduced q_{max} but these toxic substances did not completely stop AO. Ammonia oxidation activity in NAS 30 mM was only partially suppressed by AgNPs and Ag^+. Due to partial inhibition, values of Ks were estimated as indicated in Table 4-1. Monod kinetics parameters Ks and q_{max} showed that the inhibitory effect of AgNPs and Ag^+ on AO activity from NAS 30 mM followed uncompetitive–like model because both Ks and q_{max} decreased when concentrations of AgNPs and Ag^+ increased. The same inhibitory model for AgNPs and Ag^+ could imply that these two toxic substances exhibited similar mechanisms of causing toxicity effect on AO process. Previous study found that AgNPs inhibited AO process best described by uncompetitive–like model [167] which is similar to the prediction in this current study. The inhibition type of AgNPs and Ag^+ on AO from NAS 30 mM could imply that the presence of AgNPs and Ag^+ resulted in partial inactivation of functional enzymes in ammonia-oxidizing microbes. Prior study found that the heavy metals such as Ni^{2+}, Co^{2+}, Cr^{6+} showing the inhibition model of non-competitive [169] but AgNPs and Ag^+ were found to be un-completive-like models.

For NAS 0.5 mM, the amendment of AgNPs and Ag^+ into the nitrifying culture sharply reduced q_{max} (Table 4-1). This study found that when AgNPs and Ag^+ almost completely suppressed AO, the Monod curves became straight lines, thus, Monod equation cannot be applied to predict Ks values. Inhibition data supported this

discussion. It was clearly showed that AO in NAS 0.5 mM almost reached full inhibition by 90.6 ± 8.6% – 94.8 ± 4.3% and 86.3 ± 0.8% - 93.4 ± 1.2% at AgNPs of 1-100 mg/L and Ag^+ of 0.05- 0.50 mg/L, respectively. From the discussion, it can be concluded that Monod equation can be used to estimate Ks values only when AgNPs or Ag^+ partially inhibited AO.

An attempt was made to predict inhibition model for the inhibitory effect of AgNPs and Ag^+ on AO activity from NAS 0.5 mM. However, it was not well predicted the model for the effect of AgNPs and Ag^+ on AO activity from NAS 0.5 mM since AO activity was almost totally inhibited when AgNPs and Ag^+ were amended to this culture. However, it could be highly possible that type of inhibition of AgNPs and Ag^+ on AO from NAS 0.5 mM was similar to that of NAS 30 mM since the inhibition model for AgNPs and Ag^+ predicted on NAS 5 mM [167] and NAS 30 mM in the current study was the same. However, for NAS 0.5 mM the presence of AgNPs and Ag^+ could possibly fully inactivate functional enzymes of ammonia-oxidizing microbes.

4.4 Summary

Toxicity effect of AgNPs and Ag^+ on AO activity from NAS 0.5 mM and NAS 30 mM was investigated. Values of Ks obtained from the two nitrifying cultures indicated that NAS 0.5 mM were dominated by oligotrophic ammonia oxidizing microbes, whereas eutrophic ammonia oxidizers were dominant in NAS 30 mM. The experimental results showed that AgNPs and Ag^+ exhibited high toxicity to AO from the two nitrifying sludges. Silver ion from 0.05 to 0.50 mg/L inhibited AO by 52.7 ± 2.1% – 93.9 ± 1.9% and 86.3 ± 0.8% – 93.4 ± 1.24% for NAS 0.5 mM and NAS 30 mM, respectively, whereas AgNPs at 1–100 mg/L suppressed AO from NAS 0.5 mM

and NAS 30 mM by 90.6 ± 8.6% – 94.8 ± 4.3% and 45.7 ± 14.3% –75.8 ± 7.6%, respectively.

The experimental results indicated that both AgNPs and Ag^+ exhibited extremely high toxicity to AO activity for the examining cultures. Ammonia oxidizing activity from NAS 0.5 mM was more adversely impacted by AgNPs and Ag^+. The study demonstrated that both AgNPs and Ag^+ were highly toxic to AO activity, especially for ammonia oxidizers with low Ks values implying that AO from municipal WWTPs could potentially suffer more devastating impact by AgNPs and Ag^+ than industrial WWTPs. Future studies should focus on the role of individual ammonia oxidizers under occurrence of AgNPs or Ag^+.

Chapter 5 Inhibitory Kinetics and Mechanism of Ammonia Oxidation Influenced by Silver Nanoparticles: Role of Silver Particles or Ions

5.1 Introduction

Silver nanoparticles (AgNPs) are extensively used in many consumer and medical products due to its high surface area and excellent antimicrobial activity [2]. With increasing production and use, AgNPs were expected to be washed out from consumer products and unavoidably occurred in wastewater treatment plants (WWTPs) [7-9]. It was reported that the amount of silver used in global textile and plastic industries annually released to wastewater treatment systems of 190-410 tons [5]. Recently, it was detected AgNPs of up to 1.9 µg/L in effluent of WWTPs [46]. Former studies reported that silver was detected ranging from 4 µg/L to 1 mg/L and 2 to 195 mg/L in influent concentration and biosolid concentration of WWTP, respectively [41-43].

Since silver is classified as a highly toxic, persistent, and accumulated chemical, the performance of WWTPs may be adversely impacted due to the interactions between AgNPs and activated sludge [7, 15]. Nitrification process is known as the most sensitive process in WWTPs. The nitrification process includes ammonia oxidation (AO) and nitrite oxidation reactions. This AO, which was the rate-limiting step of the process, was previously found susceptible to AgNPs [7, 170]. Silver speciation related to AgNPs included AgNPs themselves and released silver ions (Ag^+). During AgNP oxidation, reactive oxygen species (ROS) could be created [2, 10, 55]. Prior studies discovered that both AgNPs and Ag^+ clearly affected a wide range of organisms including nitrifying microbes [16, 62]. Among previous works, roles of AgNPs or the released

Ag^+ to overall toxicity of AgNPs suspension were found differently due to varying experimental conditions including tested conditions, types of AgNPs, and nitrifying cultures. This inconclusive phenomenon was inadequate to finalize environmental treatment technology and management.

The aim of this chapter was to understand influence of AgNPs and Ag^+ related to AgNPs on AO process. Inhibitory mechanism and kinetics of AO activity from nitrifying sludge influenced by AgNPs and Ag^+ were investigated. Observation of microbial cell physiology, community, and viability using microscopic techniques including scanning electron microscopy (SEM), transmission electron microscopy (TEM), and confocal laser scanning microscopy (CLSM) was carried out. The result from this study can be used as fundamental information of WWTP design and operation later on.

5.2 Methodology

5.2.1 Experimental setup

The inhibitory kinetics experiments under the presence of AgNPs and Ag^+ were performed. During the experiments with AgNPs, the Ag^+ release was monitored. The experiments with Ag^+ were then performed with the concentrations equal to the release.

The nitrifying sludge was harvested and centrifuged at 5,000 rpm for 20 min and the clear supernatant was removed to collect the settled cells. The collected cells were re–suspended in SWW and centrifuged to wash. The washing process was repeated for five times to obtain the cleaned cells, which were later used for the inhibitory kinetics tests. The ammonia oxidation kinetic experiments were carried out using 250–ml flask with an effective volume of 100 mL. The initial NH_4^+–N

concentrations were in the range of 0.85 to 73 mg/L and 0.9 to 260 mg/L for AgNPs and Ag^+ experiments, respectively. The final AgNP and Ag^+ concentrations were 1, 10, and 100 mg/L and 0.05, 0.10, 0.50 and 5.00 mg/L, respectively. It is noted that the concentrations of Ag^+ (0.05-5.00 mg/L) was selected based on released Ag^+ concentrations from AgNPs.

The final biomass concentration was 50 mg/L as mass liquored suspended solid (MLSS). All tests were conducted in triplicates at DO > 2 mg/L and room temperature (28–30 ^{0}C) in batch mode for 60 h period. The pH of the neutral range (7.5–7.8) was achieved using 30 mM of HEPES. The aqueous samples of 5 mL were collected periodically to measure reduction of NH_4^+–N and production of nitrate (NO_3^-–N). The NH_4^+–N concentration was measured by salicylate–hypochlorite method [151] whereas the nitrite (NO_2^-–N) plus NO_3^-–N addressed by total NO_2^-–N was measured by colorimetric method 4500 [152] after NO_3^-–N in aqueous samples were converted to NO_2^-–N by using vanadium chloride (VCl_3, 0.8 g in 100 ml HCl 1M). The data from the experiment were used to calculate the kinetic values and inhibition percentage.

5.2.2 Silver ion release monitoring

Silver ion release monitoring experiments were performed with the AgNP concentrations of 1, 10, and 100 mg/L and initial NH_4^+–N concentrations of 20 and 100 mg/L. The aqueous samples were collected at 0 , 30, and 60 h. Approximate 8 mL of each aqueous sample was transferred into an ultracentrifuge tube (16 × 57 mm, Beckman Coulter, Inc., USA) and tightly sealed. The prepared samples were placed in ultracentrifuge machine (Optima™ MAX-XP Ultracentrifuge, Beckman Coulter, Inc., USA) and centrifuged at 165,000 × g, 4ºC, for 2 h [21] using MLN-80 rotor (16 × 58 mm, Beckman Coulter, Inc., USA). The centrifuged samples were carefully taken out

and the supernatants were gently withdrawn using 10 ml sterile syringes and transferred to glass bottles. The supernatants were sent to analyze at the certified laboratory at the Scientific and Technology Research Equipment Center (STREC, Chulalongkorn University, Thailand) using Atomic Absorbance Spectrometry (AAS, Varian Model AA280FS, Australia). The measurement of total silver in the AAS was done using Air/Acetylene flame type with the air and acetylene flow rates of 13.6 L/min and 1.80 L/min, respectively. The absorbance of silver was detected at the wavelength of 328.1 nm for 4.5 s. The detection limit of AAS was 3 µg-Ag/L.

5.3.3 Preparation of samples for transmission electron microscopy

The NAS 30 mM samples of the control and of exposed to AgNPs and Ag^+ centrifuged at the rate of 5,000 rpm for five min at 4ºC to remove the supernatants. The obtained pellets were then washed with NaCl 0.85% for five times. The washed samples were fixed with a glutaraldehyde solution 2.5%. The fixed cells were washed in phosphate buffer and a 1 % osmium tetroxide solution. The cells were mixed with melt agar of 1.5 % to form gel at 45–50ºC. The hardened agars were cut into 0.5–mm cubes. The cubes with cells were dehydrated with a series of ethanol solutions from 35 to 95%. The dehydrated cubes were saturated in a series of propylene oxide and spur resin. Next, the cubes were baked at 70ºC from 8 to 10 h. The baked cubes were cut by an ultra-microtome. The pieces with a thickness of 60–90 nm were pasted onto copper grid and stained with uranyl acetate and lead citrate to increase the contrast. The prepared specimens were observed using transmission electron microscopy (TEM, JEOL, JEM–2100, Tokyo, Japan).

5.3.4 Preparation of samples for scanning electron microscopy

The NAS 30 mM samples of the control and of exposed to AgNPs and Ag^+ centrifuged at the rate of 5,000 rpm for five minutes at 4°C to remove the supernatants. The centrifuged samples were rinsed with phosphate buffer solution (PBS, 0.1 M, pH 7.4). The washed samples were fixed by using 0.1 M PBS with 4% glutaraldehyde overnight at 4°C. The fixed samples were separated in halves in liquid nitrogen, dehydrated using a series of ethanol solutions, placed on a stub, and covered with gold under vacuum condition. The prepared samples were examined using Scanning Electron Microscopy (SEM) with an energy–dispersive spectroscopy attachment (JEOL, JSM–5410LV, Tokyo, Japan). Elemental compositions of selected areas were analyzed using Energy Dispersive X–ray (EDX, Oxford Instruments, Model X–Max^N, UK) to identify forming aggregates of AgNPs.

5.3.5 Live/dead cells after exposing to AgNPs and Ag^+

The live and dead cells of NAS 30 mM culture after exposed to AgNPs and Ag^+ were studied using staining kit (LIVE/DEAD® BacLight™ Bacterial Viability, Molecular Probes, Invitrogen) and observing under confocal laser scanning microscopy (CLSM). Live and dead cells were investigated by staining cells with an appropriate mixture of the SYTO 9 and propidium iodide stains according to the manufacturer's protocol. Both live and death cells were stained with fluorescent green from SYTO 9, whereas dead cells (damaged membranes) were only stained with fluorescent red from propidium iodide. The presence of dead cells would reduce the emission of fluorescent green. Culture of NAS 30 mM was autoclaved at 121°C for 20 min and used as positive control. The excitation/emission maxima for SYTO 9 and propidium iodide stains were about 480/500 nm and 490/635 nm, respectively. Ten images from CLSM of each

sample were used for calculation of the areas of live and dead cells using the software ImageJ [7].

5.3.6 Fluorescent 16S rRNA targeted oligonucleotide probes and in situ hybridization

Two milliliter of mixed liquor suspended solids was fixed in a 4% paraformaldehyde solution for 12 h. Fixed samples were brought into hybridization by following which procedure described elsewhere [171]. In brief, 10 µl of 16S rRNA-targeted oligonucleotide probe (Table 5-1) in hybridization buffer, were added onto each spot of the samples on microscopic slide. The slides were hybridized at 46 ^{o}C for 2 h and washed at 48 ^{o}C for 15 min. Later, DNA of all microorganisms in the sample were stained with 0.9 µM DAPI for 15 min. The hybridized samples were then observed under CLSM (FluoView FV10i, Olympus, Japan). With a helping of image analysis software (ImageJ 1.4.3.67, Broken Symmetry Software), the 22 corresponding FISH-CLSM images were determined the percent abundance of target microbes in total microbes via estimating an area occupied by microbes being hybridized with the targeted probe per one occupied by DAPI-stained microbes.

Table 5-1 Oligonucleotide probes for analyzing microorganisms in NAS 30 mM

Probe	Sequence (5' to 3')	Label	Target organisms	Formamide (%)
Nso190	CGATCCCCTGCTTTTCTCC	AF	Many but not all ammonia oxidizing *β-Proteobacteria*	55
Ntspa662	GGAATTCCGCGCTCCTCT	Cy3	*Nitrospira* genus	35
Nit3	CCTGTGCTCCATGCTCCG	Cy3	*Nitrobacter* spp.	40

5.3 Results and discussion

5.3.1 Inhibitory kinetic and mechanism of ammonia oxidation

5.3.1.1 Ammonia oxidation kinetics influenced by AgNPs

The ammonia oxidation experiment with and without AgNPs was performed. All of the tests, ammonia concentrations depleted with respect to time. The rates of ammonia reduction were used to fit Monod model as shown in Figure 5-1. Addition of AgNPs resulted in a decrease in Ks and q_{max}. Addition of AgNPs concentration of 1, 10 and 100 mg/L resulted in a sharp decrease in half-saturation constants (Ks) and maximum ammonium oxidation rates (q_{max}). Maximum ammonium oxidation activity was reduced from 0.6982 mg N/L/h to 0.1128 mg N/L/h when AgNPs concentrations increased from 0-100 mg/L. Similarly, the values of Ks at AgNPs concentrations of 0, 1, and 10 mg/L were 13.49, 5.75, 3.72 mg/L respectively.

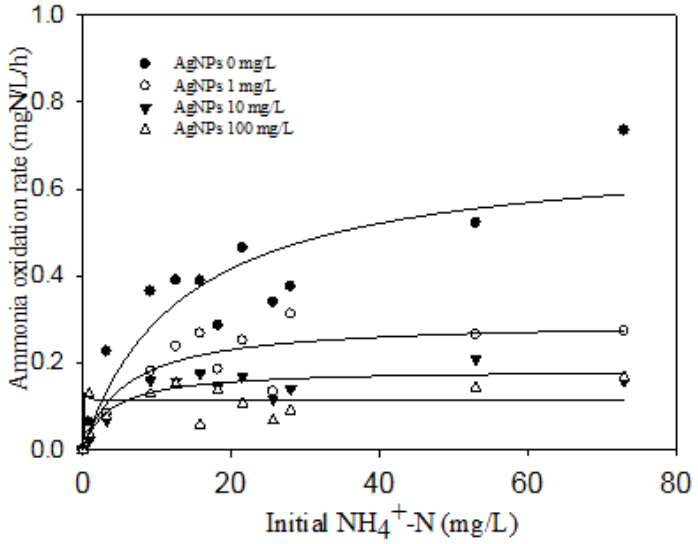

Figure 5-1 Kinetics of AO from NAS 30 mM by AgNPs

Ammonia oxidation activity was inhibited by 50.5 ± 9.48%, 63.3 ± 7.9%, and 76.8 ± 5.8% at AgNPs concentration of 1, 10, and 100 mg/L, respectively (Figure 5-2). Based on the result, it is clear that the initial AgNPs concentrations significantly affected the inhibitory magnitude ($p = 0.002$), which is in line with previous works [7, 167] that higher AgNP concentration resulted in more inhibition of AO. Giao et al. (2012) was performed the inhibition kinetics using nitrifying sludge taken from the reactor enriching nitrifiers using 5 mM NH_4^+-N while the nitrifying sludge using in this study was from 30 mM NH_4^+-N reactor. This indicate that with different nitrifying sludges higher AgNPs concentration similarly resulted in more inhibition of AO. However, up to this point, it could not conclude whether the inhibition was from AgNPs themselves or released Ag^+.

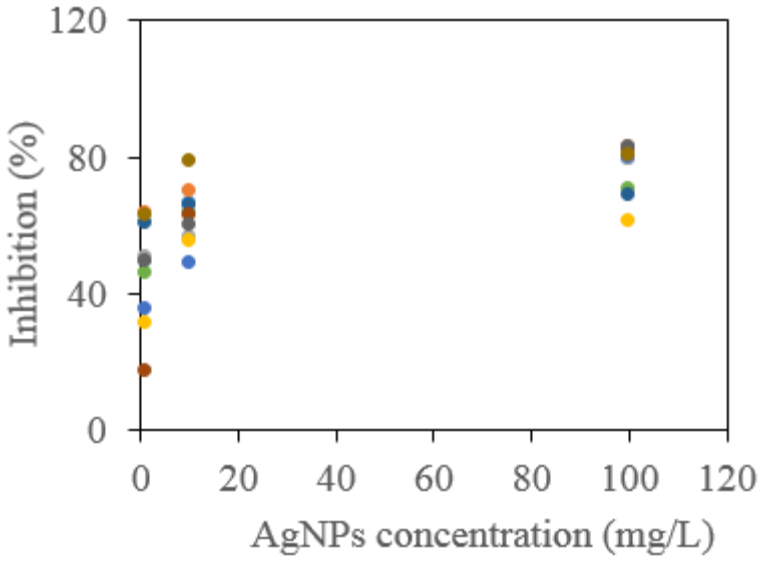

Figure 5-2 Percent inhibition of AO from NAS 30 mM by AgNPs

5.3.1.2 Ag ions release from AgNPs

Table 5-2 presented that there were more Ag^+ liberated at higher initial AgNPs concentrations.

Table 5-2 Concentration of silver ion release from AgNPs

Initial NH_4^+–N (mg/L)	Type of Medium	Initial AgNPs (mg/L)	Ag ion release from AgNPs (µg/L) Mean ± SD		
			0 h	30 h	60 h
0	SWW only	1	71.7 ± 7.6	80.0 ± 10.0	25.3 ± 0.6
0	SWW only	10	77.6 ± 10.0	232.9 ± 2.9	202.4 ± 32.1
0	SWW only	100	227.2 ± 15.3	750.9 ± 20.8	529.6 ± 10.4
20	SWW + NAS	1	4.0 ± 0.1	< DL	< DL
20	SWW + NAS	10	< DL	< DL	12.8 ± 7.5
20	SWW + NAS	100	180.9 ± 15.3	280.2 ± 36.1	211.4 ± 12.6
100	SWW + NAS	1	18.0 ± 3.2	< DL	< DL
100	SWW + NAS	10	< DL	< DL	< DL
100	SWW + NS	100	135.6 ± 20.0	578.4 ± 8.4	331.4 ± 0.0

Notes: SWW–synthetic wastewater, NAS–nitrifying activated sludge. DL is detection limit which below 3 µg Ag/L.

The release of Ag^+ increased in the period from 0 h to 30 h, but decreased in the period of 30–60 h. The ranges of liberated silver in SWW only were from 25.3 ± 0.6 µg/L to 750.9 ± 20.8 µg/L, averaged at 0.059, 0.171 and 0.503 mg/L in the experimental period of 60 h at initial AgNPs concentrations of 1, 10, and 100 mg/L, respectively. The mean amounts of Ag^+ release were close to the concentrations of Ag^+ used in the inhibitory kinetics experiment. The measured concentrations of Ag^+ in the SWW+ NAS were lower than in SWW only.

The released Ag^+ was monitored along with the ammonia oxidation inhibition in AgNPs experiments as shown in Table 5-2. The Ag^+ concentrations were measured from the experiments with SWW and SWW+NAS (the wastewater with the nitrifying sludge) at different initial ammonia and AgNPs concentrations. There was more released Ag^+ at higher initial AgNP concentrations. This could be the result of an instant dissociation of Ag^+ from AgNPs or the stock AgNPs previously contained Ag^+ since concentration of Ag^+ release was detected immediately after AgNPs were added to SWW or SWW + NAS. Prior studies found that concentration of dissolved silver increased sharply in a short time after AgNPs were added to the medium [10, 24]. The increasing Ag^+ concentration with time (from 0 to 30 h) was obviously indicated that AgNPs could gradually release Ag^+ after they are in WWTPs. The finding agreed with other studies reporting that AgNPs were the source of Ag^+ [2, 24] because they produce peroxide intermediates (H_2O_2), which oxidize metal silver to Ag^+ [79]. In this study, the concentrations of Ag^+ reduced from 30 to 60 h. The possible explanation for the reduction of Ag^+ release was due to binding to inorganic ligand such as chloride [8, 16]. In addition, Ag^+ can strongly combine with thiol groups found in biomass [51, 81].

5.3.1.3 Ammonia oxidation kinetics influenced by Ag^+

Initial AgNPs at 1, 10, and 100 mg/L released the averaged amounts of Ag^+ of 0.059, 0.171 and 0.503 mg/L in SWW only over period of 60 h. These ranges of concentrations were chosen for inhibitory kinetics experiment.

The ammonia oxidation experiment with and without AgNPs was performed. The rates of ammonia consumption were fitted in the Monod model as indicated in Figure 5-3. According to this figure, the amendment of Ag^+ resulted in rapidly decreasing both Ks and q_{max} values of the NAS 30 mM culture. Ks declined from 17.83 mg/L to 7.28, 4.98, 4.76 mg/L, whereas the q_{max} values were reduced from 0.6379 mg N/l/h to 0.2492, 0.0901, 0.0175 mg N/l/h at Ag ions concentrations of 0.05, 0.10, 0.50 mg/L, respectively (Figure 5-3).

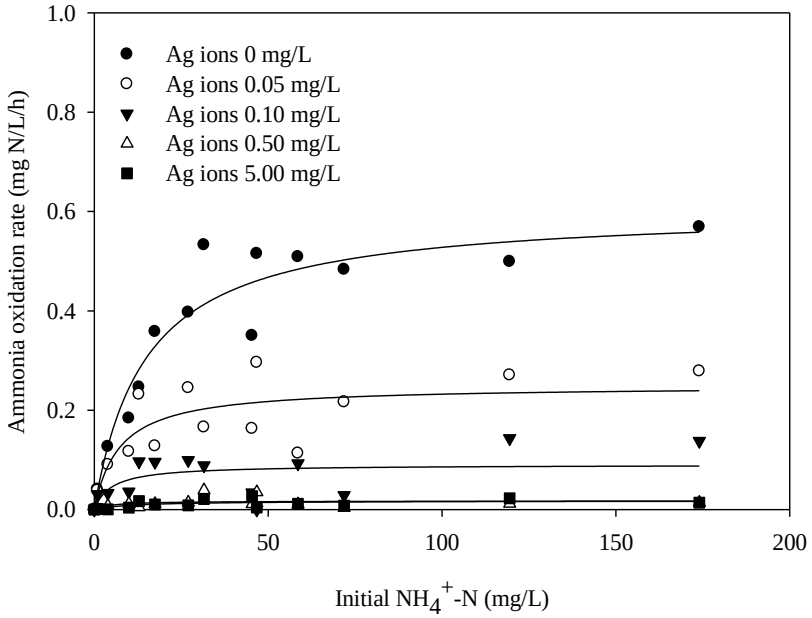

Figure 5-3 Kinetics of AO from NAS 30 mM by *Ag^+*

For AO activity, Ag^+ at 0.05, 0.10, 0.50 and 5.00 mg/L suppressed AO by 52.7 ± 2.1%, 75.3 ± 1.8%, 93.91 ± 1.9%, and 96.2 ± 1.3%, respectively (Figure 5-4). It was clearly that Ag^+ at only released range of concentrations (much lower concentrations compared to AgNPs) was much more toxic than AgNPs. This could indicate that in this study, silver toxicity to microbes was the role of Ag^+.

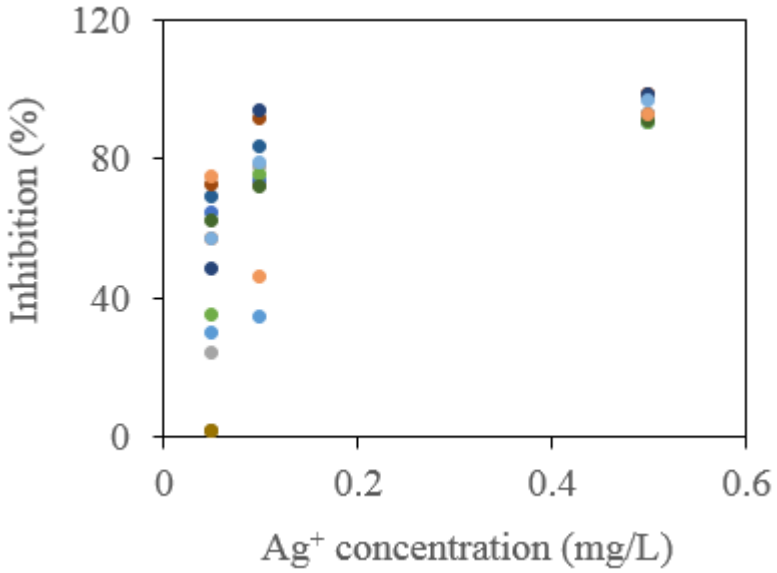

Figure 5-4 Percent inhibition of AO from NAS 30 mM by Ag^+

Previous studies also demonstrated that the toxicity of Ag^+ was higher than AgNPs to several types of organisms. The potential nitrification of both *N. europaea* biofilms and free cells was more adversely impacted by toxicity of Ag^+ than AgNPs [162]. Similarly, toxicity of Ag^+ to *Daphnia magna* and *Thamnocephalus platyurus* was also found higher than that of AgNPs [172]. Higher toxicity of Ag^+ was because Ag^+ could produce more ROS [7], easily uptaken by ion transporters and high affinity to thiol groups [81], thus exhibiting more toxic impact than AgNPs. The inhibitory constants, K_i values, supported the evidence that Ag^+ was more toxic to AO activity

than AgNPs. It was found that the K_i of Ag^+ was much lower (0.29 mg/L) than that of AgNPs (73.5 mg/L) in the current study. The Monod kinetic parameters including K_s and q_{max} showed that the inhibitory effect of AgNPs and Ag^+ on the AO activity from nitrifying sludge followed uncompetitive–like model because both K_s and q_{max} decreased when the concentrations of AgNPs and Ag^+ increased. Our previous study also found that AgNPs inhibited AO process best described by uncompetitive–like model [167] although the oxygen uptake rates were measured instead of ammonium.

It was noticed that AgNP concentrations of 1, 10, and 100 mg/L inhibited AO by 50.5 ± 9.5 %, 63.3 ± 7.9 %, and 76.8 ± 5.8 %, respectively, while Ag^+ (similar to Ag^+ released from AgNPs) at 0.05, 0.10, and 0.50 mg/L suppressed AO by 52.7 ± 2.1 %, 75.3 ± 1.8 %, and 93.9 ± 1.9 %, respectively (Figure 5-4). The inhibitory effect of AgNPs in these experiments should have been similar or higher than that influenced by Ag^+ at the released amount. However, AgNPs showed apparent lower inhibitory effect on AO compared to that of Ag^+ in the inhibitory test. This could be due to two potential reasons. Firstly, AgNPs gradually liberated Ag^+ and some factors (such as inorganic ligand, thiol groups) reduced Ag^+ under the presence of biomass. This can be seen from the Ag^+ release in SWW+NAS, which was much lower than in SWW due to the presence of nitrifying biomass (Table 5-2). The reduction of released Ag^+ could lead to lower initial Ag^+ concentrations in AgNPs experiment compared to those in Ag^+ experiment ($AgNO_3$ as a Ag^+ source). As a result, lower toxicity to AO was observed in AgNPs experiment. Secondly, Ag^+ possibly exhibited acute toxic effect on AO. It might take time for AgNPs to release Ag^+ to a level similar to the initial Ag^+ concentrations using $AgNO_3$ as a direct Ag^+ source. During that time, ammonia oxidizers could gradually adapt to the slowly increasing Ag^+ concentrations liberated

from AgNPs. Prior study reported that the oxygen uptake rate of flocculent sludge was inhibited in the short-term test (12 h) but the inhibition was absent during the long-term exposure (22 days) to AgNPs at 50 mg/L due to adaptation of the microbes in the sludge [7]. In this study, the release of Ag^+ in the AgNPs experiment and the toxicity of Ag^+ in the kinetics test suggested that Ag^+ released from AgNPs did contribute to overall toxicity of AgNPs.

5.3.2 Microbial cell physiology observation

The microbial cell physiology of the nitrifying sludge exposed to AgNPs and Ag^+ observed by SEM and TEM was shown in Figure 5-5 and 5-6. The introduction of AgNPs into the NAS 30 mM culture resulted in AgNPs–cells aggregation that was confirmed by EDX (Figure 5-5e-f). There were more AgNPs aggregated in higher AgNPs treatment (Figure 5-5b-c). The contact of AgNPs and Ag^+ with cells of NAS 30 mM resulted in same morphological change of cells from rod–shaped in the control (Figure 5-5a) to a shorter rod–shaped in the samples amended with AgNPs or Ag^+ (Figure 5-5b-c). The same morphological change on shapes of cells in this study could imply that AgNPs and Ag^+ had similar inhibitory mechanisms on microbes in NAS 30 mM. Former study used copper ions (Cu^{2+}) to expose to *Acidocella sp.* GS19h strain, the observed morphological change was similar to the current study. Morphological changes are the ways that several bacteria made to adapt to the presence of heavy metals [173]. The morphological change was due to relative reduction of cell surface (due to cell membrane reduction) with respect to cell volume. The reduction of cell surface enabled microbes to become less exposed to heavy metals [173]. In this study, the cells in NAS 30 mM culture changed its morphology to response to stressful condition resulted from AgNPs and Ag^+. In addition to morphological change, it was also

observed that filamentous seen in the control were disappeared in the samples treated with AgNPs or Ag^{+}. Many studies reported that AgNPs could reduce extracellular polymeric substances (EPS) quantity leading to inhibition of filamentation [174, 175].

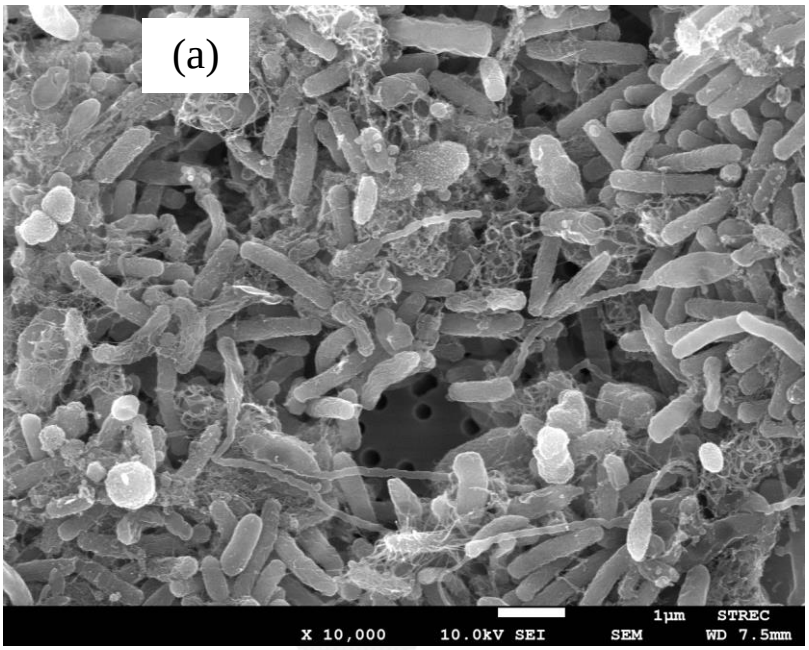

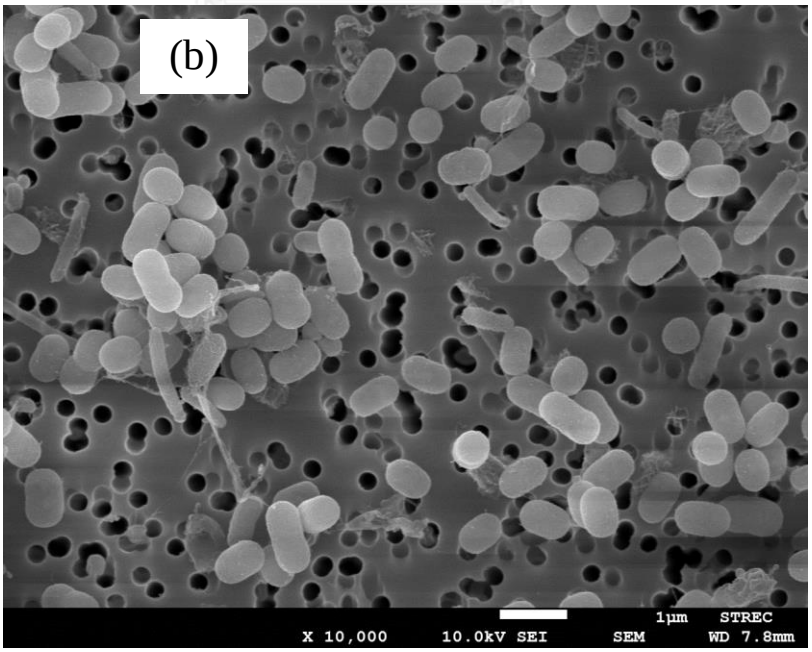

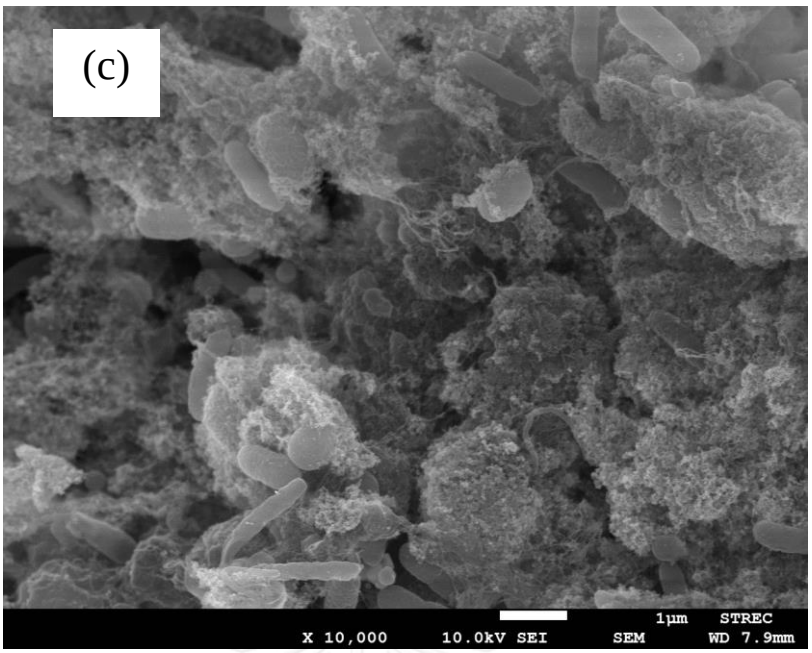
(c)
X 10,000
10.0kV SEI
SEM
1µm
STREC
WD 7.9mm

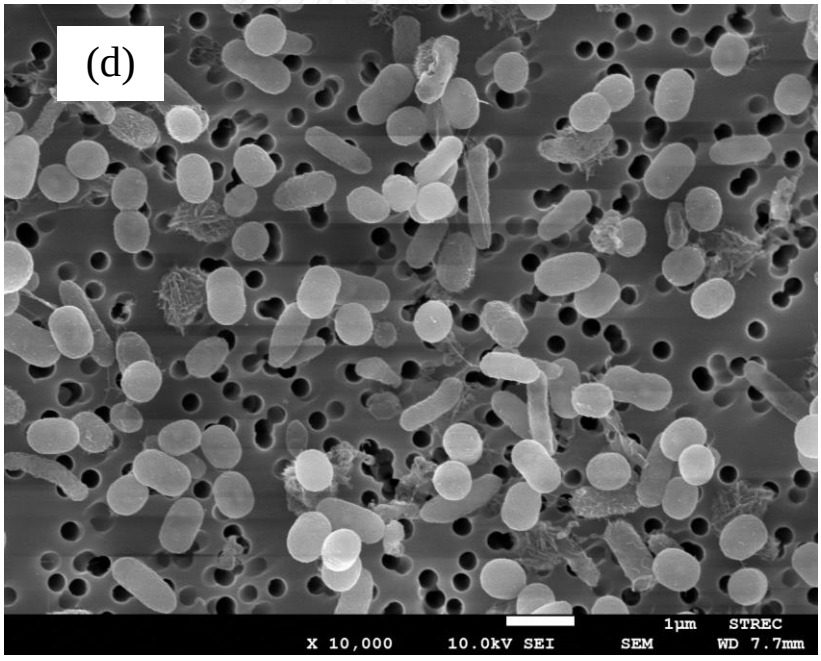
(d)
X 10,000
10.0kV SEI
SEM
1µm
STREC
WD 7.7mm

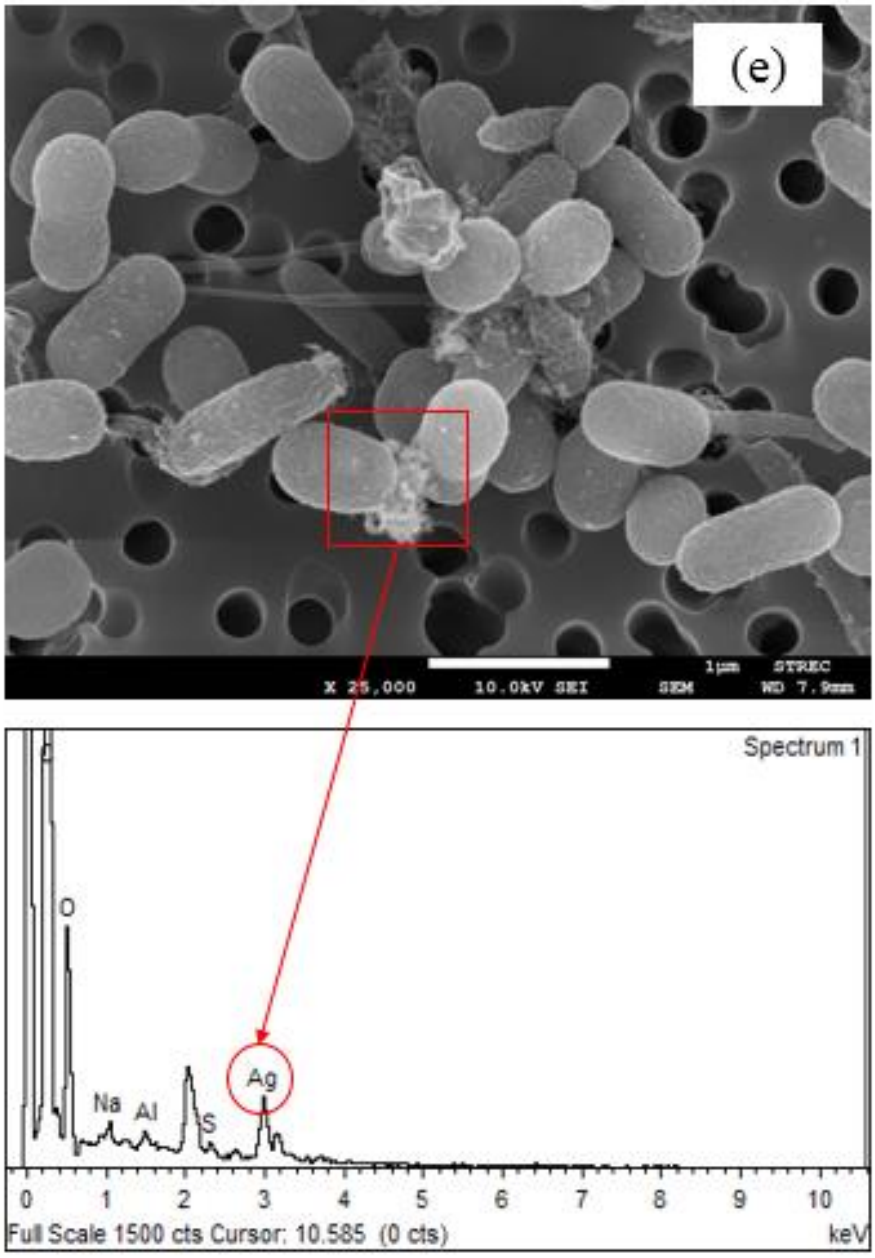
(e)
X 25,000
10.0kV SEI
SEM
1μm
STREC
WD 7.9mm
Spectrum 1
C
O
Na
Al
S
Ag
0
1
2
3
4
5
6
7
8
9
10
Full Scale 1500 cts Cursor: 10.585 (0 cts)
keV

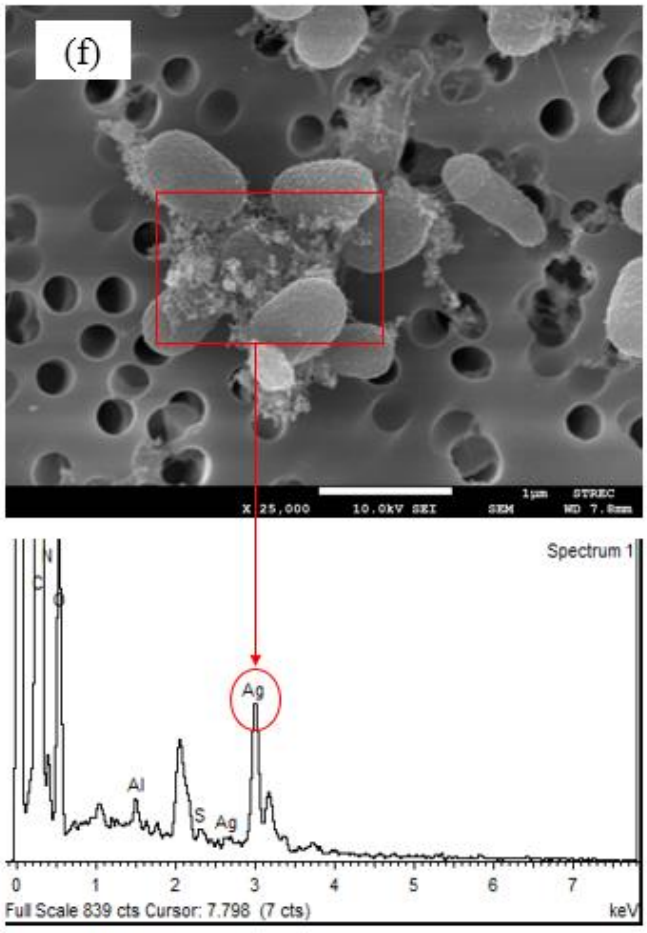

Figure 5-5 SEM micrographs for observation of NAS 30 mM after 48 h exposed to AgNPs and Ag^{+}.

Figure 5-5 showed SEM image for the control (without AgNPs or Ag^{+}) (a). In the control, microbes were in rod-shaped observed at the magnification of 10,000X. Microbes in the NAS 30 mM became shorter rod-shaped after exposing to AgNPs at 10 mg/L and 100 mg/L observed at 10,000X (b,c). Microbes in NAS 30 mM have changed to a shorter rod-shaped after exposure to Ag^{+} at 0.10 mg/L observed at 10,000X (d). AgNPs at 10 mg/L (e) and 100 mg/L (f) exposed and formed aggregates with cells observed at the magnification of 25,000X. There were more AgNPs forming aggregates with cells at higher AgNPs concentration.

In the present study, TEM results indicated that AgNPs attached on outer layer of the cells, formed pits and damaged cell membrane (Figure 5-6b-c). Damage of bacterial cell membrane by AgNPs was previously reported in the literature [15, 62, 167]. After attachment on cell membrane, AgNPs sloughed off the outer layer and caused cell death resulting in reduction of AO in nitrifying sludge. In addition, AgNPs released Ag^+ in the earlier discussion and caused additional toxicity for the cells. Beside that Ag^+ could bind to the membrane surface and inactivate activity of the functional enzyme of ammonia oxidizers [6]. The binding of AgNPs and Ag^+ on the cell surface resulted in damage of cell wall, which could be a reason leading to the absence of filamentous cells. The interior cells after exposing to Ag^+ (Figure 5-6d-e) were different from no silver control (Figure 5-6a). The area of lighter in color of the samples treated with Ag^+ was more intense than in the control. Previous study reported that bacteria responded to silver stress by forming vesicles resulting in less density of internal parts of the cell treated with Ag^+ [6]. This could be the reason to explain cells change from rod-shaped to shorter rod-shaped in the previous discussion of SEM. TEM observation also indicated that the outer layer of the cell exposed to Ag^+ was thinner than that of the cell without exposing to silver. Former finding presented that Ag^+ could interfere with peptidoglycan layer and cytoplasmic membrane [176]. The loss of defined membrane could be attributed to cell death, loss of AO activity, and absence of filamentation. The less defined membrane in cells exposed to Ag^+ than cells exposed to AgNPs could be the reason explain the more toxic impact of Ag^+ than AgNPs. The changes of cell morphology, density of internal cell matters, defined membrane and cell damages were well linked to inhibitory effect of AgNPs and Ag^+ on AO activity.

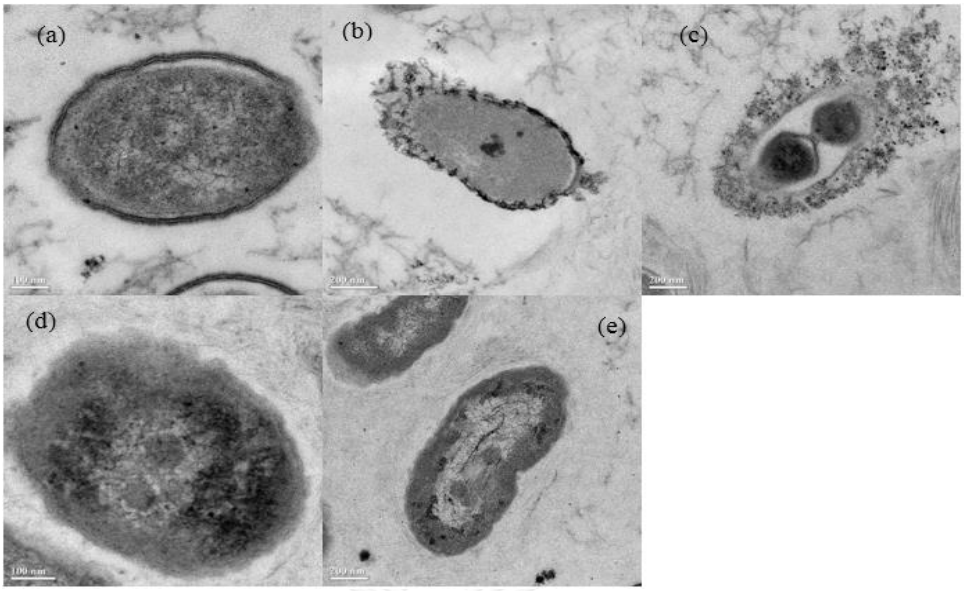

Figure 5-6 TEM images of NAS 30 mM exposed to AgNPs and Ag^{+}

Figure 5-6 indicated the control without silver (a), AgNPs 10 mg/L (b), AgNPs 100 mg/L (c), Ag^{+} 0.10 mg/L (d), and Ag^{+} 0.50 mg/L (e). AgNPs attached on the surface and caused damage of cell in the samples treated with AgNPs. Cells treated with Ag^{+} had less defined membrane and the internal parts of the cells formed vesicles indicated by a lighter in color compared to the control.

5.3.3 Microbial community and viability observation

Estimation from FISH-CLSM images (Figure 5-7) indicated that AOB were mostly dominant in nitrifying culture (59.0 ± 10.0 % of total microbes). While the nitrite-oxidizing bacteria (NOB) including *Nitrospira* sp. and *Nitrobacter* sp. accounted for 4.9 ± 4.0 % and 22.8 ± 5.7 % of total microbes, respectively. The results clearly indicated that ammonia-oxidizing culture was dominant in the nitrifying sludge. This was well fitted to the previous discussion that obvious inhibition of AO from the nitrifying culture in the inhibitory kinetics experiments with AgNPs and Ag^{+} was found.

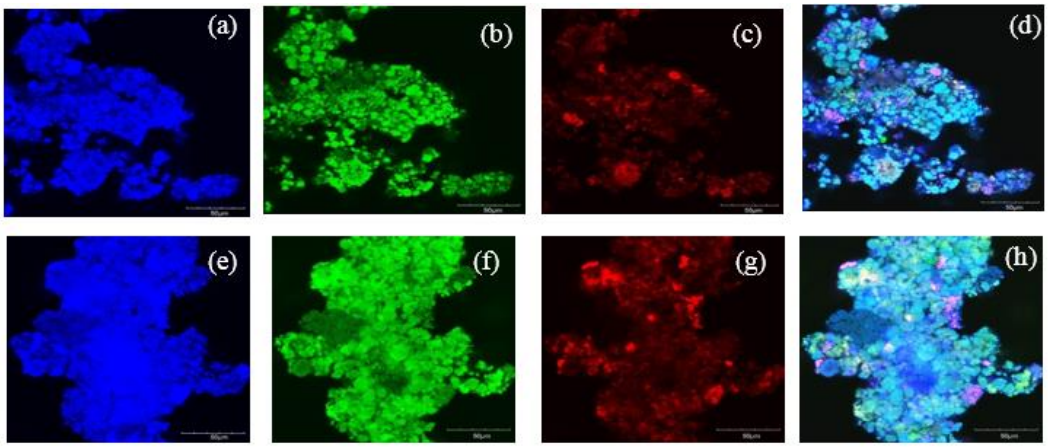

Figure 5-7 Example of FISH–CLSM images of microbes in 30 mM NAS

In Figure 5-7, total microorganisms were DAPI stained (blue), AOB was hybridized with NSO190 (green), *Nitrobactor* sp. was hybridized with Ntspa 662 (red) and *Nitrospira* sp. was hybridized with NIT3 (red). The target cells combine with both Alexa flour 488-labled probe (in green) and CY3-labled probe (in red), were in yellow. FISH signal of total microorganisms was showed in a) and e), whereas AOB was indicated in b) and f). *Nitrobactor* sp. and *Nitrospira* sp. were presented in c) and g), respectively. Combination of FISH signals of all microorganism, AOB and *Nitrobactor* sp. was illustrated in d) while combination of all microorganism, AOB and *Nitrospira* sp. was showed in h).

Since the majority of microbes found in this study was AOB, bacterial viability test was performed. The percent damage of cell membrane resulted from exposure to AgNPs and Ag^{+} was showed in Figure 5-8 whereas, example of CLSM-Images of membrane damaged by AgNPs and Ag^{+} after 48 h of exposure was showed in Figure 5-9. Live/dead microscopy results indicated that AgNPs and Ag^{+} caused damage of cell

membrane. For AgNPs, higher AgNPs concentrations resulted in higher cell membrane loss. This tendency was similar for Ag^+.

According to Figure 5-8, the damage of membrane integrity of nitrifying cells treated with AgNPs concentrations at 1, 10, and 100 mg/L accounted for 29.7 ± 16.2 %, 60.9 ± 21.6 %, and 81.8 ± 12.8 %, respectively. While nitrifying cells amended with Ag^+ at 0.10 mg/L and 0.50 mg/L resulted in membrane integrity loss by 14.1 ± 6.3 %, and 79.5 ± 15.0 %, respectively. It is clearly that Ag^+ at 0.50 mg/L caused loss of membrane integrity as high as that of AgNPs at 100 mg/L, which reaffirmed the previous finding that Ag^+ was more toxic to AO than AgNPs. In addition, the increasing percentage of dead cells agreed with the increasing inhibition magnitude of AO when AgNPs and Ag^+ concentrations increased. However, damage of membrane integrity was not significantly different ($p > 0.05$) between the silver control, AgNPs at 1 mg/L and Ag^+ at 0.10 mg/L (Figure 5-8). This was not expected since AgNPs and Ag^+ at these concentrations significantly inhibited AO by 50.5 ± 9.48 % and 52.7 ± 2.1 %, respectively. It was possible AgNPs and Ag^+ at these low concentrations could partially cause damage of membrane integrity, but the damage was not detected based on our investigation using 10 live/dead images. However, prior study reported that cell lysis was only partial reason for the inhibition of nitrification of AgNPs and Ag^+ [162]. In addition, former studies indicated that Ag^+ could inhibit functional enzymes, thus reducing AO without completely destroying the cell membrane [6, 7].

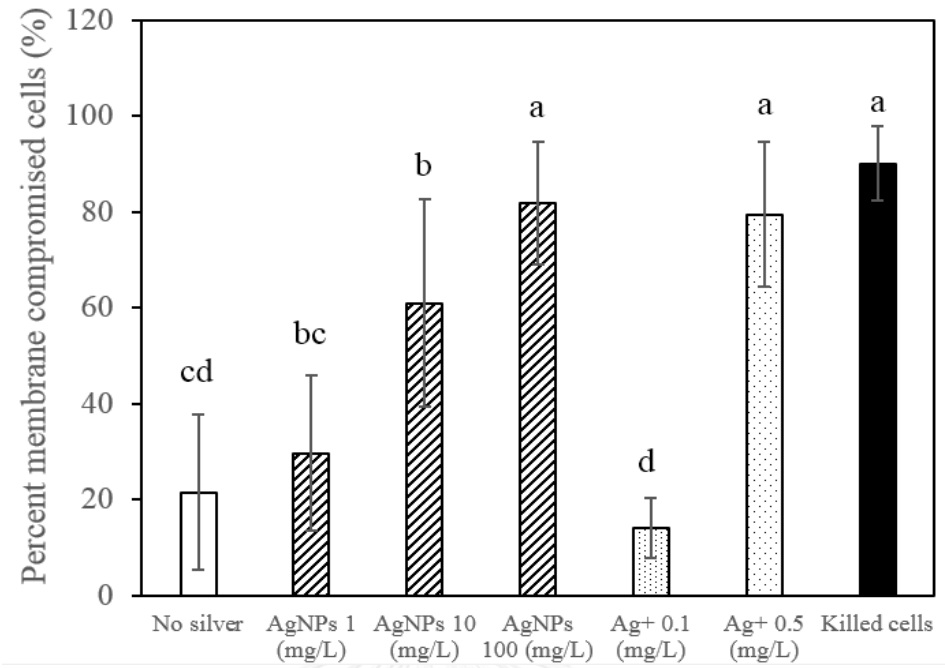

Figure 5-8 Percent of cell membrane damaged by AgNPs and Ag^{+} after 48 h of exposure

In Figure 5-8, the average percentage of LIVE/DEAD results were calculated based on ten microscopic fields. Error bars represent the standard deviation. Letters from a to d indicated the from highest levels of membrane damaged to the lowest ones. Different letters indicate statistically significant ($p < 0.05$).

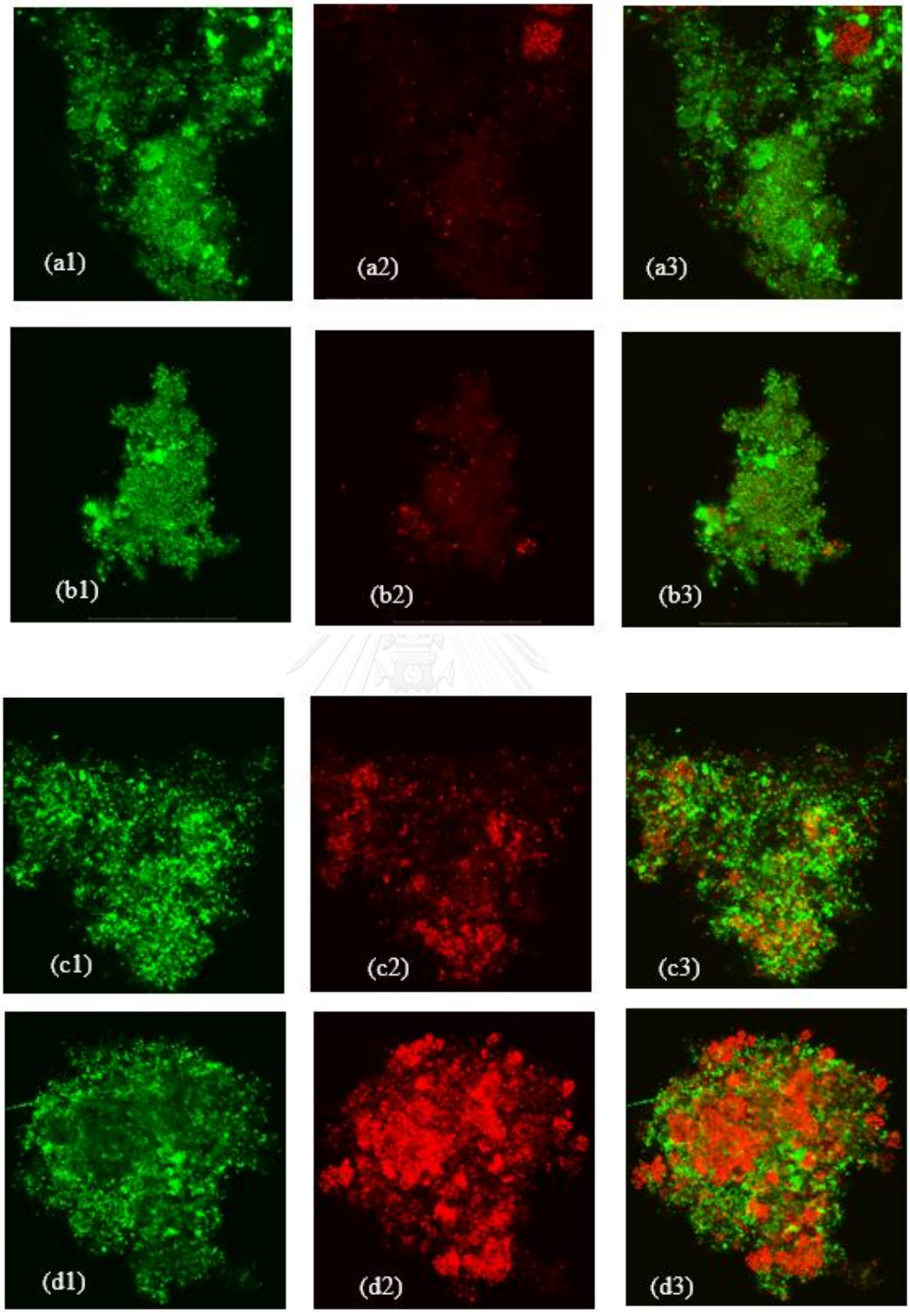
(a1)
(a2)
(a3)
(b1)
(b2)
(b3)
(c1)
(c2)
(c3)
(d1)
(d2)
(d3)

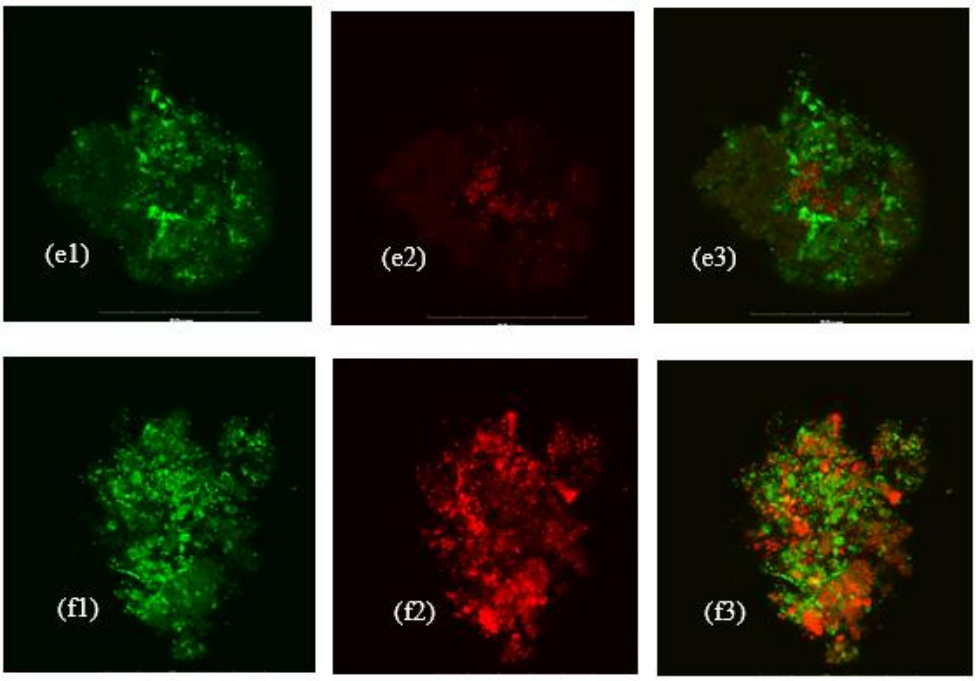

Figure 5-9 Live/Dead after NAS 30 mM exposed for 48 h to AgNPs and Ag^+

It was noted that a1, a2 and a3 showing the total cells, dead cells and overlay of total and dead cells for the control; b1, b2, and b3 showing the total cells, dead cells and overlay of total and dead cells for the sludge exposed to AgNPs 1 mg/L; b1, b2, and b3 showing the total cells, dead cells and overlay of total and dead cells for the sludge exposed to AgNPs 1 mg/L; c1, c2, and c3 showing the total cells, dead cells and overlay of total and dead cells for the sludge exposed to AgNPs 10 mg/L; d1, d2, and d3 showing the total cells, dead cells and overlay of total and dead cells for the sludge exposed to AgNPs 100 mg/L; e1, e2, and e3 showing the total cells, dead cells and overlay of total and dead cells for the sludge exposed to Ag^+ 0.1 mg/L; f1, f2, and f3 showing the total cells, dead cells and overlay of total and dead cells for the sludge exposed to Ag^+ at 0.5 mg/L.

5.3.4 Mechanism of toxicity of AgNPs and Ag^+

In this study, SEM images indicated that AgNPs attached on the microbial cells while TEM results revealed that AgNPs and Ag^+ reduced thickness of outer layer and damaged bacterial cells. In addition, Live/Dead assay confirmed that AgNPs and Ag^+ damaged membrane integrity. Previous study also found that AgNPs and Ag^+ generated reactive oxygen species (ROS) and then ROS caused damage of cell wall [6, 10, 77, 78], formed pits [15] resulting in cell death. Our findings agreed with the previously reported results that AgNPs and Ag^+ reduced AO by the mechanism of causing cell death. We proposed that AgNPs released Ag^+ and then both AgNPs and Ag^+ caused death of cells leading to inhibition of ammonia oxidation activity from the nitrifying sludge.

5.4 Summary

Amendment of AgNPs and Ag^+ into wastewater adversely inhibited the AO process. Silver ions were much more toxic to AO than AgNPs. Silver ions of 0.05 to 0.50 mg/L could inhibit AO by 53 – 94 % whereas AgNPs of 1 to 100 mg/L only reduced AO by 45 –74 %. Silver nanoparticles released the average amounts of Ag^+ at 0.059, 0.171 and 0.503 mg/L over 60-h experimental period at initial AgNPs concentrations of 1, 10, and 100 mg/L, respectively. The release of Ag^+ mainly caused toxic impact of AgNPs on nitrifying sludge. Microscopic observation indicated that AgNPs attached to microbial cell surfaces and resulted in morphological change. Microbial cells exposed to AgNPs and Ag^+ showed less defined membrane and less density of internal cell matters, which could lead to cell death. The result from this study can be used as basic information for preventing the system failure from AgNPs and the released Ag^+ by taking relevant pre-treatment measures.

Chapter 6 Mitigation of Ammonia Oxidation inhibition by Silver Nanoparticles and Silver Ions using entrapped cells

6.1 Introduction

Silver nanoparticles (AgNPs) are produced from metallic silver that has the characteristic of the antimicrobial properties of the silver ions (Ag^+). AgNPs have superiority characteristics such as high surface area per unit mass which could enhance effective antimicrobial, antifungal, antiviral and anti–inflammatory activity [29, 177]. With those, AgNPs have been used in many aspects of life and science. For instance, AgNPs are incorporated into textiles, food packaging, plastic coatings to prevent negative impact of harmful microorganisms [34, 35]. In addition, AgNPs are coated on other daily consumer products such as toys, mobile phones, clothes, toothpaste, and facial cream and in medical practices such as bandages, wound dressings to ensure consumers is safe when they are using these products [31]. It is also utilized in wastewater treatment [36]. Previous studies found that AgNPs was released during washing out consumer products [150] and consequently AgNPs were found in WWTPs [45-47] where it could release Ag^+ and impede microbial activity [48]. Former study indicated that AgNPs could cause negative effect on microbial activity especially nitrifying microorganisms in WWTPs [178] because nitrifying activity was highly susceptible to toxicity of AgNPs [16, 62, 66, 170]. Consequently, AgNPs could reduce nitrogen removal performance in wastewater facilities.

Cell entrapment technique has been proven to a potential technology for alleviation of negative impact of toxic substance doses on microbial activity since it could protect the entrapped cells less exposed to harmful chemicals [15, 129, 130, 179].

In addition, cells entrapped in entrapment materials could assist living microorganisms to resist to environmental conditions (pH change, temperature), to remain cell density, and to store longer time without reducing microbial activity [136, 180]. Prior study indicated that nitrifying cells entrapped in calcium alginate (CA), polyvinyl alcohol (PVA) could mitigate toxicity influence of AgNPs on nitrification activity which was supposed to be because of reducing contact between AgNPs and nitrifying cells. However, the evidence of less contact between cells and AgNPs was not reported. In addition, AgNPs could release Ag^+ and inhibit ammonia oxidation activity. It has been curious about the role of entrapped cells in protecting ammonia oxidation activity from toxic impact of Ag^+. Furthermore, the combination of PVA and SA has been reported showing good performance in chromium removal [181], but it has not been tested with removal of ammonia under presence of AgNPs and Ag^+.

This chapter was to investigate the role of barium alginate (BA), polyvinyl alcohol (PVA), and the mixture of polyvinyl alcohol-barium alginate (PVA–BA) in mitigating inhibition of AO from entrapped cells influenced by AgNPs and Ag^+. The micro structures of entrapped cells were observed using scanning electron microscopy (SEM) and microbial viability was observed using confocal laser scanning microscopy to elucidate mitigation effect of the entrapment materials. The results of this study could be used for possible application for treatment of wastewater contaminated with AgNPs and Ag^+.

6.2 Methodology

6.2.1 Preparation of entrapped cells

The enriched NAS 30 mM culture was harvested and centrifuged at 5,000 rpm for 20 min and the clear supernatant was removed to collect the settled cells. The collected cells were re–suspended, well–mixed, and centrifuged to wash in SWW. The washing process was repeated for 5 times to obtain the cleaned cells. The cleaned cells were used for the preparation for entrapped cells. The clean and concentrated NAS 30 mM was added to the entrapment matrices to reach final cell concentration of 2,000 mg MLSS/L.

BA-entrapped cells was prepared using alginic acid sodium salt 2% (w/v) and barium chloride 5% (w/v). Weigh 6 grams of alginic acid sodium salt and then added into 300 ml of sterile distilled water. The mixture was heated in water bath at 80^{o}C until completely dissolved and then cooled down to room temperature. The alginic acid sodium salt and NAS mixture (final cell concentration of 2,000 mg MLSS/L) were homogeneously mixed and then dropped into barium chloride ($BaCl_2$) solution of 5% using peristaltic pump at the rate of 20 rpm to produce the gel beads of 3–6 mm. Total 300 ml of mixture of cells and entrapment matrices could produce 210 grams (wet weight) of gel beads resulting in 1 gram of gel beads containing 2.85 mg of NAS 30 mM cells. The amount of gel beads was weighed (1.8 g) to add to flasks containing SWW to obtain the final MLSS concentrations of 50 mg/L in 100 ml of final operating volume.

PVA–entrapped cells was prepared by dissolving polyvinyl alcohol (PVA, 99%, fully hydrolyzed) 10% (w/v) in sterile water. Then the mixture was heated until it was totally dissolved. The heated solution was cooled down to room temperature. The cleaned NAS 30 mM was added to the cooled PVA to a final concentration of 2,000 mg MLSS/L. Total 300 ml of mixture including PVA and NAS 30 mM was used which was estimated to contain approximate 600 mg MLSS of NAS 30 mM. The gel beads of approximate 3–6 mm were produced by using peristaltic pump at the rate of 20 rpm. The produced gel beads were firstly contained in the mixture of saturated boric acid for 30 min and then transferred to 1 M sodium phosphate buffer for 2 h to harden the produced gel beads. PVA generated a crosslink with boric acid for a period from 10 min to 2 h to form a spherical structure. Then the gel beads were solidified by esterification of PVA with phosphate (sodium phosphate buffer 1 M). Approximate 200 g of gel beads in wet weight were obtained from 300 ml mixture of cells and PVA resulting each gram of gel beads contained 3 mg MLSS. The amount of 1.67 grams of gel beads were weighed and put into 250–ml flask and added SWW to 100 ml to result in final concentration of MLSS in each flask of 50 mg/L.

PVA-BA-entrapped cells was prepared by using polyvinyl alcohol (PVA, 99%, fully hydrolyzed) 10% (w/v) and alginic acid sodium salt 1% (w/v). The mixture of PVA 10% and SA 1% was heated until totally dissolved at 80^{o}C. It was then cooled down to room temperature. The final volume of the mixture of entrapment matrices and NAS 30 mM (final cell concentration of 2,000 mg MLSS/L) was 300 ml in which 600 mg MLSS was contained. The gel beads of approximate 3–6 mm were produced by using peristaltic pump at the rate of 20 rpm. The produced gel beads were firstly

contained in the mixture of saturated boric acid and $BaCl_2$ 5% for 30 min. Then the gel beads were transferred to 1 M sodium phosphate buffer for hardening in 2 h. About 290 g of gel beads in wet weight were obtained from 300 ml mixture of cells and entrapment matrices thus each gram of gel beads contained 2 mg MLSS. The amount of 2.5 grams of gel beads were weighed and put into 250–ml flask and added the synthetic media to 100 ml to result in final concentration of MLSS in each flask of 50 mg/L.

6.2.2 Experimental setup

The amount of each type of gel beads was weighed to add to experimenting flasks containing SWW to obtain the final MLSS concentrations of 50 mg/L in 100 ml of final operating volume. The AgNPs (stock 5,000 mg/L) and Ag^+ (stock 100 mg/L) were supplemented to obtain final concentrations of 1, 10, 100 mg/L and 0.05, 0.10, 0.50 mg/L, respectively. Inhibitory effect of AgNPs and Ag^+ on AO activity from BA-, PVA-, PVA-BA-entrapped cells was examined at initial ranges of NH_4^+–N concentrations of 0–170 mg/L. The experiment was conducted in aerated condition (DO = 6.0 ± 0.4 mg/L), neutral pH (7.6 ± 0.2) and at room temperature.

The abiotic controls were prepared by the same procedures with the above mentioned materials but the same volume of sterile water was used instead of NAS suspension. These controls were conducted with BA-, PVA-, and PVA-BA entrapment materials with synthetic wastewater at expected initial ammonium concentration of 50 mg/L without addition of AgNPs or Ag^+. The abiotic controls were carried out to test loss of ammonium nitrogen due to abiotic process for example evaporation of ammonia due to aeration.

Furthermore, the abiotic reaction between AgNPs and Ag^+ were also tested by in two conditions which were with only SWW and with SWW plus killed cells at initial NH_4^+-N concentration of 50 mg/L.

The control free cells (no silver added) were also conducted to compare its ammonia oxidation activity with that of the control entrapped cells (no silver added) at each initial ammonium concentration.

The aqueous samples were periodically collected to monitor AO reduction rates. Ammonium concentration reduction was plotted versus time to calculate the AO rates or slope values which were addressed in the unit of mg N/L/h. Then the percent inhibition was calculated by comparing rates of ammonium reduction in entrapped cells control with those of entrapped cells added with AgNPs or Ag^+. Scanning electron microscopy was used to observe microbial cells and internal structures in the BA-, PVA-, and PVA-BA-entrapped cells. Live/dead assays were performed for examining viability of microbial cells in the entrapped cells after exposed to AgNPs and Ag^+.

6.2.2.1 Preparation of free cells from the entrapped cells for Live/dead

Ten gel beads after 60h exposed to various AgNPs and Ag^+ were collected, washed five times with distilled water, then washed five times with NaCl 0.85%. The washed cells were broken out using a pair of tweezers. The separated entrapped cells were dipped in ten milliliters of NaCl 0.85% and then gently squeezed using two tweezers to let the cells out of the entrapment matrices. Then the suspended cells were centrifuged at 5,000 rpm for 5 min. The supernatant was discarded, and the pellets were collected. The centrifugal step was to concentrate the concentration of suspended cells obtained from the entrapped cells. Approximate 250 µL NaCl 0.85% solution was added to the pellet

and then stained using staining kit (LIVE/DEAD® BacLight™ Bacterial Viability, Molecular Probes, Invitrogen) and observing under confocal laser scanning microscopy (CLSM). The staining procedure was described in the Chapter 3. The suspended cells control (taken directly from NAS 30 mM reactor) and killed cells (autoclaved at 121 °C, for 15 min) were also stained for estimation of microbial viability to compared with the entrapped cells and check the staining chemicals, respectively. Percentage of live and dead was estimated based on 10 CLSM-images. The results were presented as % dead cells ± SD.

6.2.2.2 Measurement of AgNP concentrations

Change of AgNPs at the concentrations of 1, 10 and 100 mg/L on different entrapment matrices including BA–, PVA–, and PVA–BA–entrapped cells were tested. The experiment was conducted using 5 grams of each type of entrapped cells plus 100 ml synthetic wastewater (the same component with inhibitory test) at the same initial NH_4^+–N concentration of 50 mg/L. The experimenting flasks were covered with aluminum foil tightly to prevent water evaporation. The flasks were shaken on a rotary shaker at the rate of 200 rpm at room temperature. The aqueous samples were collected at 0, 2, 24, 48 and 72 h to quantify AgNPs amounts in aqueous phase using spectrophotometer.

Silver nanoparticles have its own localized surface plasmon resonance (LSPR) and AgNPs in the well–dispersed form or non–agglomerated form has a maximum absorbance (λmax) at near 400 nm [157]. Zook et al. (2011) used the intensity of the λmax to quantify the concentration of AgNPs in solution by measuring LSPR. UV–visible spectroscopy is often used to observe LSPR which will provide information

regarding the agglomeration state of AgNPs suspensions and amount of AgNPs [60, 157]. This method can be also applied in differentiating the AgNPs form with other forms such as Ag^+ or agglomerated forms. In addition, this method could be used to distinguish AgNPs remaining in solutions from total silver [157].

From stock silver nanoparticles of 100 mg/L, a serial standard of AgNPs concentrations ranged from 0 to 40 mg/L were prepared in synthetic wastewater (SWW). The AgNP suspensions were measured from 250–600 nm by using spectrophotometry (UV–Visible Spectrophotometer Biomate 3S, Thermo Scientific, Madison, WI). The peak absorbance (400–405 nm) at each AgNP concentrations were used to establish linear relationship with AgNPs standard concentrations. The linear equation was obtained.

The samples from entrapped cells experiments with AgNPs were collected and dilutions were made when appropriate. Then the collected samples were measured exactly the same way with the measurements of the AgNPs serial standard solutions to obtain the peak absorbance. The obtained absorbance was used to calculate AgNPs concentrations in the samples by interpolating from the linear regression equation.

6.2.2.3 Scanning electron microscopy for entrapped cells

SEM was performed to observe for microbial cells and bead physiology. The BA- and PVA- and PVA-BA entrapped cells were prepared for SEM observations according to a procedure described elsewhere [15]. Briefly, the entrapped cell beads from the experiment were collected, washed with distilled water. The collected gel beads were fixed using 1% osmium tetroxide for 1 h. Then, the fixed gel beads were rinsed with distilled water for 10 min per time for 3 times. After that, they were dehydrated with a

series of ethanol from 30-95%. Then, the absolute ethanol was applied as the last step of the dehydration. The dehydrated beads pieces were dried using a critical point dryer (Balzers, CPD 020, Liechtenstein). Then, the beads were divided into two parts using a razor blade in liquid nitrogen, attached to a stub, and coated with gold. The dried BA and PVA and PVA-BA beads were observed using SEM with an energy-dispersive spectroscopy attachment (JEOL, JSM-5410LV, Tokyo, Japan). Elemental compositions of selected areas were analyzed using Energy Dispersive X–ray (EDX, Oxford Instruments, Model X–MaxN, UK) to identify forming aggregates of AgNPs.

6.3 Results and Discussion

6.3.1 Influence of AgNPs and Ag^+ on AO in BA–entrapped cells

The inhibition of AgNPs and Ag^+ on AO in the BA–entrapped cells were presented in Table 6-1 and Table 6-2. Generally, BA–entrapped cells significantly reduced negative impact of AgNPs and Ag^+ on AO compared to those of suspended cells (mean inhibition data at various AgNPs and Ag^+ concentrations were obtained from Chapter 5), especially at lower ranges of AgNPs (1-10 mg/L) and Ag^+ (0.05-0.10 mg/L) concentrations. In chapter 5, it was found that addition of AgNPs at 1, 10, 100 mg/L reduced the average of AO activity by 50.5 ± 9.5%, 63.3 ± 7.9% and 76.8 ± 5.8% in suspended cells, whereas only reduced AO activity by 12.5 ± 11.1, 36.9 ± 24.9% and 61.8 ± 24.8% in entrapped cells, respectively. At lowest AgNPs (1 mg/L) BA–entrapped cells could better protect AO from lethal effect of AgNPs than at high AgNPs (10 and 100 mg/L). This could be possibly explained because abundance of AgNPs in the bulk media release Ag^+ then the released Ag^+ transported into inner parts of the gel beads where AgNPs could have had more contact with ammonia oxidizing cells. Higher

AgNPs could facilitate forming aggregates and deposit on the surfaces of the entrapped cells which limited DO and NH_4^+-N transfer to the cells entrapped inside the gel beads. Prior study suggested that the dense network contained fine pores of the cross-linking between barium and alginate could limit diffusion of DO into the inner parts of the BA-entrapped cells [138]. Cells entrapped in alginate could be protected from the harmful effect of AgNPs due to limitation of AgNPs in transporting into contact with cells [15].

Table 6-1 Percent inhibition of AgNPs on AO from BA–entrapped cells

NH_4^+-N (mg/L)	AgNP 1 mg/L	AgNP 10 mg/L	AgNP 100 mg/L
6.7	5.9 ± 0.4 $^{b\,(c)}$	18.7 ± 0.6 $^{a\,(d)}$	19.0 ± 1.7 $^{a\,(e)}$
26.4	22.9 ± 1.0 $^{c\,(ab)}$	49.6 ± 1.0 $^{b\,(a)}$	73.9 ± 0.3 $^{a\,(c)}$
45.9	0.0 ± 0.0 $^{c\,(d)}$	24.3 ± 0.6 $^{b\,(c)}$	86.8 ± 0.1 $^{a\,(a)}$
75.0	24.1 ± 1.2 $^{c\,(a)}$	66.0 ± 0.7 $^{b\,(a)}$	78.2 ± 0.5 $^{a\,(b)}$
100.0	22.1 ± 1.9 $^{c\,(b)}$	62.5 ± 1.3 $^{b\,(b)}$	73.0 ± 0.9 $^{a\,(c)}$
156.5	0.0 ± 0.0 $^{b\,(d)}$	0.0 ± 0.0 $^{b\,(e)}$	39.7 ± 2.3 $^{a\,(d)}$
Mean	**12.5 ± 11.1** ^{c}	**36.9 ± 24.9** ^{b}	**61.8 ± 24.8** ^{a}

Note: Different letters indicate statistical differences ($p<0.05$). Letters in the parentheses show the statistical differences for ammonia oxidation respect to initial NH_4^+-N. Letters without parentheses indicate the statistical differences for respect to initial AgNPs concentrations. Letters from a to e indicated the from highest levels of inhibition to the lowest ones.

BA–entrapped cells was also able to effectively reduce negative impact of Ag^+ on AO. In the entrapped cells, Ag^+ at 0.05, 0.10 and 0.50 mg/L inhibited AO by 2.7 ± 3.42%, 15.9 ± 13.6%, and 41.0 ± 24.4%, respectively (Table 6-2). These inhibitory effects were also much lower than those in the free cells. In the suspended cells, Ag^+ at 0.05, 0.10 and 0.50 mg/L inhibited AO by 52.7 ± 2.1%, 75.3 ± 1.8%, and 93.9 ± 1.9%, respectively. BA–entrapped cells was highly effective in maintaining AO activity at Ag^+ at 0.05 and 0.10 mg/L. However, Ag^+ at 0.50 mg/L still showed high inhibitory effect on ammonia oxidation process. Higher concentration of Ag^+ in the bulk media could lead to higher diffusion of Ag^+ into the gel beads due to turbulence resulted from aeration and concentration gradient.

Table 6-2 Inhibition of Ag^+ on AO from BA–entrapped cells

NH_4^+-N (mg/L)	Ag^+ 0.05 mg/L	Ag^+ 0.10 mg/L	Ag^+ 0.50 mg/L
6.7	7.0 ± 0.2 $^{a\,(b)}$	17.9 ± 1.3 $^{c\,(c)}$	25.1 ± 0.2 $^{b\,(d)}$
26.4	6.4 ± 0.8 $^{c\,(a)}$	33.8 ± 1.0 $^{b\,(a)}$	58.7 ± 0.5 $^{a\,(a)}$
45.9	0.0 ± 0.0 $^{b\,(c)}$	0.0 ± 0.0 $^{b\,(e)}$	2.3 ± 0.9 $^{a\,(e)}$
75.0	0.0 ± 0.0 $^{c\,(c)}$	25.6 ± 0.5 $^{b\,(b)}$	63.9 ± 0.1 $^{a\,(b)}$
100.0	0.0 ± 0.0 $^{c\,(c)}$	1.8 ± 2.8 $^{b\,(d)}$	55.0 ± 0.9 $^{a\,(c)}$
Mean	**2.7 ± 3.42** ^{c}	**15.9 ± 13.6** ^{b}	**41.0 ± 24.4** ^{a}

Note: Different letters indicate statistical differences ($p<0.05$). Letters in the parentheses show the statistical differences for ammonia oxidation respect to initial NH_4^+-N. Letters without parentheses indicate the statistical differences for respect to initial Ag+ concentrations. Letters from a to e indicated the from highest levels of inhibition to the lowest ones.

Table 6-3 Estimation of AO activity remaining in BA–entrapped

Silver (mg/L)	% AO remain in BA–entrapped cells	% AO remain in free cells
AgNPs		
1	76–100	37–56
10	33–100	21–53
100	13–81	18–34
Ag ions		
0.05	93–100	22–76
0.10	66–100	6–30
0.50	36–98	2–7

Table 6-3 estimated that BA–entrapped cells remained AO activity up to 81–100% and 98–100% under AgNPs from 1–100 mg/L and Ag^+ from 0.05–0.50 mg/L, respectively. The experimental results indicated that BA–entrapped cells could be effectively used to mitigate inhibitory effect of AgNPs or Ag^+ on AO.

The study of using BA for mitigation of inhibitory effect of AgNPs or Ag^+ on AO process is limited. Previous studies mainly focused on calcium alginate [15, 130, 182]. Calcium alginate or CA (SA 2% + $CaCl_2$ 3.5%, w/v) was used as entrapment material to mitigate toxic influence of AgNPs on nitrification activity in the previous study [15]. The result showed that CA–entrapped cells remained AO by 90% and 65% under presence of AgNPs at 0.05 and 5.00 mg/L, respectively. In this study, cells entrapped in BA could maintain maximum AO rates by 100%, 100%, and 81% at AgNPs at 1, 10, and 100 mg/L, respectively. A primary comparison showed that the mitigated efficiency in the former study also as effective as those found in this current. Prior study showed that change of gelating agent using $CaCl_2$ to $BaCl_2$ could improve

quality of the produced gel beads [137]. BA beads proved to have better physical–chemical properties than the more commonly used CA beads and the immobilized cells in BA gel retained a high yield and activity [137]. Recently, a study reported that activated sludge entrapped with BA could enhance wastewater treatment better than free activated sludge. More specifically, BA–entrapped cells could remove 54% of chemical oxygen demand (COD), whereas the corresponding suspended cells reduced only 33% of COD [130]. This study did not deal with toxic substance and ammonium was not significant in the treated wastewater so the comparison was not possible.

This was the first time BA–entrapped cells were used to protect AO activity from lethal impact of AgNPs and Ag^+. In overall, BA–entrapped cells performed high effectiveness in remaining AO rates from toxicity effect of AgNPs and Ag^+. Since BA did not bind Ag^+ the mechanism for the protection could be possibly because the bead surfaces and the cells located in the nearest surfaces of the beads disturbed the transfer of Ag^+ into the inner parts of the beads. In contrast, AgNPs were strongly attached on BA and this could block transfer of DO and NH_4^+-N to the cells locating at inner parts of the BA–gel beads, thus stronger reducing AO at high AgNPs concentration. Figure 6-1 showed that AgNPs at 10 and 100 mg/L had more yellow color on the surfaces indirectly indicated that more AgNPs deposited on the entrapped cells beads at higher AgNPs concentration.

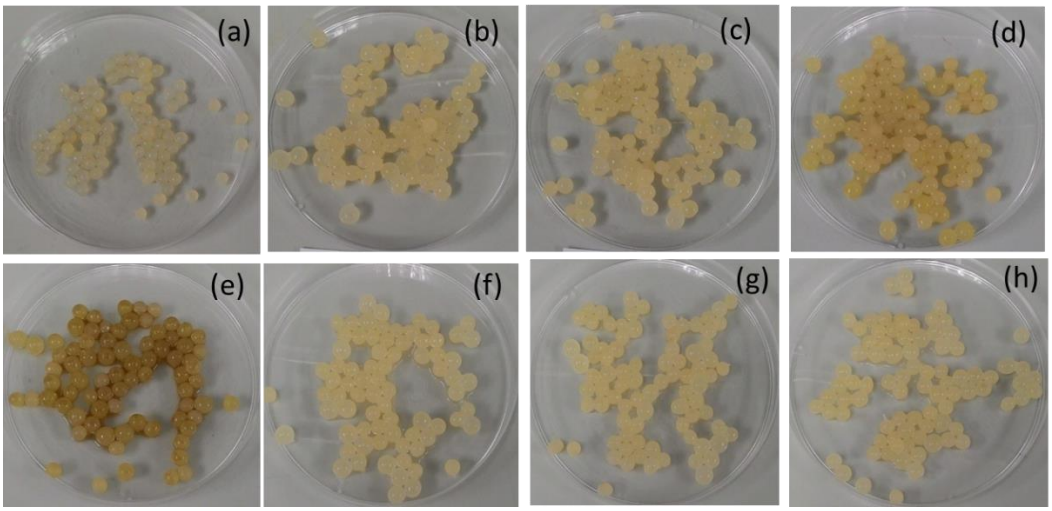

Figure 6-1 Photos of BA before and after experiment with AgNPs and Ag^+

Figure 6-1 showed photos of BA (a) before experiment, (b) after experiment-no silver, (c) after experiment at agNP 1 mg/L, (d) after experiment at AgNP 10 mg/L, (e) after experiment at AgNP 100 mg/L, (f) after experiment at Ag^+ 0.05 mg/L, (g) after experiment at Ag^+ 0.10 mg/L and (h) after experiment at Ag^+ 0.50 mg/L. Size and shape of the entrapped cells after 60 h of experiment remained similar. AgNPs were observed to bind to BA-entrapped cells (d-e) higher at higher AgNPs concentrations.

6.3.2 Influence of AgNPs and Ag^+ on AO in PVA–entrapped cells

Table 6-4 and Table 6-5 showed influence of AgNPs and Ag^+ on AO in PVA–entrapped cells, respectively. These tables indicated that PVA was also a good entrapment matrix to mitigate toxicity effect of AgNPs and Ag^+ on AO, especially at low silver concentrations. The inhibition was concentration dependent. It was found that AgNPs at 1, 10, and 100 mg/L inhibited AO from PVA–entrapped cells by 23.2 ± 17.3%, 56.5 ± 16.2%, and 66.2 ± 14.3%, respectively (Table 6-4). These values were lower compared to those in the suspended cells indicated that PVA–entrapped cells performed better AO activity than free cells under presence of AgNPs. Silver ions at 0.05, 0.10 and 0.50 mg/L caused inhibition

of AO by 25.6 ± 14.4%, 33.1 ± 14.2%, 56.7 ± 9.6%, respectively (Table 6-5). Similarly, the inhibitory effect of Ag^+ on AO activity in PVA–entrapped cells was lower compared to those in the suspended cells.

Table 6-4 Percent inhibition of AgNPs on AO from PVA–entrapped cells

NH_4^+-N (mg/L)	AgNP 1 mg/L	AgNP 10 mg/L	AgNP 100 mg/L
7.6	22.4 ± 0.4 $^{c\,(b)}$	29.4 ± 0.3 $^{b\,(f)}$	43.3 ± 0.2 $^{a\,(e)}$
24.7	21.8 ± 0.2 $^{c\,(b)}$	41.8 ± 0.1 $^{b\,(e)}$	52.2 ± 0.3 $^{a\,(d)}$
43.5	17.7 ± 0.9 $^{c\,(c)}$	62.3 ± 0.3 $^{b\,(d)}$	74.2 ± 0.4 $^{a\,(b)}$
63.2	2.6 ± 0.3 $^{c\,(e)}$	75.1 ± 1.2 $^{b\,(a)}$	83.7 ± 0.1 $^{a\,(a)}$
95.5	57.7 ± 0.3 $^{c\,(a)}$	66.6 ± 0.4 $^{b\,(b)}$	73.9 ± 0.2 $^{a\,(b)}$
171.6	16.7 ± 0.4 $^{c\,(d)}$	63.8 ± 0.6 $^{b\,(c)}$	69.9 ± 0.4 $^{a\,(c)}$
Mean	**23.2 ± 17.3** ^{b}	**56.5 ± 16.2** ^{a}	**66.2 ± 14.3** ^{a}

Note: Different letters indicate statistical differences ($p<0.05$). Letters in the parentheses show the statistical differences for ammonia oxidation respect to initial NH_4^+-N. Letters without parentheses indicate the statistical differences for respect to initial AgNPs concentrations. Letters from a to f indicated the from highest levels of inhibition to the lowest ones.

Table 6-5 Percent inhibition of Ag^+ on AO from PVA–entrapped cells

NH_4^+-N (mg/L)	Ag^+ 0.05 mg/L	Ag^+ 0.10 mg/L	Ag^+ 0.50 mg/L
7.6	37.2 ± 0.3 $^{c\,(b)}$	41.0 ± 0.5 $^{b\,(b)}$	61.9 ± 0.2 $^{a\,(b)}$
24.7	24.2 ± 0.5 $^{c\,(d)}$	30.2 ± 0.3 $^{b\,(d)}$	38.9 ± 0.5 $^{a\,(d)}$
43.5	17.3 ± 0.4 $^{c\,(e)}$	38.1 ± 0.4 $^{b\,(c)}$	69.2 ± 0.2 $^{a\,(a)}$
63.2	29.8 ± 0.5 $^{c\,(c)}$	37.3 ± 1.2 $^{b\,(c)}$	60.2 ± 0.4 $^{a\,(b)}$
95.5	44.2 ± 0.7 $^{c\,(a)}$	47.6 ± 0.1 $^{b\,(a)}$	55.7 ± 0.1 $^{a\,(c)}$
171.6	0.9 ± 0.4 $^{c\,(f)}$	4.6 ± 0.3 $^{b\,(e)}$	54.6 ± 2.4 $^{a\,(c)}$
Mean	**25.6 ± 14.4** ^{b}	**33.1 ± 14.2** ^{b}	**56.7 ± 9.6** ^{a}

Note: Different letters indicate statistical differences ($p<0.05$). Letters in the parentheses show the statistical differences for ammonia oxidation respect to initial NH_4^+-N. Letters without parentheses indicate the statistical differences for respect to initial Ag^+ concentrations. Letters from a to f indicated the from highest levels of inhibition to the lowest ones.

Table 6-6 presented that ammonia oxidation in the PVA–entrapped cells was remained up to 97%, 71%, and 57% at AgNPs concentrations of 1, 10, 100 mg/L, respectively. Similarly, AO in the PVA–entrapped cells remained up to 99%, 95% and 61% at Ag^+ concentrations of 0.05, 0.10 and 0.50 mg/L, respectively. From the remaining activity of AO, it was clearly showed that PVA-entrapped cells could mitigate toxicity impact resulted from AgNPs and Ag^+.

Table 6-6 Estimation of AO activity remaining in PVA–entrapped cells

Silver (mg/L)	% AO remain in PVA–entrapped cells	% AO remain in free cells
AgNPs		
1	42–97	37–56
10	25–71	21–53
100	16–57	18–34
Ag ions		
0.05	56–99	22–76
0.10	52–95	6–30
0.50	31–61	2–7

Previous studies reported that PVA was commonly used for entrapment technique because it is not harmful to activated sludge microorganisms [141, 182] and it can be produced massively at a low cost [137]. In the prior study, PVA at 10% (w/v) was applied to entrap microbes to degrade atrazine [17] from agricultural soil. The results revealed that PVA–entrapped cells performed better atrazine removal than suspended cells because free cells had a problem with leaching in sand column test. The study indicated that entrapped cells could help to solve the problem of cell leaching while the current study showed that the entrapped cells helped to prevent cells from contacting

with AgNPs or Ag^+. In the other study, Siripattanakul–Ratpukdi et al. (2014) proved that PVA at 10% used for the entrapment of NAS 5 mM could reduce the adverse effects of AgNPs on nitrification activity. For instance, PVA–entrapped cells could remain AO by 88%, 82%, and 44% at AgNPs at 0.5, 1, and 5 mg/L, respectively [15]. This current study found that PVA–entrapped cells remained AO up to 97% at AgNPs of 1 mg/L, 71% at AgNPs of 10 mg/L and only 57% at AgNPs of 100 mg/L. The effectiveness of using PVA to protect AO from negative impact of AgNPs in this study had similar tendency to the previous study that higher AgNPs concentration inhibited higher ammonia oxidation/nitrification. It could be said that the removal efficiency in the current study was higher than the previous study. The higher efficiency could be because the nitrifying culture was enriched at higher NH_4^+–N concentration leading to better AO activity. In addition, the air was continuously supplied at remained the level of DO > 5 mg/L in the current study, whereas it was supplied to a saturation point (DO = 8 mg/L) and then stopped. This could limit DO diffuse into the gel beads. The higher size of AgNPs (14 nm) could be another factor effect on the efficiency of the ammonia removal. The bigger AgNPs size could enhance deposition of AgNPs on the surfaces of the beads. The deposition of AgNPs were indirectly observed via more intense yellow color in the PVA-entrapped cells treated with higher AgNPs concentrations (Figure 6-2 c-e). All in all, this study suggested that PVA–entrapped cells could lessen inhibitory effect on AO of Ag^+ and AgNPs.

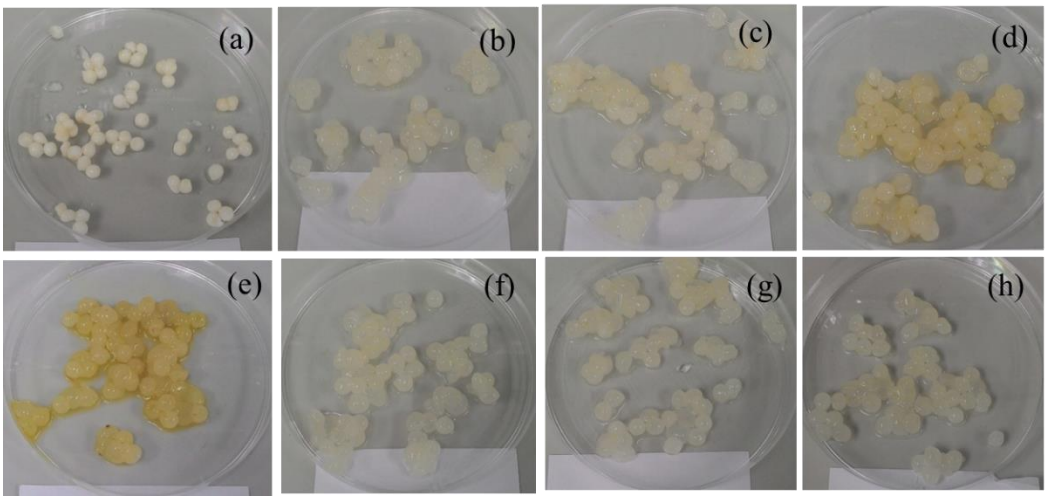

Figure 6-2 Photos of PVA before and after experiment with AgNPs and Ag^+

Figure 6-2 showed example of PVA-entrapped cells (a) before experiment, (b) after experiment-no silver, (c) after experiment at AgNP 1 mg/L, (d) after experiment at AgNP 10 mg/L, (e) after experiment at AgNP 100 mg/L, (f) after experiment at Ag^+ 0.05 mg/L, (g) after experiment at Ag^+ 0.10 mg/L and (h) after experiment at Ag^+ 0.50 mg/L. The size of the PVA-entrapped cells after 60 h of experimental period became bigger possibly due to water absorption. The gel beads became weak and deformed but not broken. It was observed that AgNPs bound on the surface of the PVA gel beads at 10 and 100 mg/L (in yellow color).

6.3.3 Influence of AgNPs and Ag^+ on AO in PVA–BA entrapped cells

The percentage of inhibitory impact of AgNPs on AO activity in suspended cells and entrapped cells was calculated and presented in Table 6-7. Experimental results indicated that AgNPs at 1 mg/L showed low inhibition (13.5 ± 15.9%) on AO activity at most initial NH_4^+–N concentrations in PVA–BA entrapped cells, whereas AO activity in free cells was more seriously inhibited (50.5 ± 9.5%) at this AgNPs

concentration. AgNPs at 10 mg/L suppressed AO in the entrapped cells by 25.9 ± 17.1% and in free cells by 63.3 ± 7.9%. At the highest AgNPs concentration of 100 mg/L, AO activity was retarded by 43.5 ± 18.9% in the entrapped cells while the activity was stopped by 76.8 ± 5.8% in the free cells. The results clearly showed that AO could be remained under AgNPs toxicity when nitrifying cells entrapped in PVA–BA matrix.

Table 6-7 Percent inhibition of AgNPs on AO from PVA–BA–entrapped cells

NH_4^+-N (mg/L)	AgNP 1 mg/L	AgNP 10 mg/L	AgNP 100 mg/L
9.6	0.0 ± 0.0 $^{c\,(d)}$	6.9 ± 0.1 $^{b\,(e)}$	24.8 ± 0.2 $^{a\,(f)}$
22.0	0.0 ± 0.0 $^{c\,(d)}$	50.9 ± 0.2 $^{b\,(a)}$	64.6 ± 0.2 $^{a\,(b)}$
36.7	0.0 ± 0.0 $^{c\,(d)}$	22.6 ± 0.1 $^{b\,(c)}$	28.6 ± 1.5 $^{a\,(d)}$
74.8	11.6 ± 0.4 $^{c\,(c)}$	24.3 ± 0.4 $^{b\,(c)}$	26.3 ± 0.3 $^{a\,(e)}$
97.6	40.5 ± 1.2 $^{c\,(a)}$	45.6 ± 3.1 $^{b\,(b)}$	70.0 ± 0.4 $^{a\,(a)}$
156.5	16.4 ± 5.7 $^{b\,(b)}$	17.8 ± 0.9 $^{b\,(d)}$	46.6 ± 1.2 $^{a\,(c)}$
Mean	**13.5 ± 15.9** ^{c}	**25.9 ± 17.1** ^{b}	**43.5 ± 18.9** ^{a}

Note: Different letters indicate statistical differences ($p<0.05$). Letters in the parentheses show the statistical differences for ammonia oxidation respect to initial NH_4^+-N. Letters without parentheses indicate the statistical differences for respect to initial AgNPs concentrations. Letters from a to f indicated the from highest levels of inhibition to the lowest ones.

Inhibitory effect of Ag^+ on AO activity in PVA–BA entrapped cells and free cells was showed in Table 6-8. Silver ions at 0.05 mg/L inhibited AO in the PVA-BA entrapped cells by 7.0 ± 7.9%, whereas 52.7 ± 2.1% of AO activity in free cells were suppressed at the same Ag^+ concentration. Silver ion at 0.10 mg/L inhibited AO in the

entrapped cells by 24.1 ± 16.6% while it retarded AO in free cells up to 75.3 ± 1.8%. Similarly, AO in suspended cells was almost totally inhibited whereas it was partially suppressed in the entrapped cells (44.9 ± 1.9%). These findings revealed that PVA-BA-entrapped cells performed AO activity better than those of suspended cells under toxic effect of Ag^+.

Table 6-8 Percent inhibition of Ag^+ on AO from PVA–BA–entrapped cells

NH_4^+-N (mg/L)	Ag^+ 0.05 mg/L	Ag^+ 0.10 mg/L	Ag^+ 0.50 mg/L
9.6	0.0 ± 0.0 $^{c\,(d)}$	8.6 ± 0.1 $^{b\,(e)}$	57.2 ± 0.2 $^{a\,(b)}$
22.0	21.7 ± 0.5 $^{c\,(a)}$	35.8 ± 0.7 $^{b\,(b)}$	69.5 ± 0.0 $^{a\,(a)}$
36.7	2.7 ± 1.4 $^{c\,(c)}$	4.8 ± 0.8 $^{b\,(f)}$	25.4 ± 1.8 $^{a\,(d)}$
74.8	10.1 ± 0.7 $^{c\,(b)}$	31.1 ± 1.2 $^{b\,(c)}$	39.6 ± 0.7 $^{a\,(c)}$
97.6	0.0 ± 0.0 $^{c\,(d)}$	49.9 ± 3.7 $^{b\,(a)}$	57.5 ± 1.7 $^{a\,(b)}$
156.5	0.0 ± 0.0 $^{c\,(d)}$	14.5 ± 2.5 $^{b\,(d)}$	20.6 ± 1.4 $^{a\,(e)}$
Mean	**7.0 ± 7.9** ^{c}	**24.1 ± 16.6** ^{b}	**44.9 ± 1.9** ^{a}

Note: Different letters indicate statistical differences ($p<0.05$). Letters in the parentheses show the statistical differences for ammonia oxidation respect to initial NH_4^+-N. Letters without parentheses indicate the statistical differences for respect to initial Ag^+ concentrations. Letters from a to f indicated the from highest levels of inhibition to the lowest ones.

The remaining activity of AO in the PVA–BA entrapped cells was presented in Table 6-9. This table indicated that PVA–BA entrapped cells remained AO up to 75–100% and 79–100% at AgNPs 1–100 mg/L and Ag^+ at 0.05–0.50 mg/L, respectively. This study pointed out that PVA–BA could be highly effectively used to protect nitrifying bacteria from toxicity of both AgNPs and Ag^+.

Table 6-9 Estimation of AO activity remaining in PVA–BA–entrapped

Silver (mg/L)	% AO remaining in PVA–BA entrapped cells	% AO remaining in free cells
AgNPs		
1	60–100	37–56
10	49–93	21–53
100	30–75	18–34
Ag ions		
0.05	78–100	22–76
0.10	64–95	6–30
0.50	30–79	2–7

Currently, study using mixture of PVA and BA as entrapment matrix to mitigate toxicity effect of AgNPs and Ag^+ on ammonia oxidation process was not available. The present study clearly indicated that the PVA–BA entrapped cells were good in remaining AO from toxicity of AgNPs and Ag^+. Previous research mainly focused on PVA-CA, the mixture of PVA (8%) and sodium copolymer alginate (1%) and gelating agent 1% $CaCl_2$. Prior study found that the PVA-CA-entrapped cells could enhance nitrilase activity up to 98% [148]. The PVA-CA was used for immobilized cells to improve microbial activity and prolong the storage duration. PVA-CA was also used to entrap the cells *of Ochrobactrum* sp. applied in removing of Cr (VI) in the previous

study [181]. The overall removal rate of Cr (VI) was similar for free cells and entrapped cells. However, the more beneficiary of entrapped cells is that it could be applied in high concentration of Cr (VI) and the entrapped cells could be used several times [181].

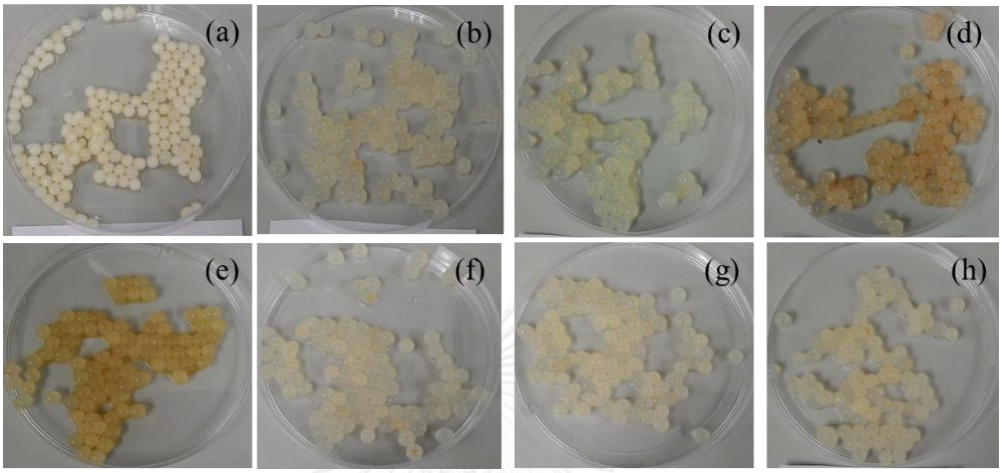

Figure 6-3 Photos of PVA-BA before and after experiment with AgNPs and Ag^+

Figure 6-3 demonstrated shapes of PVA-BA (a) before experiment, (b) after experiment-no silver, (c) after experiment at agNP 1 mg/L, (d) after experiment at AgNP 10 mg/L, (e) after experiment at AgNP 100 mg/L, (f) after experiment at Ag^+ 0.05 mg/L, (g) after experiment at Ag^+ 0.10 mg/L and (h) after experiment at Ag^+ 0.50 mg/L. The size of the mixture of PVA-BA gel beads after 60 h of experimental period become larger due to absorption of water but the shapes of the gel beads remained similar. The addition of SA into PVA improved quality of PVA in term of shape in SWW comparing to PVA only.

6.3.4 Abiotic process influencing on ammonium reduction

Ammonia reduction may have been influenced by other factors such as stripping out due to aeration process. Therefore, some abiotic tests were performed to elucidate abiotic factors influencing on ammonia reduction.

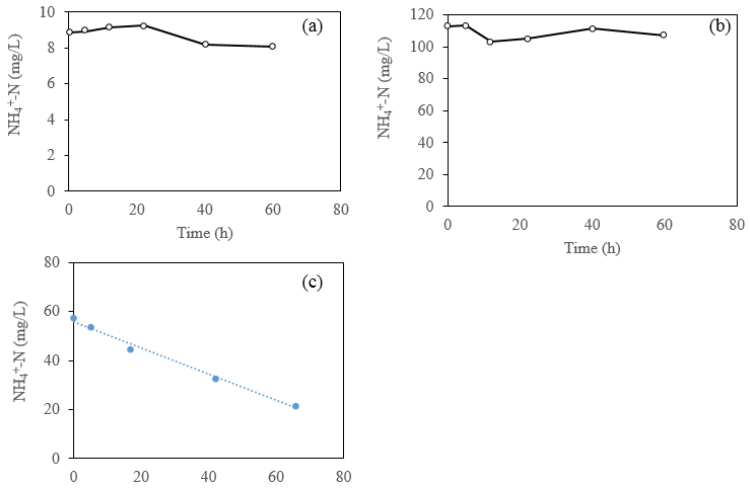

Figure 6-4 Test of sorption of ammonia on BA-entrapment matrix.

In Figure 6-4, (a) and (b) were change of low and high initial NH_4^+-N concentration under no aeration condition, whereas (c) was change of initial NH_4^+-N under aeration condition.

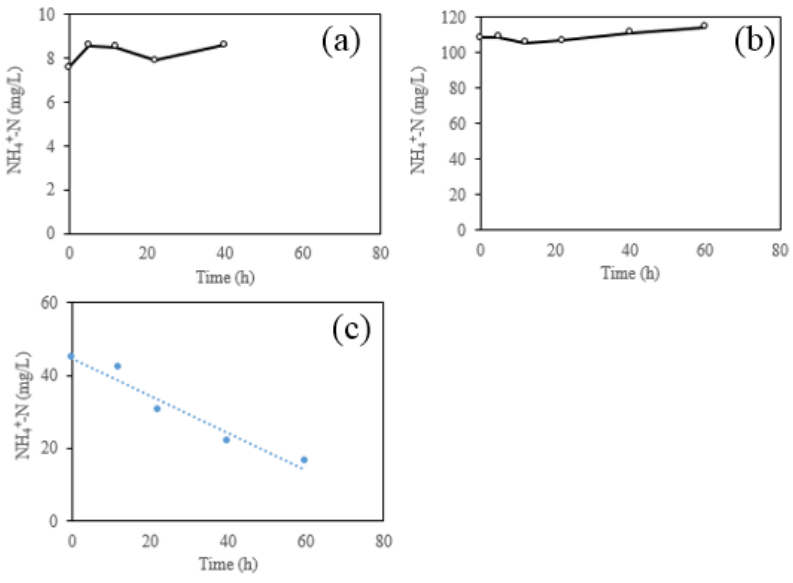

Figure 6-5 Test of sorption of ammonia on PVA-entrapment matrix.

It is noted that (a) and (b) were change of low and high initial NH_4^+-N concentration under no aeration condition, whereas (c) was change of initial NH_4^+-N concentration under aeration condition.

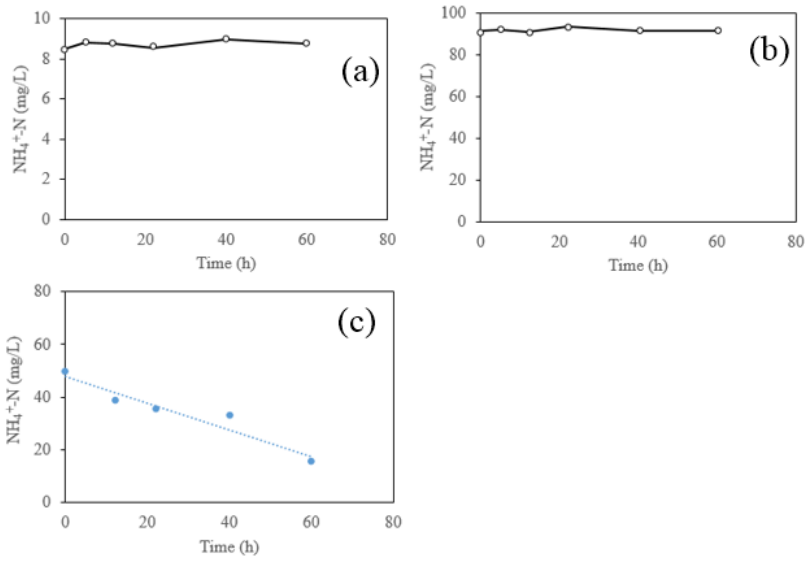

Figure 6-6 Test of sorption of ammonia on PVA-BA entrapment matrix.

In the Figure 6-6, (a) and (b) were change of low and high initial NH_4^+-N concentration under no aeration condition, whereas (c) was change of initial NH_4^+-N concentration under aeration condition.

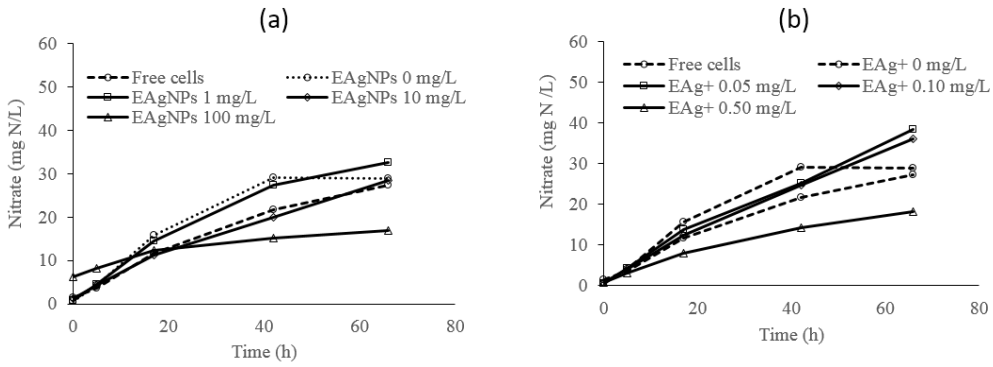

Figure 6-7 Production of nitrate from BA-entrapped cells under AgNPs (a) and Ag^+ (b) at initial NH_4^+-N of 50 mg/L.

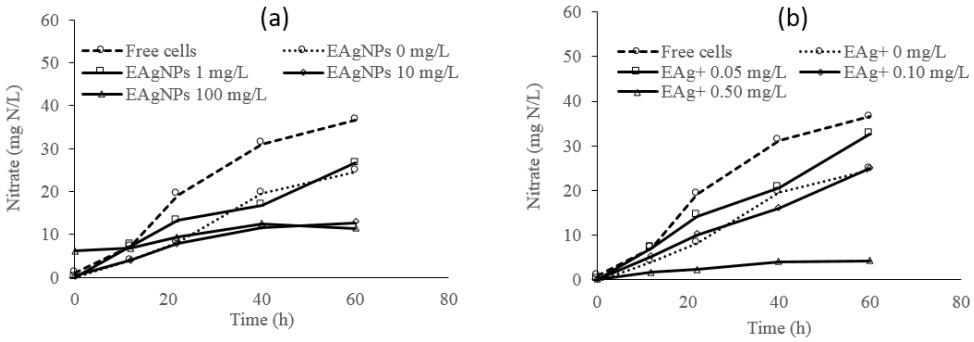

Figure 6-8 Production of nitrate from PVA-entrapped cells under AgNPs (a) and Ag^+ (b) at initial NH_4^+-N of 50 mg/L.

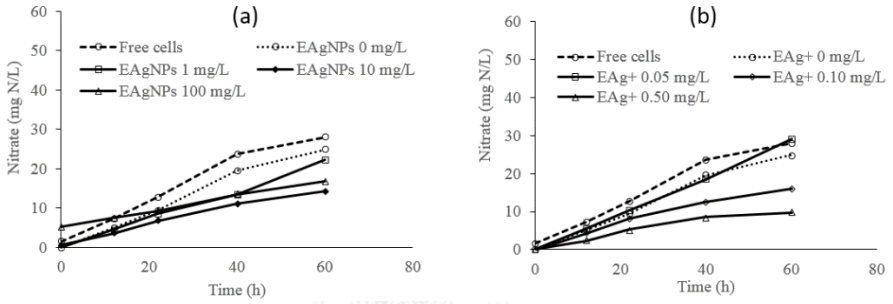

Figure 6-9 Production of nitrate from PVA-entrapped cells under AgNPs (a) and Ag^+ (b) at initial NH_4^+-N of 50 mg/L.

Figure 6-4 to 6-6 presented the change of ammonia concentrations in aerated and non-aerated conditions using BA-, PVA-, and PVA-BA-entrapment matrices (without nitrifying cells). Figure 6-4 a-b to Figure 6-6 a-b indicated that ammonium was not lost due to the entrapment matrices under no aeration since concentration of ammonium remained unchanged over 60-h- experimental period and nitrate was not produced. In contrast, in aerated condition, ammonium was lost at a rate of 0.54, 0.51, and 0.51 mg N/L/h due to evaporation for BA-, PVA-, and PVA-BA-entrapment matrices (without nitrifying cells). Therefore, the reduction of ammonium concentration in the inhibitory kinetics experiments was resulted from ammonia

oxidizing activity performed by microbes and ammonia loss due to evaporation. DO was used at approximate 6 mg/L since it was the optimum values applied for microbial activity in entrapped cells [138]. By comparing ammonium reduction of the entrapped cells control (entrapment material + nitrifying cells + no AgNPs or Ag^{+}) and the entrapped cells with addition of various AgNPs or Ag^{+} concentrations at the same initial ammonium concentrations, problem of ammonium loss due to evaporation could be solved, thus ammonium consumption by microbes was still valid for the discussion of inhibitory effect by AgNPs and Ag^{+}. The ammonium consumed by ammonia oxidizing microbes was reaffirmed by measurement of nitrate production under no silver, AgNPs and Ag^{+} supplement at the similar initial ammonium concentrations that were used for the study of ammonium loss in aeration conditions. The results presented in Figure 6-7 to 6-9 indicated that nitrate was produced at all experimental conditions meaning that ammonia oxidation process responsible for the production of nitrate. Inhibition calculated based on nitrate production also indicated similar tendency to inhibition calculated based on ammonium reduction.

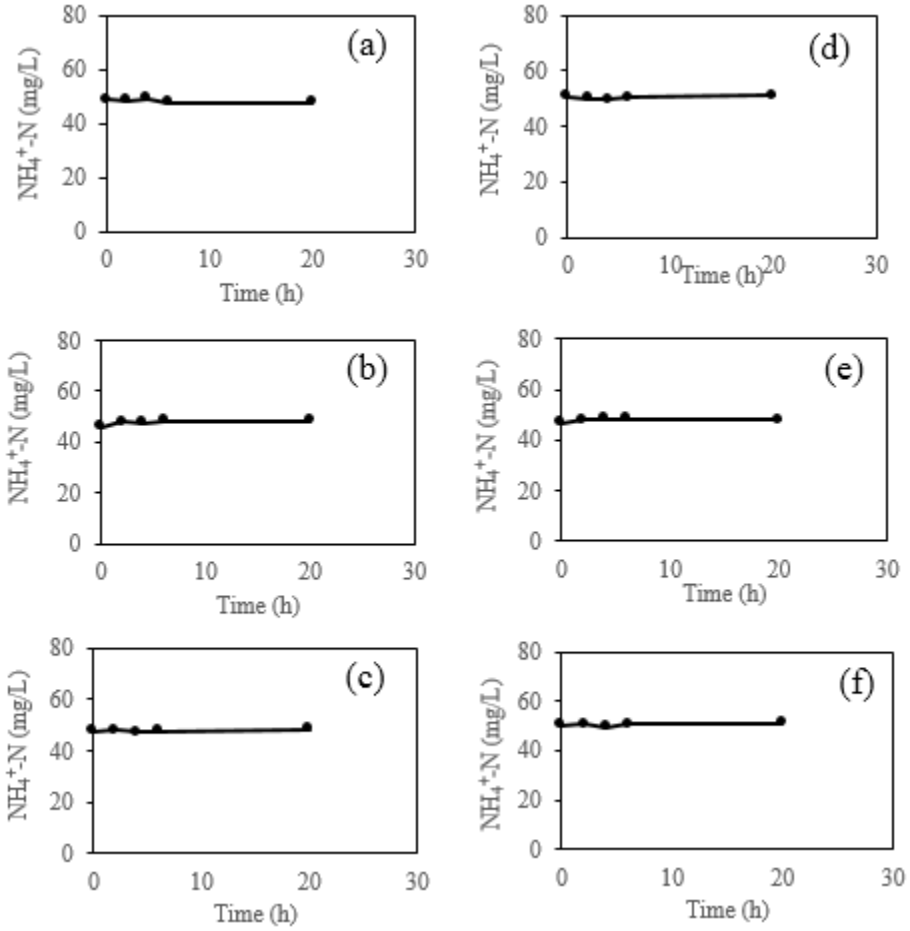

Figure 6-10 Change of initial NH_4^+-N concentration of 50 mg/L under presence of SWW with AgNPs or Ag^+.

In Figure 6-10, (a) was AgNPs at 1 mg/L, (b) AgNPs at 10 mg/L, (c) AgNPs at 100 mg/L, (d) Ag^+ at 0.05 mg/L, (e) Ag^+ at 0.1 mg/L, and (f) Ag^+ at 0.5 mg/L.

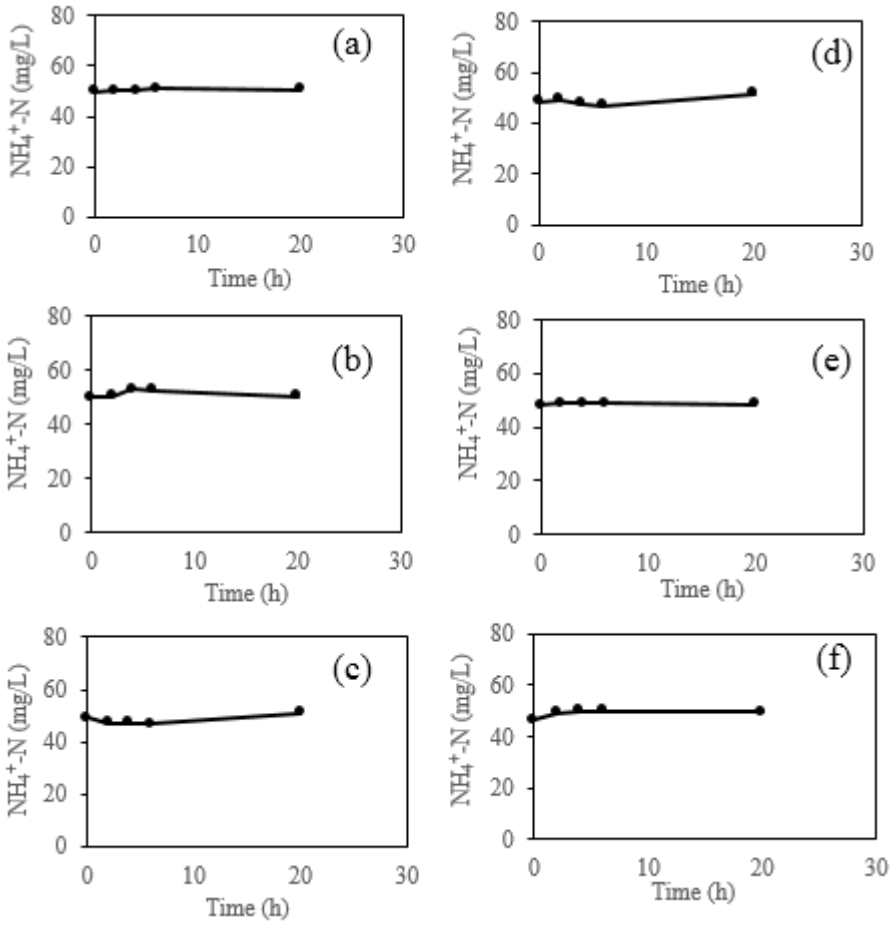

Figure 6-11 Change of initial NH_4^+-N concentration of 50 mg/L under presence of SWW plus autoclaved NAS 30 mM with AgNPs or Ag^+.

The label for Figure 6-11 was (a) AgNPs at 1 mg/L, (b) AgNPs at 10 mg/L, (c) AgNPs at 100 mg/L, (d) Ag^+ at 0.05 mg/L, (e) Ag^+ at 0.1 mg/L, and (f) Ag^+ at 0.5 mg/L. Figure from 6-10 to 6-11 clearly showed that the concentration of NH_4^+-N concentration in SWW only and SWW + autoclaved NAS 30 mM, respectively under presence of AgNPs and Ag^+ did not change and nitrate production was not detected over 20 h of experimental period indicating that there was no chemical reaction between ammonia and AgNPs and Ag^+. It was noted that aeration was not applied in these experiments.

The inhibitory kinetics results indicated that the entrapped cells using BA, PVA, and PVA-BA could alleviate harmful effect of AgNPs and Ag^+ via observing ammonia oxidation activity. Similar to suspended cells, AgNPs and Ag^+ influenced on AO from the entrapped cells follow concentration-dependent manner. In most cases, the impact of AgNPs on AO from the entrapped cells were higher than those of Ag^+ this could be possibly because AgNPs bind to bead surfaces and interfere transfer of oxygen and ammonia into the gel beads. Both AgNPs and Ag^+ still exhibited high toxicity to AO at high concentration (100 mg/L and 0.50 mg/L, for AgNPs and Ag^+, respectively) from entrapped cells but much lower compared to suspended cells.

On the other hand, the abiotic influence tests indicated that the use of the entrapped cells needed high oxygen to lessen limitation of oxygen diffusion into the gel beads. Therefore, for the further application, ammonia stripping out needed to be avoided.

6.3.5 Microscopic observation of internal structures of the entrapped cells

SEM images of BA-entrapped cells were performed and presented in Figure 6-10. As can be seen that several colonies of cells were found in the BA-matrices (Figure 6-10b-c). The cells did not occupy inside the pores, but the cells were surrounded by the BA-matrices. This was because numerous internal pores formed by ionic cross-linking between alginate and barium ions had very small diameters. These diameters of the sizes were estimated to range from 0.1-0.3 μm (Figure 6-10a). Previous study indicated that cross-linking between barium and alginate created a dense network with abundance of fine pores [138]. These pore sizes were smaller than the sizes of the cells (1-2 μm) and much smaller than sizes of colonies of the cells. This was the reason the cells could not stay inside the porous structures

but they were surrounded instead. Due to this porous structure, nitrifying cells inside the BA beads could perform ammonia oxidation since oxygen (0.155 nm in diameter) and ammonia (0.101 nm in diameter) and water (0.275 nm in diameter) could move in and reach the cells. However, toxic substances such as AgNPs (2-12 nm) and Ag^+ (0.115 nm in diameter) could also occur the entrapped cells since the diameters of these toxic substances are much smaller than diameters of the porous structure of BA-entrapped cells. Theoretically, AgNPs should have entered into the BA beads by transporting torturously inside and contacted with the cells. In this experiment, AgNPs was indirectly observed on the surface of BA-entrapped cells (in yellow color showed in Figure 6-1d), but AgNPs clusters were not detected inside the testing beads using EDS. This could mean that BA minimally reduced entrance of AgNPs into the beads. The minimal entrance of AgNPs maybe because AgNPs deposited on the surface of the entrapped cells, formed aggregates and interaction with cells in the outer layer of the beads. However, some cells were observed changing their shape from long rod-shaped to a shorter rod-shaped (Figure 6-10b-d). The change of cell morphology could be the response of cells under presence of AgNPs and Ag^+. The change of shape of the cells from long rod-shaped to shorter rod-shaped under presence of AgNPs or Ag^+ was consistent with the result found in Chapter 5.

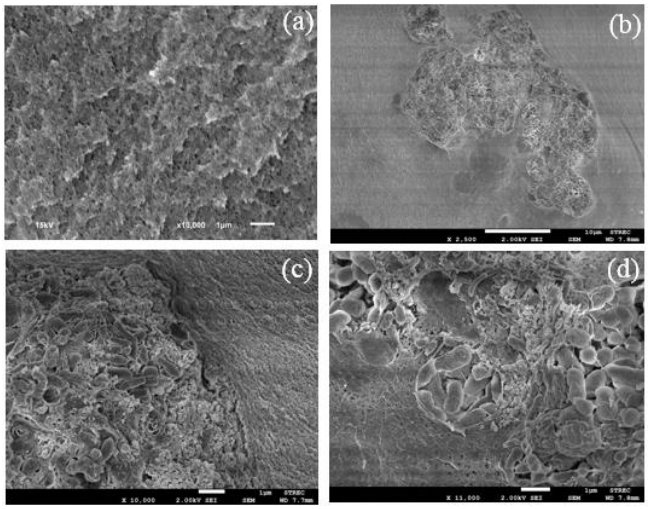

Figure 6-12 SEM micrographs for observation of BA-entrapped cells after 60-h exposed to AgNPs at 10 mg/L

The labels of Figure 6-12 were (a) the micro porous structures formed by ionic-cross linking between alginate and barium ions. The sizes of the pores were estimated far less than 1 µm observed at 10,000X. (b) cross-section of the BA-entrapped beads with several colonies of the cells found in the BA matrices observed at 2500X. (c) microbial cells were surrounded by BA-matrices observed at 10,000X. (d) A cluster of the cells with long and short-rod shapes observed at 11,000X.

Microscopic observation of the produced PVA-entrapped cells was presented in Figure 6-13. The internal pores were generated by the PVA-boron cross-linking between PVA and boric acid and they were also observed in the previous studies [15, 143]. It was estimated that PVA had the diameters of the internal pores ranged from 10-20 µm which were much larger than those of BA-entrapped cells and diameters of other molecules in the media including H_2O, NH_3, O_2, AgNPs, and Ag^+. The cells were observed distributed in the internal porous structures of PVA (Figure 6-13b-d). The porous structures of PVA allowed the diffusion of dissolved oxygen, ammonia and other nutrients to reach the cells. As a result, reduction of initial ammonium and production of nitrate were observed in the ammonia oxidation inhibition test. The

porous spaces also allowed transport of AgNPs and Ag^+ into the contact with the cells. However, with the observed entrapped cells beads, AgNPs were not detected inside the PVA-beads using EDS indicating that internal porous structures of PVA reduced contact between AgNPs and cells. In the previous part, it was found that AgNPs were easily detected forming cluster with suspended cells, but it was not found in the entrapped cells. This could be the role of entrapped cells in preventing contact between AgNPs and cells. In addition, phosphorylation of PVA on the exterior shell of the bead could further limit transportation of substances in the media into inside the beads (Figure 6-14). As can be seen from the Figure 6-16 that maximum ammonium oxidation rate in the PVA-entrapped cells was slightly lower than that in corresponding suspended cells. Changes of cell morphology from long-rod shaped to a shorter rod-shaped was also observed at AgNPs 10 mg/L (Figure 6-13b) after 60 h exposure. It could be possible that cells have changed their shape to respond to stressful condition resulted from the Ag^+ release from AgNPs and AgNPs. However, AgNPs were not detected in some beads even though AgNPs were found deposited on the surface of PVA-entrapped cells (Figure 6-2d). This could suggest the release of Ag^+ possibly play main role in toxicity of AgNPs suspension in the experimental condition.

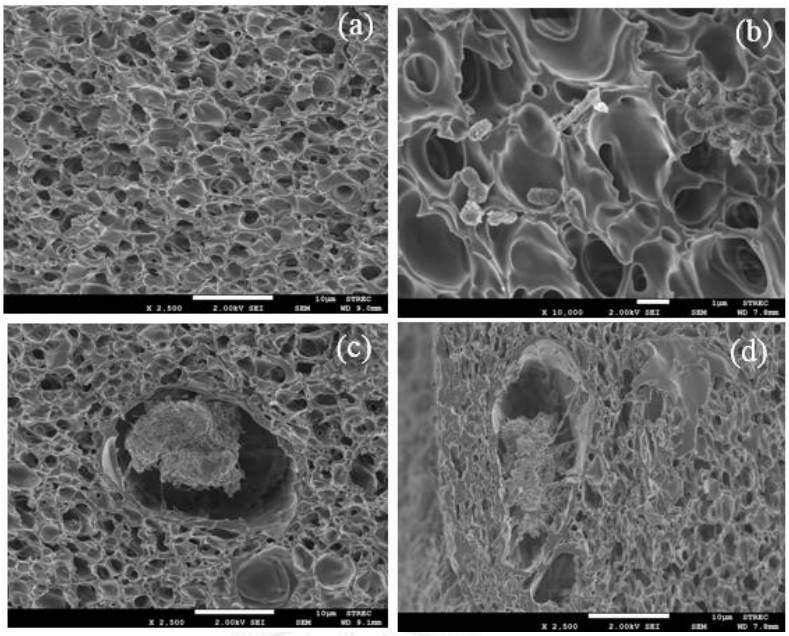

Figure 6-13 SEM micrographs for observation of PVA-entrapped cells after 60-h exposed to AgNPs at 10 mg/L.

In this Figure 6-13, (a) Cross-section of the PVA-entrapped bead without nitrifying cells observed at 2,500X. The micro porous structures formed by cross linking between PVA and boric acid. The sizes of the pores were estimated from 10- 20 µm observed at 10,000X. (b) Nitrifying cells distributed in the internal spaces of PVA beads observed at 10,000X. (c-d) clusters of cells in observed in at 2,500X.

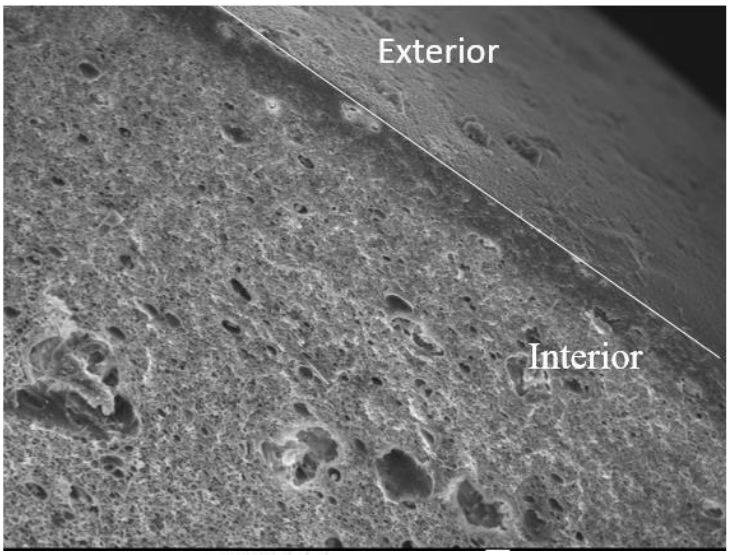

Figure 6-14 SEM micrograph demonstrating exterior and interior parts of PVA-entrapped cells observed at 400X.

The internal structure of PVA-BA entrapped cells was observed and illustrated in Figure 6-15. When BA was incorporated into the PVA, it makes the internal porous structure of PVA become more dense (Figure 6-15a) compared to PVA only. In addition, PVA-BA beads were less sticky and easier to handle than PVA-entrapped cells. The internal diameters of pore sizes of PVA-BA entrapped cells were probably larger than those of PVA (Figure 6-15b). The addition of SA into PVA could perturb the formation of PVA crystallites and disordered-crystalline phase and reduced density of cross-linking [183]. Cells were observed in the porous structures of PVA-BA (Figure 6-15a-b). The internal porous structures of PVA-BA allowed essential nutrients reached the cells inside the beads that could support them in utilizing ammonia. The external layer of PVA-BA entrapped cells was more roughness than that of PVA-entrapped cells (Figure 6-16). Prior study proposed that big difference in the miscibility degree between PVA and SA could result in significant surface roughness differences between PVA

only and PVA-SA [148, 183, 184]. The reported observation of roughness surface could be the same for this study. The white balls on the external layer of PVA-BA entrapped cells were barium alginate which was confirmed by EDX. This external layer could further limit transport of essential nutrients as well as toxic substances into the beads. However, ammonium oxidation rate in the PVA-BA entrapped cells and corresponding suspended cells were almost the same indicating that ammonia and oxygen were not limited inside the PVA-BA entrapped cells (Figure 6-17). Similar to BA and PVA-BA, none of AgNPs were detected inside the tested PVA-BA beads which could mean that PVA-BA limited transportation and penetration of AgNPs into the bead. However, the change of the shape of cells and inhibition of ammonia oxidation indicated that silver having impact on nitrifying bacteria located in the PVA-BA-entrapped cells.

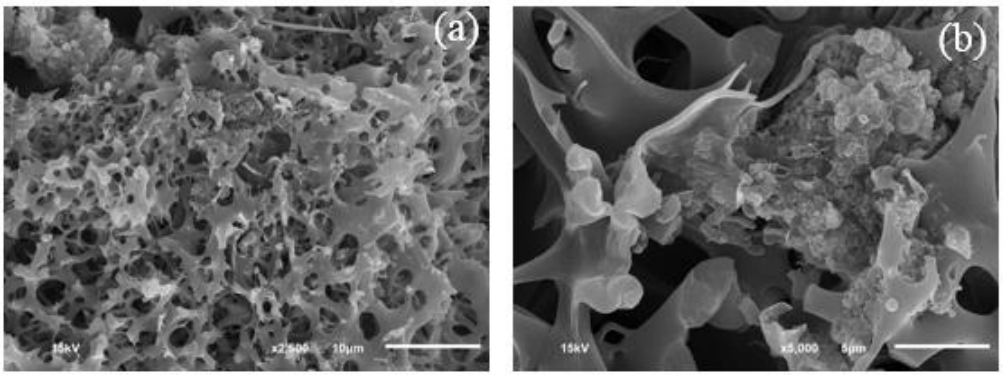

Figure 6-15 SEM micrographs for observation of PVA-BA- entrapped cells after 60-h exposed to AgNPs at 10 mg/L.

In Figure 6-15, (a) Cross-section of the PVA-BA entrapped bead with nitrifying cells observed at 2,500X. (b) The micro porous structures formed by the mixture between PVA and BA observed at 5,000X. The internal porous structure were relatively similar to those of PVA only, but PVA-BA were more dense branches.

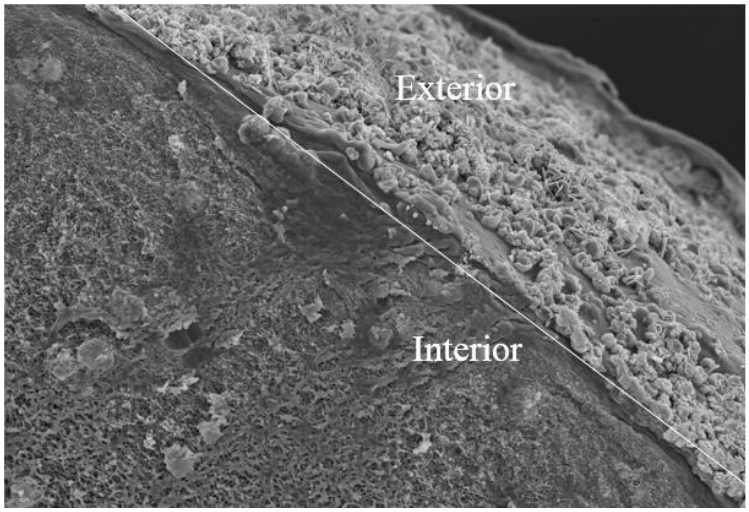

Figure 6-16 SEM micrograph demonstrating exterior and interior parts of PVA-BA entrapped cells.

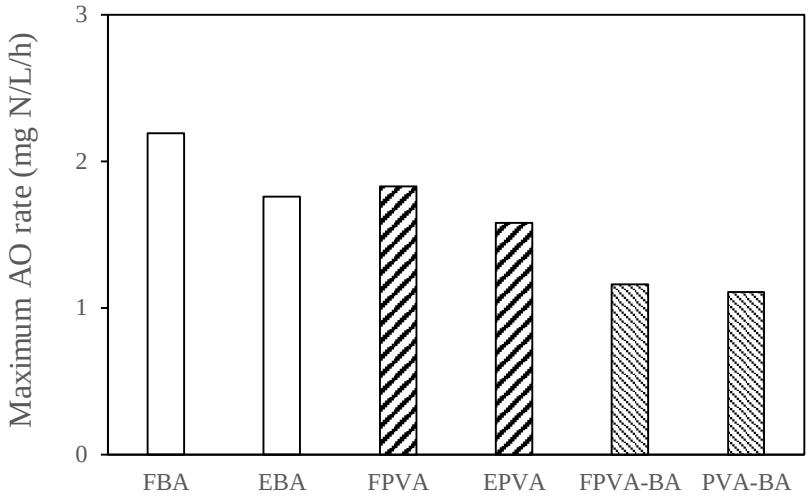

Figure 6-17 Maximum AO rates in the entrapped cells and corresponding free cells under control conditions

In Figure 6-17, F is abbreviation of free cells; E is abbreviation of entrapped cells. For example, FBA, FPVA, FPVA-BA were the free cells kinetics conducted at the same time with BA-entrapped cells (EBA), PVA-entrapped cells (EPVA) and PVA-BA-entrapped cells (PVA-BA).

Microscopic observation of the entrapped cells using BA, PVA and PVA-BA indicated that the internal porous structures of these beads were different which could result in difference in ammonium oxidation rates for the cells entrapped in. The maximum ammonium oxidation rates in the entrapped cells using PVA-BA or BA were equal or higher than those in corresponding free cells, respectively. In contrast, maximum ammonium oxidation rate in the entrapped cells was lower than that of corresponding suspended cells for the case of PVA only (Figure 6-17). This observation was also reported in the previous study [185]. In addition, difference in AO rates may be due to quantity and activity survived bacteria after entrapment processes [141]. A former study reported that the percent of live cells in the entrapment (39–62%) was less than those in the corresponding suspended culture (54–74%) before the entrapment was made [186]. In addition, this could be because PVA demonstrates significant feature of oxygen barrier due to its firm-forming characteristic [187]. The interior pores sizes of the entrapped cells should not limit transfer of oxygen and ammonia into the beads since they were much larger than those of oxygen and ammonia. The difference could be from the structure of external layers. Previous study suggested that the beads with pore sizes of 2 μm should not cause any constraint for transfer oxygen and substrate into the gel bead matrices [188]. However, the entrapped cells could limit transportation and penetration of the nutrients and the toxic substances AgNPs into the beads due to agglomeration in the bulk media, deposition on the surfaces of the beads, and barriers from the cells-entrapment matrices. The reduction of ammonia oxidation rates at AgNPs 10 mg/L indicated the impact of silver species. SEM results revealed that shapes of some cells in the gel beads changed from long rod-shaped to shorter-rod shaped suggesting the impact of silver species on microbial cells entrapped in the materials.

AgNPs were not found in the entrapped cells, but they could harm ammonia oxidation process via release of Ag^+ as found in the previous part of this study.

6.3.6 Microbial viability observation in the entrapped cells

Testing of viability of cells in the BA-entrapped cells after 60-h exposure to AgNPs and Ag^+ was performed and the results were presented in Figure 6-18. It was clearly indicated that the proportions of dead cells between free cells (collected directly from the enriching reactor NAS 30 mM) and the entrapped cells control (entrapped cells without AgNPs or Ag^+) were insignificantly different which could mean that BA was not toxic to microbial cells and the BA-entrapped cells preparation process did not cause cell death. Prior study reported that sodium alginate gelated with calcium ions was not harmful to microbes [136, 186]. Other study also demonstrated that barium alginate microbeads did not affect cell viability [189]. The replace of calcium ions by barium ions did not cause any harmful effect for nitrifying cells under this experimental condition. Increasing the amounts of AgNPs and Ag^+ addition into the BA-entrapped cells resulted in an increase in percentage of membrane compromised cells (Figure 6-18). This indicated that the cause of damage of cell membrane was from AgNPs and Ag^+. AgNPs from 1-100 mg/L resulted in membrane integrity damaged by 18.9 ± 14.7% - 52.2 ± 7.9%, whereas Ag^+ 0.05-0.50 mg/L caused membrane integrity damaged by 10.1 ± 8.9% - 23.2 ± 13.3%. This result agreed with the data of AO inhibition. In the previous experiments with suspended cells, it was found that AgNPs from 1-100 mg/L damaged membrane integrity by 29.7 ± 16.2% - 81.8 ± 12.8 % and Ag^+ 0.10-0.50 mg/L damaged by 14.1 ± 6.3% - 79.5 ± 15.0%. Comparing the proportions of dead cells between free cells and entrapped cells after exposed to AgNPs and Ag^+ clearly showed

that cells entrapped in BA were less damaged by AgNPs and Ag^+ than those of suspended cells.

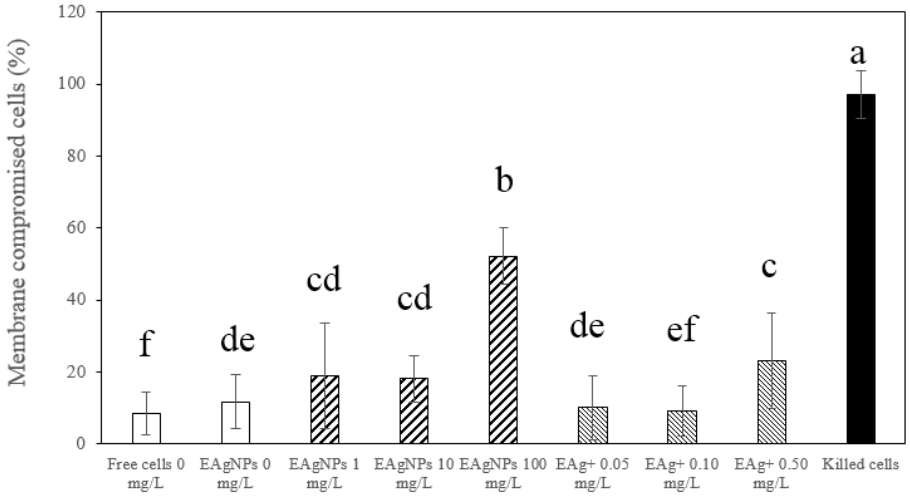

Figure 6-18 Percent of cell membrane from BA-entrapped cells damaged by AgNPs and Ag^+ after 60 h of exposure to AgNPs and Ag^+.

The average percentage of Live/Dead results were calculated based on 10 CLSM images. Error bars represent the standard deviation. Different letters indicate statistically significant ($p < 0.05$). Letters from a to f indicated the from highest levels of membrane damaged to the lowest ones.

The Live/dead results of PVA-entrapped cells after 60-h exposed to silver species was presented in Figure 6-19. Similar to BA-entrapped cells, PVA was non-toxic to microbial cells since dead cells proportions between the free cells control and the PVA-entrapped cells control were not statistically significantly difference ($p > 0.05$). PVA was previously reported not substantial cause dead for the microbes being entrapped [143, 186]. It was found that AgNPs at 1-10 mg/L and Ag^+ at 0.05 mg/L did not show pronounced damage on membrane integrity of the cells entrapped in PVA (Figure 6-19). Increasing supplement of AgNPs from 10-100 mg/L (15.9 ± 13.1% –

34.6 ± 13.4%) and Ag^+ from 0.10-0.50 mg/L (20.2 ± 8.0% – 42.8 ± 15.3%) resulted in more significant difference in damaging membrane integrity of the entrapped cells compared to the lower ones. Ag^+ at 0.50 mg/L resulted in higher proportions of cell death than that at AgNPs at 100 mg/L. This could be Ag^+ have smaller diameter thus easily reached inside the beads and caused cell damage or Ag^+ was much more toxic than AgNPs. However, cells entrapped in PVA was less damaged by AgNPs and Ag^+ compared to free cells. This could be because porous structures of PVA stopped AgNPs and Ag^+ moving freely from bulk media to internal parts of the PVA beads, thus protecting the cells. During examining internal structure of PVA-entrapped cells using, EDX was applied to detect AgNPs, however, AgNPs were not detected inside the beads. It could be the role of PVA-entrapped cells and it is also possible that AgNPs influenced on the microbial cells in the bead by releasing Ag^+.

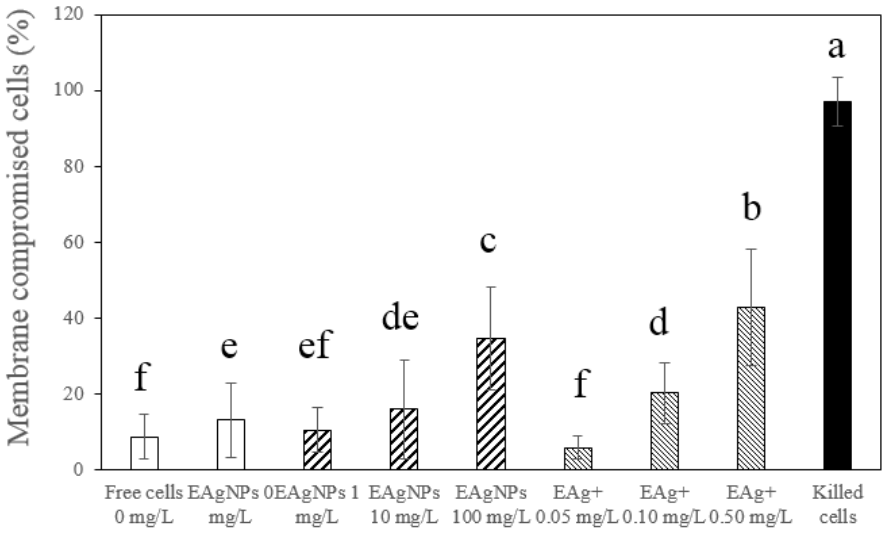

Figure 6-19 Percent of cell membrane from PVA-entrapped cells damaged by AgNPs and Ag^+ after 60 h of exposure to AgNPs and Ag^+.

The average percentage of Live/Dead results were calculated based on 10 CLSM images. Error bars represent the standard deviation. Different letters indicate statistically significant ($p < 0.05$). Letters from a to f indicated the from highest levels of membrane damaged to the lowest ones.

Proportion of dead cells after letting the nitrifying cells entrapped in PVA-BA exposed to AgNPs and Ag^+ for the period of 60-h was presented in Figure 6-20. On the contrary to BA- and PVA-entrapped cells, the percent of dead cells between PVA-BA-entrapped and free cells under control condition were significantly different ($p < 0.05$). In the previous discussion, BA and PVA are non-toxic to microbial cells, so the mixture of the two should not cause toxicity for the entrapped cells. Therefore, more damaged cells in PVA-BA entrapped cells control could be possibly the result of mixing two types of entrapment materials and white balls on the exterior shell resulting in less diffusion of oxygen and ammonia into the beads. It could be other reason, for example, cells damaged during breaking the beads.

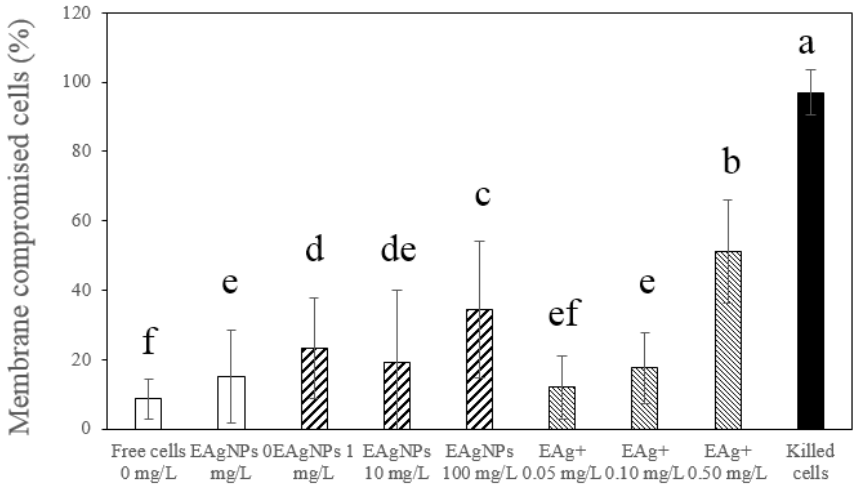

Figure 6-20 Percent of cell membrane from PVA-BA-entrapped cells damaged by AgNPs and Ag^+ after 60 h of exposure to AgNPs and Ag^+.

The average percentage of Live/Dead results were calculated based on 10 CLSM images. Error bars represent the standard deviation. Different letters indicate statistically significant ($p < 0.05$). Letters from a to f indicated the from highest levels of membrane damaged to the lowest ones.

The damage of membrane integrity in the treatments with entrapped cells control (15.1 ± 13.3%), entrapped cells with AgNPs at 1 mg/L (23.1 ± 14.5%), and entrapped cells with Ag^+ 0.05-0.10 mg/L (12.1 ± 9.1% - 17.6 ± 10.3%) was not significantly different. However, increased concentrations of AgNPs and Ag^+ to 100 mg/L and 0.5 mg/L, respectively resulted in significant higher membrane integrity damaged by 34.4 ± 19.7% and 51.0 ± 14.9%, respectively. This data supported inhibition data since high inhibition of ammonia oxidation activity was also found high at AgNPs 100 mg/L and Ag^+ 0.50 mg/L. However, the Live/dead results clearly indicated that PVA-BA could effectively reduce damage of cell membrane under presence of AgNPs and Ag^+ compared to those of free cells. SEM micrographs indicated that PVA-BA played role in reducing cell damaged since it generated porous structures which could minimize the entrance of AgNPs and Ag^+ into the internal parts of the gel bead. An attempt was made to detect AgNPs in the bead using EDX but no AgNPs were detected. It could be because PVA-BA entrapped cells limit transportation and penetration of AgNPs into contact with cells.

In overall, live and dead results indicated that the entrapment materials including BA, PVA, and PVA-BA were non-toxic to the entrapped microbes. This characteristic of high cell viability is important for future use of these entrapment materials for practical purposes [144]. This further indicated that simplified form of

SWW wastewater used throughout in the experiments of the entire study was suitable for short-term test with ammonia oxidation process. Increasing AgNPs or Ag^+ concentration resulted in an increase of percentage of membrane compromised cells indicating that AgNPs or Ag^+ were the main cause of membrane integrity damage. The data of membrane integrity damage agreed with data of inhibition test discussed in the early section. Previous studies reported that exposed to silver species resulted in cell dead [6, 7]. Live and dead and inhibition results were supported by SEM results that cells entrapped in the entrapment materials were less membrane integrity damaged compared to the suspended cells after exposed to AgNPs and Ag^+. In addition, SEM results showed that AgNPs were not observed in the entrapped cells while AgNPs clusters were obviously observed in free cells. This leads to conclusion that entrapment materials reduced chance for cells to contact with AgNPs by minimizing the freely moving of AgNPs into the entrapped cells. Prior studies suggested that torturous transport and sorption of AgNPs were the main cause for lessening the nitrification inhibition [15]. However, it could be possible that AgNPs released Ag^+ and then Ag^+ diffused into the entrapped cells resulting in damage of cell membrane. It conclusion, higher dead cells resulted in higher inhibition of ammonia oxidation in suspended cells, and this tendency was the same for the entrapped cells but cells entrapped in entrapment materials were less damaged by AgNPs and Ag^+ that it was found in suspended cells. This is the beneficial role of the entrapment materials.

6.3.7 Stability test of the entrapped cells in synthetic wastewater

The stability of BA, PVA, and PVA-BA-entrapped cells in synthetic wastewater was performed by using rotary shaker at the rate of 200 rpm for 30 days. The photos of the

beads were presented in Figure 6-21. As can be seen that BA-beads and PVA-BA gel beads became weaker due to water absorption but they still remained their shape. However, PVA-beads were weak and deformed. This phenomenon was also observed in the previous study [136]. It showed that addition of BA into PVA could help to improve stability of PVA in synthetic wastewater. This result was in line with other studies that combination of PVA and BA resulted in more stability of the produced gel beads and could be stored for a long time [137, 148]. PVA bead were deformed because of its water-soluble and hydrophilic natures. Among the types of entrapped cells, BA was the most stable, and then PVA-BA over 30 days of shaking in synthetic wastewater containing various AgNPs concentrations. Previous study also reported that BA was stable during long-term operation and supported growth of the entrapped microbes [138].

It was also observed that the yellow color of AgNPs suspension was disappeared in the treatment with BA-entrapped cells. The disappearance of the yellow color could indirectly indicate that the nano sizes of AgNPs have been lost due to formation of AgNPs aggregates [157]. Yellow color in the treatment using PVA- and PVA-BA-entrapped cells was more intense than that observed in BA-entrapped cells. It could mean that AgNPs in the treatments with PVA, PVA-BA were less aggregated than that in BA-entrapped cells.

Changes of AgNPs concentrations due to different types of the entrapment matrices in the stability experiment were presented in Table 6-10. It was found that AgNPs concentrations significantly reduced by 73.8% and 78.8%, and 48.4% at AgNPs concentrations of 1, 10 and 100 mg/L, respectively in BA–entrapped cells, after

experimental period of 72 h. This result was in line with the observation that yellow color was disappeared on the surface of the BA-entrapped beads. The reduction of AgNPs concentration in the BA–entrapped cells found in this study was in accordance with the prior study which showed that alginate could strongly bind to AgNPs [190]. The binding of aggregates of AgNPs on the surface of BA-entrapped cells could block the ways of movement of dissolved oxygen and ammonia into the internal parts of the BA-entrapped cells beads which could retard ammonia oxidation process taking place in the beads. Data in Table 6-10 also indicated that exposure of AgNPs to PVA–and PVA–BA entrapped cells did not result in significant reduction of AgNPs concentrations over 72-h of the experimental period. It could imply that the AgNPs remained in nano form. These results agreed with the previous discussion that yellow color still remained on the surfaces of PVA- and PVA-BA entrapped cells.

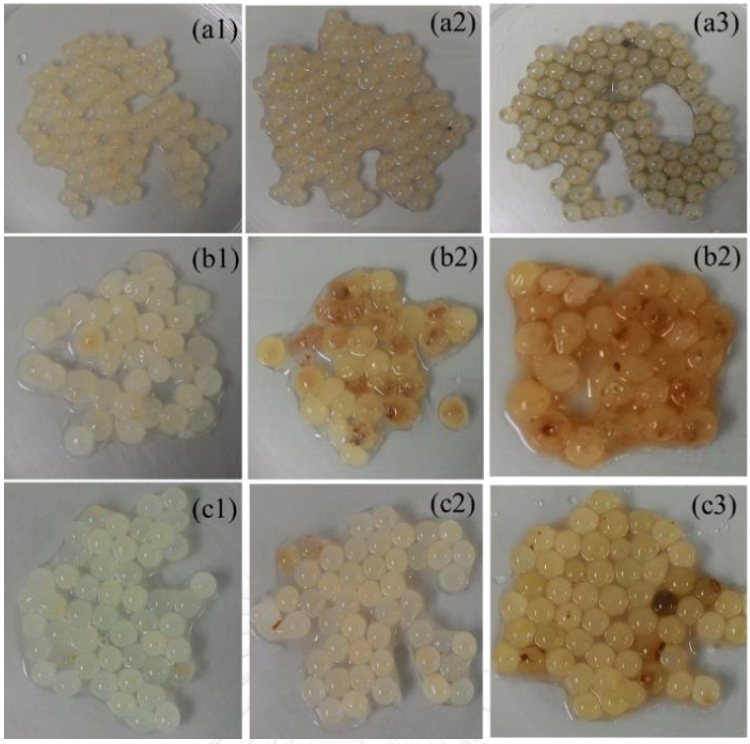

Figure 6-21 Photos of cells entrapped in different entrapment matrices after 30 days shaken at 200 rpm.

In Figure 6-21, (a1) BA at AgNPs 1 mg/L, (a2) BA at AgNPs 10 mg/L, and (a3) BA at agNP 100 mg/L; (b1) PVA at AgNP 1 mg/L, (b2) PVA at AgNP 10 mg/L, and (b3) PVA at AgNPs 100 mg/L; (c1) PVA-SA at AgNPs 1 mg/L, (c2) PVA-BA at AgNPs 10 mg/L and (c3) PVA-BA at AgNPs 100 mg/L.

Table 6-10 Changes of AgNPs due to different types of entrapped–cells

Type of entrapped cells	Time (h)	AgNPs 1 mg/L	AgNPs 10 mg/L	AgNPs 100 mg/L
BA	0	1.11 ± 0.07 [a]	10.12 ± 0.54 [a]	81.60 ± 0.98 [b]
	2	0.73 ± 0.01 [b]	7.76 ± 0.24 [b]	88.41 ± 2.83 [a]
	24	0.35 ± 0.01 [c]	3.25 ± 0.07 [c]	83.56 ± 1.41 [b]
	48	0.30 ± 0.01 [cd]	2.45 ± 0.06 [d]	57.18 ± 3.84 [c]
	72	0.29 ± 0.00 [d]	2.15 ± 0.04 [d]	42.11 ± 0.95 [d]
PVA	0	1.03 ± 0.09 [a]	9.92 ± 0.68 [a]	83.63 ± 5.00 [c]
	2	1.11 ± 0.05 [a]	10.59 ± 0.56 [a]	96.6 ± 4.89 [a]
	24	1.15 ± 0.06 [a]	10.48 ± 0.65 [a]	102.04 ± 2.72 [a]
	48	1.15 ± 0.06 [a]	10.70 ± 0.16 [a]	91.24 ± 2.27 [ab]
	72	1.08 ± 0.03 [a]	10.12 ± 0.59 [a]	96.53 ± 6.29 [a]
PVA–BA	0	1.04 ± 0.04 [b]	9.81 ± 0.63 [a]	91.67 ± 1.30 [bc]
	2	1.14 ± 0.03 [a]	10.33 ± 0.45 [a]	95.73 ± 0.98 [b]
	24	1.04 ± 0.02 [b]	10.27 ± 0.40 [a]	102.33 ± 0.22 [a]
	48	0.98 ± 0.01 [c]	10.18 ± 0.38 [a]	87.04 ± 2.05 [e]
	72	0.97 ± 0.01 [c]	10.07 ± 0.33 [a]	90.01 ± 4.65 [cd]

Note: Different letters indicate statistically significant ($p < 0.05$) respect to time. Letters from a to d indicated the concentrations of AgNPs changed from highest to the lowest ones.

6.3.8 Comparative mitigation of the entrapment matrices on AO influenced by AgNPs and Ag^+

The entrapment materials presented the high effectiveness in mitigating toxicity impact of AgNPs and Ag^+ (at low concentrations) on AO in the entrapped cells. However, BA and PVA-BA retained high cell viability and they were more stable entrapped beads in long-term shaken in SWW. Thus, use of BA and PVA-BA for further development and treatment of AgNPs contaminated wastewater could be a promising technology.

Table 6-11 Maximum percent of AO remaining under AgNPs and Ag^+ stress

Type of entrapped cells	Type of silver	Maximum AO remaining (%)
BA	AgNPs	81–100%
	Ag ions	98–100%
PVA	AgNPs	57–97%
	Ag ions	61–99%
PVA–BA	AgNPs	75–100%
	Ag ions	79–100%

6.4 Summary

Toxic impact of AgNPs and Ag^+ on ammonia oxidation process was mitigated using BA, PVA and PVA–BA. The findings demonstrated the entrapped cells using BA, PVA, and PVA–BA remained AO up to 81–100%, 57–97%, and 75–100% at AgNPs from 1–100 mg/L, whereas remained AO up to 98–100%, 61–99%, and 79–100% under Ag^+ concentrations from 0.05–0.50 mg/L, respectively. Live and dead results revealed that cells entrapped in BA, PVA, and PVA-BA were less damage of membrane integrity

than that of free cells under toxic condition of AgNPs and Ag^+. In addition, the entrapment materials were non-toxic to microbial cells in short term test. Increasing AgNPs and Ag^+ concentration led to increase of membrane compromised cells which could indicate that damage of cell membrane was caused by AgNPs or Ag^+ or the two species. SEM results showed that AgNPs were not detected in the entrapped cells. Microscopic observation of internal structures of the entrapped cells suggested that the porous structures of the internal parts of the entrapped cells could help to limit transportation and penetration of AgNPs into the internal parts of the entrapped cells beads. Since AgNPs were not detected inside the beads and entrapment materials were not the cause of membrane integrity damage led to a suggestion that Ag^+ possibly play role in toxicity of AgNPs suspension. Among the entrapped cell types, BA and PVA-BA were the most promising entrapment materials because they showed low dead cells and more stable in synthetic wastewater. Future study on long-term impact of AgNPs and Ag^+ on ammonia oxidation activity and microbial community change in entrapped cells should be investigated.

Chapter 7 Conclusions and Recommendations

7.1 Conclusions

Conclusion 1: Toxicity effect of AgNPs and Ag^+ against AO was compared between NAS 0.5 mM and NAS 30 mM. The study demonstrated that both AgNPs and Ag^+ were highly toxic to AO activity, especially for the nitrifying culture with low Ks values which could imply that AO from municipal WWTPs could bear more devastating impact by AgNPs and Ag^+ than industrial WWTPs. Concentrations of AgNPs of 1-100 mg/L inhibited AO activity by 90.6 ± 8.6% – 94.8 ± 4.3% and 44.9 ± 2.4% – 73.8 ± 1.5%, whereas Ag^+ concentration of 0.05 – 0.50 mg/L inhibited by 86.3 ± 0.8% – 93.4 ± 1.24% and 52.7 ± 2.14% – 93.9 ± 1.89% for NAS 0.5 mM and NAS 30 mM, respectively. Inhibitory kinetics results suggested that Ag^+ was much more toxic than that of AgNPs, and AO activity in NAS 30 mM was able to better tolerate to toxicity effect of AgNPs and Ag^+. The difference in inhibitory effect could be attributed to variation in physical characteristics and microbial community structures of ammonia oxidizing microbes in the two nitrifying cultures.

Conclusion 2: Inhibitory kinetics and mechanisms of AO from NAS 30 mM influenced by AgNPs and Ag^+ were studied. Amendment of AgNPs and Ag^+ into wastewater adversely inhibited on AO process. Silver ions of 0.05 to 0.50 mg/L inhibited AO by 53 – 94% whereas AgNPs of 1 to 100 mg/L reduced AO by 45 –74%. Silver ions was much more toxic to AO than AgNPs. Silver nanoparticles released the averaged amounts of Ag^+ at 0.059, 0.171 and 0.503 mg/L over 60-h experimental period

at initial AgNPs concentrations of 1, 10, and 100 mg/L, respectively. The release of Ag^+ mainly caused toxic impact of AgNPs on AO from nitrifying sludge. Microscopic observation indicated that AgNPs attached to microbial cell surfaces and resulted in morphological change. Microbial cells exposed to AgNPs and Ag^+ become less defined membrane and density of internal cell matters leading to cell death. This study suggested that the primary mechanism for toxicity of AgNPs was the liberation of Ag^+ and then both of silver species caused cell death.

Conclusion 3: The inhibitory effect of AgNPs and Ag^+ on AO from NAS 30 mM could be effectively mitigated by using cell entrapment technique. The study found that BA, PVA, and PVA-BA entrapped cells could remain AO activity at 81–100%, 57–97%, and 75–100% at AgNPs 1-100 mg/L, whereas the remained AO activity up to 98–100%, 61–99%, and 79–100% under Ag^+ concentrations from 0.05-0.50 mg/L, respectively. Live and dead results revealed that cells entrapped in BA, PVA, and PVA-BA were less damage of membrane integrity than that of free cells under toxic condition of AgNPs and Ag^+ which could further confirm benefit of using entrapped cells to mitigate negative influence of AgNPs and Ag^+ on AO. The main mechanisms for reducing toxicity of AgNPs and Ag^+ by using entrapped cells were that the entrapment matrices limit transportation and penetration of AgNPs into the entrapped cells beads thus reducing contact between ammonia oxidizing cells and silver due to porous internal structures generated from the entrapment materials.

The entrapped cells could be possibly applied to reduce toxicity impact of AgNPs and Ag^+ on ammonia oxidation process from NAS 0.5 mM. However, the efficiency of the protection could be possibly lower since the proportions of active biomass were

significantly lower compared to that of NAS 30 mM. Alternatively, additional treatment unit, for example tank rich sulfide, could be inserted to precipitate silver species before letting the wastewater contaminated with AgNPs and Ag^+ entering the aeration tank in wastewater treatment systems.

7.2 Application in the environmental field

This study found that AgNPs caused toxicity for ammonia oxidation process through released Ag^+. This information can be used for preventing the WWTP system failure from AgNPs and the released Ag^+ by taking relevant pre-treatment measures (precipitation of AgNPs and Ag^+ before letting the wastewater contaminated with silver move into the biological treatment units) for both AgNPs and Ag^+. The result of this study can be used to communicate with the practitioners to better manage AgNPs discharged to potential reduction of environmental impact.

The entrapped cells using entrapment materials could be used for treating ammonia under presence of AgNPs and Ag^+ or both.

It is noted that the toxicity of AgNPs could be enhanced in aeration-based wastewater treatment system through releasing Ag^+. In anaerobic wastewater treatment system, the toxicity of AgNPs may be lowered since silver exhibited high affinity to sulphide leading to precipitation of silver species. Therefore, the results of this study would be valuable for consideration when design and operation of activated sludge systems such as those in municipal and industrial wastewater treatment systems.

7.3 Recommendations

Silver nanoparticles are toxic to microorganisms, particularly ammonia oxidizing microorganisms in municipal WWTP. Therefore, production and use of AgNPs should be more strictly and properly managed to prevent its detrimental effect on nitrogen removal performance.

Future study should investigate the role of EPS in relation of toxicity of AgNPs and Ag^+ on the nitrifying cultures. In addition, further research should be extended to examine toxicity impact of AgNPs and Ag^+ on individual groups of nitrifying bacteria who complete nitrification process.

Future study should focus on optimization of strength of the gel beads as well as storage conditions. In addition, AgNPs and Ag^+ may sorb on the surface of the gel beads, for example BA entrapment matrix, so proper treatment (stabilization of the used gel beads by using binding agents such as cement) is needed for the used entrapped cells. Furthermore, diffusion coefficients of AgNPs and Ag^+, ammonium, and dissolved oxygen into BA-, PVA-, and PVA-BA-gel beads should be identified to provide detailed scientific information to select the best materials for the treatment of wastewater contaminated AgNPs or Ag^+.

Further research should also focus on shifting communities of ammonia oxidizing culture in the entrapped materials as well as corresponding suspended cells due to toxicity impact of AgNPs and Ag^+. Long-term effects by toxicity of AgNPs and Ag^+ are also recommended for future study to observe whether the AO activity will be recovered by development of resistant genes to cope with the toxicity of silver or not. This should be studied for entrapped cells and corresponding free cells.

REFERENCES

1. Kholoud, M.M., et al., *Synthesis and applications of silver nanoparticles.* Arabian Journal of Chemistry, 2010. **3**: p. 135-140.
2. Massarsky, A., V.L. Trudeau, and T.W. Moon, *Predictiong the environmental impact of nanosilver.* Environmental Toxicology and Pharmacology, 2014. **38**: p. 861-873.
3. Choi, O. and Z. Hu, *Size Dependent and Reactive Oxygen Species Related Nanosilver Toxicity to Nitrifying Bacteria.* Environmental Science and Technology, 2008. **42**(12): p. 4583-4588.
4. Luoma, S., *Silver Nanotechnologies and the Environment: Old Problems or New Challenges? Washington, D.C: Woodrow Wilson International Center for Scholars.* 2008.
5. Siripattanakul-Ratpukdi, S. and M. Fürhacker, *Review: Issues of Silver Nanoparticles in Engineered Environmental Treatment Systems.* Water Air Soil Pollution, 2014. **2014**: p. 225:1939.
6. Arnaout, C.L. and C.K. Gunsch, *Impacts of Silver Nanoparticle Coating on the Nitrification Potential of Nitrosomonas europaea.* Environmental Science and Technology, 2012. **46**: p. 5387-5395.
7. Gu, L., et al., *Comparison of nanosilver removal by flocculent and granular sludge and short- and long-term inhibition impacts.* Water Research, 2014. **58**: p. 62-70.
8. Choi, O., et al., *Role of sulfide and ligand strength in controlling nanosilver toxicity.* Water Research, 2009. **43**: p. 879-886.
9. Westerhoff, P.K., M.A. Kiser, and K. Hristovski, *Nanomaterial removal and transformation during biological wastewater treatment.* Environmental Engineering Science, 2013. **30**: p. 109-17.
10. Yuan, Z., et al., *Interaction of silver nanoparticles with pure nitrifying bacteria.* Chemosphere, 2013. **90**: p. 1404-1411.
11. Limpiyakorn, T., et al., *Abundance of amoA genes of ammonia-oxidizing archaea and bacteria in activated sludge of full-scale wastewater treatment plants.* Bioresource Technology, 2011. **102**: p. 3694-3701.
12. Bai, Y., et al., *Abundance of ammonia-oxidizing bacteria and archaea in industrial and domestic wastewater treatment systems.* FEMS Microbiology Ecology, 2012. **80**: p. 323-330.
13. Sonthiphand, P., *Thesis. Microbial ecology of ammonia oxidation in the Grand River. University of Waterloo, Canada.* 2014.
14. Limpiyakorn, T., et al., *Effects of Ammonium and Nitrite on Communities and Populations of Ammonia-Oxidizing Bacteria in Laboratory-Scale Continuous-Flow Reactors.* FEMS Microbiological Ecology, 2007. **60**: p. 501-512.
15. Siripattanakul-Ratpukdi, S., et al., *Mitigation of nitrification inhibition by silver nanoparticles using cell entrapment technique* Journal of Nanoparticle Research, 2014. **2014**: p. 16:2218.
16. Yang, Y., et al., *Pyrosequencing reveals higher impact of silver nanoparticles than Ag^+ on the microbial community structure of activated sludge.* Water Research, 2014. **48**: p. 317-325.

17. Siripattanakul, S., et al., *A feasibility study of immobilized and free mixed culture bioaugmentation for treating atrazine in infiltrate.* Journal of Hazardous Materials, 2009. **168**: p. 1373-1379.
18. Tolaymat, T.M., et al., *An evidence-based environmental perspective of manufactured silver nanoparticle in syntheses and applications: A systematic review and critical appraisal of peer-reviewed scientific papers.* Science of the Total Environment, 2010. **408**: p. 999-1006.
19. Sereemaspun, A., et al., *Inhibition of human cytochrome P450 enzymes by metallic nanoparticles: A preliminary to nanogenomics.* International Journal of Pharmacology, 2008. **4**(6): p. 492-495.
20. Panacek, A., et al., *Antifungal activity of silver nanoparticles against Candida spp.* Biomaterials, 2009. **30**: p. 6333–6340.
21. Beer, C., et al., *Toxicity of silver nanoparticles - Nanoparticle or silver ion?* Toxicology Letters, 2012. **208**: p. 286-292.
22. Dougherty, G.M., et al., *The zeta potential of surface functionalized metallic nanorod particles in aqueous solution.* Electrophoresis, 2007. **29**: p. 1131-1139.
23. Ghandour, W., et al., *The uptake of silver ions by Escherichia coli K12: Toxic effects and interaction with copper ions.* Applied Microbiology and Biotechnology, 1988. **28**(6): p. 559−565.
24. Lee, Y.-J., et al., *Ion-release kinetics and ecotoxcity effect of silver nanoparticles.* Environmental Ecotoxicology and Chemistry, 2012. **31**(1): p. 155-159.
25. GrandViewResearch, *Global Silver Nanoparticles Market By Application (Electronics & Electrical, Healthcare, Food & Beverages, Textiles) Is Expected To Reach USD 2.54 Billion By 2022. Available from https://www.grandviewresearch.com/press-release/global-silver-nanoparticles-market (Accessed on 10 October 2016).* 2015.
26. Hendren, C.O., et al., *Estimating production data for five engineered nanomaterialsas a basis for exposure assessment.* Environmental Science & Technology, 2011. **45**(7): p. 2562-2569.
27. Piccinno, F., et al., *Industrial production quantities and uses of ten engineered nanomaterials in Europe and the world.* Journal of Nanoparticle Research, 2012. **14**: p. 1109-1119.
28. Lara, H.H., et al., *Bactericidal effect of silver nanoparticles against multidrug-resistant bacteria.* World Journal of Microbiology and Biotechnology, 2010. **26**: p. 615-621.
29. Clement, J.L. and P.S. Jarrett, *Antibacterial silver.* Metal-Based Drugs, 1994. **1**: p. 467-482.
30. Murphy, M., et al., *Current Development of Silver Nanoparticle Preparation, Investigation, and Application in the Field of Medicine.* Journal of Nanomaterials, 2015. **2015**: p. 1-12.
31. Pantic, I., *Application of silver nanoparticles in experimental physiology and clinical medicine: current status and future prospects.* Reviews on Advanced Materials Science, 2014. **2014**(37): p. 15-19.
32. Huang, Z., et al., *Controllable synthesis and biomedical applications of silver nanomaterials.* Journal of Nanoscience and Nanotechnology, 2011. **11**: p. 9395-408.

33. Stones, M. *Nanoscience to boost food safety, quality and shelf life*. Avaiblable at http://www.foodproductiondaily.com/content/search?SearchText=nanosilver 2009 February 2, 2010].
34. Chaudhry, Q.M., et al., *Applications and implications of nanotechnologies for the food sector.* Food Additives & Contaminants, 2008. **25**(3): p. 241-258.
35. Haider, A. and I.-K. Kang, *Preparation of Silver Nanoparticles and Their Industrial and Biomedical Applications: A Comprehensive Review.* Advances in Materials Science and Engineering, 2015. **2015**: p. 1-16.
36. Tiwari, D.K., J. Behari, and P. Sen, *Application of Nanoparticles in Wastewater Treatment.* World Applied Sciences Journal, 2008. **3**(3): p. 417-433.
37. Con, T.H. and D.K. Loan, *Preparation of Silver Nano–particles and Use as a Material for Water Sterilization.* EnvironmentAsia, 2011. **4**(2): p. 62-66.
38. Chaturvedi, S., P.N. Dave, and N.K. Shah, *Applications of nano-catalyst in new era.* Journal of Saudi Chemical Society, 2012. **16**: p. 307-325.
39. Benn, T., et al., *The Release of Nanosilver from Consumer Products Used in the Home.* Journal of Environmental Quality, 2009. **39**(6): p. 1875-1882.
40. Kulthong, K., et al., *Determination of silver nanoparticle release from antibacterial fabrics into artificial sweat.* Particle and Fibre Toxicology, 2010. **7**: p. 1-8.
41. Schildkraut, D.E., et al., *Determination of silver ions at sub microgram-per-liter levels using anodic square-wave stripping voltammetry.* Environmental Ecotoxicology and Chemistry, 1998. **17**: p. 642-649.
42. Shafer, M.M., J.T. Overdier, and D.E. Armstong, *Removal, partitioning, and fate of siver and other metals in wastewater treatment plants and effluent-receiving streams.* Environmental Ecotoxicology and Chemistry, 1998. **17**: p. 630-641.
43. USEPA, *Targeted National Sewage Sludge Survey Statistical Analysis Report.* U.S. Environmental Protection Agency Office of Water (4301T) 1200 Pennsylvania Avenue, NW Washington, DC 20460, 2009. **EPA-822-R-08-018**.
44. Bouwmeester, H., et al., *Review of health safety aspects of nanotechnologies in food production.* Journal of Regulatory Toxicology and Pharmacology, 2009. **53**: p. 52-62.
45. Mitrano, D.M., et al., *Detecting nanoparticulate silver using single-particle inductively coupled plasma-mass spectrometry.* Environmental Toxicology and Chemistry, 2011. **31**: p. 115–121.
46. Hoque, M.E., et al., *Detection and characterization of silver nanoparticles in aqueous matrices using asymmetric-flow field flow fractionation with inductively coupled plasma mass spectrometry.* Journal of Chromatography A, 2012. **1233**: p. 109–115.
47. Li, L., et al., *Quantification of nanoscale silver particles removal and release from municipal wastewater treatment plants in Germany.* Environmental Science and Technology, 2013. **47**: p. 7317–7323.
48. Wang, Y., P. Westerhoff, and K.D. Hristovski, *Fate and biological effects of silver, titanium dioxide, and C60 (fullerene) nanomaterials during simulated wastewater treatment processes.* Journal of Hazardous Materials, 2012. **201-202**: p. 16-22.

49. Zhang, Y., et al., *Stability of commercial metal oxide nanoparticles in water.* Water Research, 2007. **42**: p. 2204-2212.
50. Blaser, S.A., et al., *Estimation of cumulative aquatic exposure and risk due to silver: contribution of nano-functionalized plastics and textiles.* Science of the Total Environment 2008. **390**: p. 396-409.
51. Morones, J.R., et al., *The bactericidal effect of silver nanoparticles.* Journal of Nanotechnology, 2005. **16**: p. 2346-2353.
52. Pal, S., Y.K. Tak, and J.M. Song, *Does the antibactericidal activity of silver nanoparticles depend on the shape of the nanoparticle? A study of gram-negative bacterium Escherichia coli.* Applied Environmental Microbiology, 2007. **73**: p. 1712-1720.
53. Martinez-Castanon, G.A., et al., *Synthesis and antibacterial activity of silver nanoparticles with different sizes.* Journal of Nanoparticle Research, 2008. **10**: p. 1343-1348.
54. Radniecki, T.S., et al., *Influence of liberated silver from silver nanoparticles on nitrification inhibition of Nitrosomonas europaea.* Chemosphere, 2011. **85**: p. 43-49.
55. Li, L., et al., *A metabolic study on the responses of daphnia magna exposed to silver nitrate and coated silver nanoparticles.* Ecotoxicology and Environmental Safety, 2015. **119**: p. 66-73.
56. Yuan, Z.-H., et al., *Long-term impacts of silver nanoparticles in an anaerobic–anoxic–oxic membrane bioreactor system.* Chemical Engineering Journal, 2015. **276**: p. 83-90.
57. Levard, C., et al., *Environmental transformations of silver nanoparticles: impact on stability and toxicity.* Environmental Science and Technology, 2012. **46**: p. 6900-6941.
58. McShan, D., P.C. Ray, and H. Yu, *Molecular toxicity mechanism of nanosilver.* Journal of Food and Drug Analysis, 2014. **22**: p. 116-127.
59. Fabrega, J., et al., *Silver nanoparticle impact on bacterial growth: effect of pH, concentration, and organic matter.* Environmental Science and Technology, 2009. **43**: p. 7585-7290.
60. Mumper, C.K., et al., *Influence of ammonia on silver nanoparticle dissolution and toxicity to Nitrosomonas europaea.* Chemosphere, 2013. **93**: p. 2493-2498.
61. Zhang, C., Z. Liang, and Z. Hu, *Bacterial response to a continuous long-term exposure of silver nanoparticles at sub-ppm silver concentrations in a membrane bioreactor activated sludge system.* Water Research, 2013. **50**: p. 350-358.
62. Choi, O., et al., *The inhibitory effects of silver nanoparticles, silver ions, and silver chloride colloids on microbial growth.* Water Research 2008. **42**: p. 3066-3074.
63. Liang, Z., A. Das, and Z. Hu, *Bacterial response to a shock load of nanosilver in activated sludge treatment system.* Water Research, 2010. **44**: p. 5432-5438.
64. Beddow, J., et al., *Effects of engineered silver nanoparticles on the growth and activity of ecologically important microbes.* Environmental Microbiology Reports, 2014. **6**(5): p. 448-458.
65. Quan, X., et al., *Response of aerobic granular sludge to the long-term presence to nanosilver in sequencing batch reactors: Reactor performance, sludge*

property, microbial activity and community. Science of the Total Environment, 2015. **506-507**(2015): p. 226-233.

66. Jeong, E., et al., *Effects of silver nanoparticles on biological nitrogen removal processes.* Water Science and Technology, 2012. **65**(7): p. 1298-1303.
67. Chen, Y., et al., *Long-Term Effects of Copper Nanoparticles on Wastewater Biological Nutrient Removal and N_2O Generation in the Activated Sludge Process.* Environmental Science and Technology, 2012. **46**: p. 12452-12458.
68. Zhang, J., et al., *Response to shock load of engineered nanoparticles in an activated sludge treatment system: Insight into microbial community succession.* Chemosphere, 2016. **144**: p. 1837-1844.
69. Luo, Z., et al., *Gold and silver nanoparticle effects on ammonia-oxidizing bacteria cultures under ammoxidation.* Chemosphere, 2015. **120**: p. 737-742.
70. Wise, S., *Silver nanospheres are cytotoxic and genotoxic to fish cells.* Aquatic Toxicology 2010. **16**: p. 914-925.
71. Kim, Y.S., et al., *Twenty-eight-day oral toxicity, genotoxicity, and gender-related tissue distribution of silver nanoparticles in Sprague-Dawley rats.* Journal of Inhalation Toxicology, 2008. **20**(6): p. 575-583.
72. Lu, L., et al., *Silver nanoparticles inhibit hepatitis B virus replication.* Journal of Antiviral Therapy, 2008. **13**(2): p. 252-262.
73. Laresea, F.F., et al., *Human skin penetration of silver nanoparticles through intact and damaged skin.* Toxicology and Applied Pharmacology, 2009. **255**: p. 33–37.
74. Wong, K.K.Y. and X. Liu, *Silver nanoparticles - The real "silver bullet" in clinical medicine?* MedChemComm, 2010. **1**(2): p. 125-131.
75. Marambio-Jones, C. and E.M.V. Hoek, *A review of the antibacterial effects of silver nanomaterials and potential implications for human health and the environment.* Journal of Nanoparticle Research, 2010. **12**(5): p. 1531-1551.
76. Lee, W., K.-J. Kim, and D.G. Lee, *A novel mechanism for antibacterial effect of silver nanoparticles on Escherichia coli.* Biomaterials, 2014. **27**: p. 1191-1201.
77. Sharma, V.K., R.A. Yngard, and Y. Lin, *Silver nanoparticles:green synthesis and their antimicrobial activities.* Advances in Colloid and Interface Science, 2009. **145**: p. 83-96.
78. Hwang, E.T., et al., *Analysis of the toxic mode of action of silvernanoparticles using stress-specific bioluminescent bacteria.* Small, 2008. **4**: p. 746-750.
79. Liu, J. and R.H. Hurt, *Ion release kinetics and particle persistence in aqueous nano-silver colloids.* Environmental Science and Technology, 2010. **44**(6): p. 2169-2175.
80. Dibrov, P., et al., *Chemiosmotic Mechanism of Antimicrobial Activity of Ag^+ in Vibrio cholerae.* Antimicrobial Agents and Chemotherapy, 2002. **46**(8): p. 2668-2670.
81. Gordon, O., et al., *Silver coordination polymers for prevention of implant infection:thiol interaction, impact on respiratory chain enzymes, andhydroxyl radical induction.* Antimicrobial Agents and Chemotherapy, 2010. **54**: p. 4208-4218.

82. Park, H.D., et al., *Occurrence of Ammonia-Oxidizing Archaea in Wastewater Treatment Plant Bioreactors.* Applied and Environmental Microbiology, 2006. **72**(8): p. 5643-5647.
83. Zhang, T., et al., *Occurrence of ammonia-oxidizing Archaea in activated sludges of a laboratory scale reactor and two wastewater treatment plants.* Applied Microbiology, 2009. **107**(3): p. 970-977.
84. Sauder, L.A., et al., *Low-ammonia niche of ammonia-oxidizing archaea in rotating biological contactors of a municipal wastewater treatment plant.* Environmental Microbiology, 2012. **14**(9): p. 2589-2600.
85. Strous, M., et al., *The sequencing batch reactor as a powerful tool for the study of slowly growing anaerobic ammonium-oxidizing microorganisms.* Applied Microbiology and Biotechnology, 1998. **50**(5): p. 589-596.
86. Shen, L.D., et al., *Enrichment of Anammox bacteria from three sludge sources for the startup of monosodium glutamate industrial wastewater treatment system.* Journal of Hazardous Materials, 2012. **199-200**: p. 193-199.
87. Jung, J.Y., et al., *Factors affecting the activity of anammox bacteria during start up in the continuous culture reactor.* Water Science and Teachnology, 2007. **55**(1-2): p. 459-468.
88. Niu, J., et al., *Evaluation of autotrophic growth of ammonia oxidizers associated with granular activated sludge carbon used for drinking water purification by DNA-stable isotope probing.* Water Research, 2013. **47**: p. 7053-7067.
89. Gao, J., et al., *Abundance and diversity based on amoA genes of ammonia-oxidizing archaea and bacteria in ten wastewater treatment systems.* Applied Microbiology and Biotechnology, 2014. **98**: p. 3339-3354.
90. Bock, E. and M. Wagner, *Oxidation of Inorganic Nitrogen Compounds as an Energy Source.* Prokaryotes, 2006. **2**: p. 457-495.
91. Phurkhold, U., et al., *16S rRNA and amoA-based phylogeny of 12 novel betaproteobacterial ammonia-oxidizing isolates: extension of the dataset and proposal of a new linage within the nitrosomonads.* Systematic and Evolutionary Microbiology, 2003. **53**: p. 1485-1494.
92. Kayee, P., et al., *Ammonia half-saturation constants of sludge with different community compositions of ammonia-oxidizing bacteria.* Environmental Engineering Research, 2016. **21**(2): p. 140-144.
93. Wang, X., et al., *Community analysis of ammonia-oxidizing bacteria in activated sludge of eight wastewater treatment systems.* Journal of Environmental Sciences, 2010. **22**(4): p. 627-634.
94. Zhang, T., et al., *Ammonia-oxidizing archaea and ammonia-oxidizing bacteria in six full-scale wastewater treatment bioreactors.* Applied Microbiology and Biotechnology, 2011. **91**(4): p. 1215-1225.
95. Sonthiphand, P. and T. Limpiyakorn, *Change in ammonia-oxidizing microorganisms in enriched nitrifying activated sludge.* Applied Microbiology and Biotechnology, 2011. **89**: p. 843-853.
96. Walker, C.B., et al., *Nitrosopumilus maritimus genome reveals unique mechanisms for nitrification and autotrophy in globally distributed marine crenarchaea.* PNAS, 2010. **107**(19): p. 8818-8823.

97. Junier, P., et al., *Phylogenetic and functional marker genes to study ammoniaoxidizing microorganisms (AOM) in the environment.* Applied Microbiology and Biotechnology 2010. **85**(3): p. 425-440.
98. Rotthauwe, J.H., K.P. Witzel, and W. Liesack, *The Ammonia Monooxygenase Structural Gene Amoa as a Functional Marker: Molecular Fine-Scale Analysis of Natural Ammonia-Oxidizing Populations.* Applied Environmental Microbiology, 1997. **63**: p. 4704–4712.
99. Treusch, A.H., et al., *Novel Genes for Nitrite Reductase and Amo-Related Proteins Indicate a Role of Uncultivated Mesophilic Crenarchaeota in Nitrogen Cycling.* Environmental Microbiology, 2005. **7**: p. 1985–1995.
100. Leininger, S., et al., *Archaea predominate among ammonia oxidizing prokaryotes in soils.* Nature, 2006. **442**(806-809).
101. Konneke, M., et al., *Isolation of an autotrophic ammonia oxidizing marine archaeon.* Nature, 2005. **437**: p. 543-546.
102. Lehtovirta-Morley, L.E., et al., *Effect of nitrification inhibitors on the growth and activity of Nitrosotalea devanaterra in culture and soil.* Soil Biology and Biochemistry, 2013. **62**: p. 129-133.
103. USEPA, *Process design manual for nitrogen control. Prepared for the Office of Technology Transfer of the USEPA, Brown and Caldwell, Walnut Creek, California.* 1993.
104. Aoi, Y., et al., *Microbial ecology of nitrifying bacteria in wastewater treatment process examined by Fluorescence in situ Hybridization.* Journal of Bioscience and Bioengeneering, 2000. **90**(3): p. 234-240.
105. Jung, M.Y., et al., *Enrichment and Characterization of an Autotrophic Ammonia-Oxidizing Archaeon of Mesophilic Crenarchaeal Group I.1a from an Agricultural Soil.* Applied and Environmental Microbiology, 2011. **77**(24): p. 8635-8647.
106. Park, B.J., et al., *Cultivation of Autotrophic Ammonia-oxidizing Archaea from Marine Sediments in Coculture with Sulfur-Oxidizing Bacteria.* Applied and Environmental Microbiology, 2010. **76**(22): p. 7575-7578.
107. Laanbroek, H.J., P.L.E. Bodelier, and S. Gerards, *Oxygen consumption kinetics of Nitrosomonas europaea and Nitrobacter hamburgensis grown in mixed continuous cultures at different oxygen concentrations.* Archives of Microbiology, 1994. **161**: p. 156–162.
108. Luo, Z., et al., *Dynamics of ammonia-oxidizing archaea and bacteria in relation to nitrification along simulated dissolved oxygen gradient in sediment–water interface of the Jiulong river estuarine wetland, China.* Environmental Earth Science, 2014. **72**(7): p. 2225–2237.
109. Viotti, P., et al., *Oxygen control and improved denitrification efficiency by dosing ferrous ions in the anoxic reactor.* Desalination and Water Treatment, 2016. **57**(39): p. 18240-18247.
110. Tourna, M., et al., *Nitrososphaera viennensis, an ammonia oxidizing archaeon from soil.* PNAS, 2011. **108**(20): p. 8420-8425.
111. Lehtovirta-Morley, L.E., et al., *Cultivation of an obligate acidophilic ammonia oxidizer from a nitrifying acid soi.* PNAS, 2011. **108**: p. 15892-15897.

112. Urakawa, H., et al., *Low Temperature Decreases the Phylogenetic Diversity of Ammonia-Oxidizing Archaea and Bacteria in Aquarium Biofiltration Systems.* Applied and Environmental Microbiology, 2008. **74**(3): p. 894-900.
113. de la Torre, J.R., et al., *Cultivation of a thermophilic ammonia oxidizing archaeon synthesizing crenarchaeol.* Environmental Microbiology, 2008. **10**(1): p. 810-818.
114. Strauss, E.A., *The effects of organic carbon and nitrogen availability on nitrification rates in stream sediments. University of Notre Dame, Indiana.* 2000.
115. Abell, G.C., et al., *Niche Differentiation of Ammonia-Oxidising Archaea (AOA) and Bacteria (AOB) in Response to Paper and Pulp Mill Effluent.* Microbiology of Aquatic Systems, 2014. **67**(4): p. 758-768.
116. Wang, Y.F., X.Y. Li, and J.D. Gu, *Differential responses of ammonia/ammonium-oxidizing microorganisms in mangrove sediment to amendment of acetate and leaf litter.* Applied Microbiology and Biotechnology, 2014. **98**: p. 3165-3180.
117. Chen, X.P., et al., *Ammonia-oxidizing archaea: important players in paddy rhizosphere soil?* Environmental Microbiology, 2008. **10**(8): p. 1978-1987.
118. Ding, K., et al., *Abundance and distribution of ammonia-oxidizing archaea in Tibetan and Yunnan plateau agricultural soils of China* Frontiers of Environmental Science & Engineering, 2014. **8**(5): p. 693-702.
119. Merbt, S.N., et al., *Differential photoinhibition of bacterial and archaeal ammonia oxidation.* FEMS Microbiology Letters, 2012. **327**: p. 41-46.
120. French, E., et al., *Ecophysiological characterization of ammonia-oxidizing archaea and bacteria from freshwater.* Applied Environmental Microbioly, 2012. **78**: p. 5773–5780.
121. Ginestet, P., et al., *Estimation of nitrifying Bacterial Activities by Measuring Oxygen Uptake Rate in the presence of the Metabolic Inhibitor Allylthiourea and Azide.* Applied and Environmental Microbiology, 1998. **64**(6): p. 2266-2268.
122. Martens-Habbena, W., et al., *The production of nitric oxide by marine ammonia-oxidizing archaea and inhibition of archaeal ammonia oxidation by a nitric oxide scavenger.* Environmental Microbiology, 2014. **17**(7): p. 2261-2274.
123. Mosier, A., M.B. Lund, and C.A. Francis, *Ecophysiology of an Ammonia-Oxidizing Archaeon Adapted to Low-Salinity habitats.* Microbial Ecology, 2012. **64**: p. 955-963.
124. Shen, T., et al., *Responses of the terrestrial ammonia-oxidizing archaeon Ca. Nitrososphaera viennensis and ammonia-oxidizing bacterium nitrosospira multiformis to nitrification inhibitors.* FEMS Microbiological Letter, 2013. **344**: p. 121-129.
125. Lawrence, A.W. and P.L. McCarty, *Unified basis for biological treatment design and operation.* Journal of the Sanitary Engineering Division, 1970: p. 757-779.
126. Kargi, F. and A. Uygur, *Nutrient removal performance of a sequencing batch reactor as a function of the sludge age.* Enzyme and Microbial Technology, 2002. **31**: p. 842-847.

127. Hallin, S., et al., *Community survey of ammonia-oxidizing bacteria in full-scale activated sludge processes with different solids retention time.* Journal of Applied Microbiology, 2005. **99**: p. 629-640.
128. Khan, E., et al., *Determination of biodegradable dissolved organic carbon using entrapped mixed microbial cells.* Water Research, 2003. **37**: p. 4981-4991.
129. Saez, J.M., C.S. Benimeli, and M.J. Amoroso, *Lindane removal by pure and mixed cultures of immobilized actinobacteria.* Chemosphere, 2012. **89**: p. 982-987.
130. Siripattanakul-Ratpukdi, S., *Entrapped cell system for decentralized hospital wastewater treatment: inhibitory effect of disinfectants.* Environmental Technology, 2012. **33**(20): p. 2319-2328.
131. Ha, J., C.R. Engler, and S.J. Lee, *Determination of diffusion coefficients and diffusion characteristics for chlorferon and diethylthiophosphate in Ca-alginate gel beads.* Biotechnology and Bioengineering, 2008. **100**: p. 698-706.
132. Lee, K.Y. and D.J. Mooney, *Alginate: properties and biomedical applications.* Progress in Polymer Science, 2012. **37**(1): p. 106-126.
133. Grant, G.T., et al., *Biological interactions between polysaccharides and divalent cations - egg-box model.* FEBS Letters, 1973. **32**: p. 195-198.
134. Kashima, K. and M. Imai, *Advanced Membrane Material from Marine Biological Polymer and Sensitive Molecular-Size Recognition for Promising Separation Technology.* Advancing Desalination, 2012.
135. Julian, T.N., G.W. Radebaugh, and S.J. Wisniewski, *Permeability characteristics of calcium alginate films.* Journal of Controlled Release, 1988. **7**: p. 65-169.
136. Siripattanakul, S. and E. Khan, *Fundamentals and Applications of Entrapped Cell Bioaugmentation for Contaminant Removal.* Emerging Environmental Technologies, 2010. **2**: p. 147-170.
137. Paul, F. and P.M. Vignais, *Photophosphorylation in bacterial chromatophores entrapped in alginate gel: improvement of the physical and biochemical properties of gel beads with barium as gel-inducing agent.* Enzyme and Microbial Technology, 1980. **2**(4): p. 281-287.
138. Siripattanakul-Ratpukdi, S. and T. Tongkliang, *Municipal Wastewater Treatment Using Barium Alginate Entrapped Activated Sludge: Adjustment of Utilization Conditions.* International Journal of Chemical Engineering and Applications, 2012. **3**(5).
139. Baker, M.I., et al., *A review of polyvinyl alcohol and its uses in cartilage and orthopedic applications.* Journal of Biomedical Materials Research Part B: Applied Biomaterials, 2012. **100**: p. 1451-1457.
140. Gaaz, T.S., et al., *Properties and Applications of Polyvinyl Alcohol, Halloysite Nanotubes and Their Nanocomposites.* Molecules, 2015. **20**: p. 22833-22847.
141. Pramanik, S. and E. Khan, *Effects of Cell Entrapment on Growth Rate and Metabolic Activity of Pure Cultures Commonly Found in Biological Wastewater Treatment.* Biochemical Engineering Journal, 2009. **46**(3): p. 286-293.
142. Ochiai, H., et al., *Mechanical and Thermal Properties of Poly(vinyl alcohol) Crosslinked by Borax.* Polymer Journal, 1976. **8**(1): p. 131-133.

143. Siripattanakul, S., et al., *Effect of cell-to-matrix ratio in polyvinyl alcohol immobilized pure and mixed cultures on atrazine degradation.* Water, Air, and Soil Pollution: Focus, 2008. **8**(3-4): p. 257-266.
144. Chen, K.-C. and Y.-F. Lin, *Immonilization of microorganisms with phosphorylated polyvinyl alcohol (PVA) gel.* Enzyme and Microbial Technology, 1994. **16**(1): p. 79-83.
145. Wu, K.-Y.A. and K.D. Wisecarver, *Cell Immobilization Using PVA-Crosslinked with Boric Acid.* Biotechnology and Bioengineering, 1992. **39**: p. 447-449.
146. Yujian, W., et al., *Immobilization of Acidithiobacillus ferrooxidans with complex of PVA and sodium alginate.* Polymer Degradation and Stability, 2006. **91**: p. 2408–2414.
147. Tuncer Çaykara, T. and S. Demirci, *Preparation and Characterization of Blend Films of Poly(Vinyl Alcohol) and Sodium Alginate.* Journal of Macromolecular Science, Part A: Pure and Applied Chemistry, 2006. **44**: p. 1113-1121.
148. Liu, Z.-Q., et al., *Biosynthesis of iminodiacetic acid from iminodiacetonitrile by immobilized recombinant Escherichia coli harboring nitrilase.* Journal of Molecular Microbiology and Biotechnology, 2012. **22**: p. 35-47.
149. Kantartzi, S.G., et al., *Kinetic characterization of nitrifying pure cultures in chemostate.* Global NEST Journal, 2006. **8**(1): p. 43-51.
150. Benn, T.M. and P. Westerhoff, *Nanoparticle silver released into water from commercially available sock fabric.* Environmental Science Technology, 2008. **42**: p. 4133-4139.
151. Bower, C.E. and T. Holm-Hansen, *A Salicylate-Hypochlorite Method for Determining Ammonia in Seawater.* Fishery and Aquaculture Science, 1980. **37**: p. 794-798.
152. APHA, *American Public Health Association. Standard methods for the examination of water and wastewater, 20th edition, Washington DC, USA.* 1998.
153. Ahrari, F., et al., *The antimicrobial sensitivity of Streptococcus mutans and Streptococcus sangius to colloidal solutions of different nanoparticles applied as mouthwashes.* Dental Research Journal, 2015. **12**(1): p. 44-49.
154. Thanakitpairin, A., W. Pungrasmi, and S. Powtonsook, *Nitrogen and Phosphorus Removal in the Recirculating Aquaculture System with Water Treatment Tank Containing Baked Clay Beads and Chinese Cabbage.* EnvironmentAsia, 2014. **7**(1): p. 81-88.
155. Panáček, A., et al., *Silver Colloid Nanoparticles: Synthesis, Characterization, and their Antibacterial Activity.* The Journal of Physical Chemistry B, 2006. **110**(33): p. 16248-16253.
156. Elechiguerra, J.L., et al., *Interaction of silver nanoparticles with HIV-1.* Journal of Nanobiotechnology, 2005. **3**(6): p. 1-10.
157. Zook, J.M., et al., *Measuring silver nanoparticle dissolution in complex biological and environmental matrices using UV-visible absorbance.* Analytical and Bioanalytical Chemistry, 2011. **401**: p. 1993-2002.
158. Kroll, A., et al., *Extracellular Polymeric Substance (EPS) of Freshwater Biofilms Stabilize and Modify CeO_2 and Ag Nanoparticles.* PLOS ONE, 2014. **9**(10): p. 1-16.

159. Mock, J.J., et al., *Shape effects in plasmon resonance of individual colloidal silver nanoparticles* The Journal of Chemical Physics, 2002. **116**(15): p. 6755-6759.
160. Stehr, G., et al., *The ammonia-oxidizing nitrifying population of the River Elbe estuary.* FEMS Microbiology Ecology, 1995. **17**: p. 177-186.
161. Giska, J.R., *The Effects of Silver Ions and Nanoparticles. Oregon State University, Corvallis, OR.* 2013.
162. Barker, L.K., *Effects of Silver Ions and Nanoparticles on Suspended Cells and Biofilms of Nitrosomonas europaea. Master Thesis, University of Oregon State.* 2014.
163. Sheng, Z. and Y. Liu, *Effects of silver nanoparticles on wastewater biofilms.* Water Research, 2011. **45**(18): p. 6039-6050.
164. Kang, F., P.J. Alvarez, and D. Zhu, *Microbial Extracellular Polymeric Substances Reduce Ag^+ to Silver Nanoparticles and Antagonize Bactericidal Activity.* Environmental Science & Technology, 2014. **2014**(48): p. 316-322.
165. Thuptimdang, P., et al., *Effect of silver nanoparticles on Pseudomonas putida biofilms at different stages of maturity.* Journal of Hazardous Materials, 2015. **290**: p. 127-133.
166. Barker, L.K., *Effects of Silver Ions and Nanoparticles on Suspended Cells and Biofilms of Nitrosomonas europaea.* 2014.
167. Giao, N.T., T. Limpiyakorn, and S. Siripattanakul-Ratpukdi, *Inhibition Kinetics of Ammonia Oxidation Influenced by Silver Nanoparticles.* Water Air Soil Pollution, 2012. **223**: p. 5197-5203.
168. Blum, D.J.W. and R.E. Speece, *The Toxicity of Organic Chemicals to Treatment Processes.* Water Science and Teachnology, 1992. **3**(25): p. 23-31.
169. Bitton, G., *Wastewater Microbiology*. Third Edition. 2005: John Wiley & Sons.
170. Yang, Y., et al., *Impacts of silver nanoparticles on cellular and transcriptional activity of introgen-cycling bacteria.* Environmental Ecotoxicology and Chemistry, 2013. **32**(7): p. 1488-1494.
171. Amann, R., W. Ludwig, and K.H. Schleifer, *Phylogenetic identification and in situ detection of individual microbial cells without cultivation.* Microbiological Reviews, 1995. **59**: p. 143-69.
172. Blinova, I., et al., *Toxicity of two types of silver nanoparticles to aquatic crustaceans Daphnia magna and Thamnocephalus platyurus.* Environmental Science and Pollution Research, 2013. **20**(5): p. 3456-3463.
173. Chakravarty, R., et al., *Morphological Changes in an Acidocella Strain in Response to Heavy Metal Stress.* Research Journal of Microbiology, 2007. **2**(10): p. 742-748.
174. Badireddy, A.R., et al., *Role of extracellular polymeric substances in bioflocculation of activated sludge microorganisms under glucose-controlled conditions.* Water Research, 2010. **44**(15): p. 4505-16.
175. Lara, H.H., et al., *Effect of silver nanoparticles on Candida albicans biofilms: an ultrastructural study.* Journal of Nanobiotechnology, 2015. **13**(91): p. 1-12.
176. Jung, W.K., et al., *Antibacterial Activity and Mechanism of Action of the Silver Ion in Staphylococcus aureus and Escherichia coli.* Applied and Environmental Microbiology, 2008. **74**(7): p. 2171−2178.

177. Ahamed, M., M.S. AlSalhi, and M.K.J. Siddiqui, *Silver nanoparticle applications and human health.* Clinica Chimica Acta, 2010. **411**(23-24): p. 1841–1848.
178. Chopra, I., *The increasing use of silver-based products as antimicrobial agents: a useful development or a cause for concern.* Journal of Antimicrobial Chemotherapy, 2007. **59**: p. 587-590.
179. Lucchesi, G.I., et al., *Immobilization of P. Putida a (ATCC 12633) cells using ca-alginate: Environmental applications for the removal of cationic surfactants pollutants in industrial wastewater.* Alginic Acid: Chemical Structure, Uses and Health Benefits, 2015. **2015**: p. 105-118.
180. Hu, J. and Q. Yang, *Microbial degradation of di-n-butyl phthalate by Micrococcus sp. immobilized with polyvinyl alcohol.* Desalination and Water Treatment, 2015. **56**: p. 2457-2463.
181. Hora, A. and V.K. Shetty, *Kinetics of bioreduction of hexavalent chromium by poly vinyl alcohol-alginate immobilized cells of Ochrobactrum sp. Cr-B4 and comparison with free cells.* Desalination and Water Treatment, 2016. **57**: p. 8981–8989.
182. Pramanik, S., et al., *Effects of cell entrapment on nucleic acid content and microbial diversity of mixed cultures in biological wastewater treatment.* Bioresource Technology, 2010. **102**: p. 3176-3183.
183. Kamoun, E.A., et al., *Poly (vinyl alcohol)-alginate physically crosslinked hydrogel membranes for wound dressing applications: Characterization and bio-evaluation.* Arabian Journal of Chemistry, 2015. **8**(1): p. 38-47.
184. Sun, X. and H. Uyama, *A poly(vinyl alcohol)/sodium alginate blend monolith with nanoscale porous structure.* Nanoscale Research Letters, 2013. **8**(1): p. 1-5.
185. Rongsayamanont, C., et al., *Relationship between respirometric activity and community of entrapped nitrifying bacteria: Implications for partial nitrification.* Enzyme and Microbial Technology, 2010. **46**: p. 229-236.
186. Wadhawan, T., et al., *A new method to determine initial viability of entrapped cells using fluorescent nucleic acid staining.* Bioresource Technology, 2011. **2011**(102): p. 1622-1627.
187. Limpan, N., et al., *Influences of degree of hydrolysis and molecular weight of poly (vinyl alcohol)(PVA) on properties of fish myofibrillar protein/PVA blend films.* Food Hydrocolloids, 2012. **29**: p. 226–233.
188. Li, H., et al., *Bioremediation of contaminated surface water by immobilized Micrococcus roseus.* Environmental Technology, 2005. **26**(8): p. 931-939.
189. Vecchiatini, R., et al., *Effect of dynamic three-dimensional culture on osteogenic potential of human periodontal ligament-derived mesenchymal stem cells entrapped in alginate microbeads.* Journal of Periodontal Research, 2015. **50**(4): p. 544-553.
190. Ostermeyer, A.K., et al., *Influence of Bovine Serum Albumin and Alginate on Silver Nanoparticle Dissolution and Toxicity to Nitrosomonas europaea.* Environmental Science & Technology, 2013. **47**(24): p. 14403–14410.

APPENDIX

Appendix A Inhibitory effect of AgNPs and Ag^+ on ammonia oxidation of NAS 30 mM

Table A-1 Inhibitory constants (K_i) for AgNPs and Ag^+ on NAS 30 mM

	K_i (mg/L)	
NAS	AgNPs	Ag^+
30 mM	73.5	0.2856

Table A-2 ANOVA for live and dead with NAS 30 mM

Silver	Concentration (mg/L)	%Death
No silver	0	21.5 ± 16.2 ^{cd}
AgNPs	1	29.7 ± 16.2 ^{bc}
AgNPs	10	60.9 ± 21.6 ^{b}
AgNPs	100	81.8 ± 12.8 ^{a}
Ag^+	0.10	14.1 ± 6.3 ^{d}
Ag^+	0.50	79.5 ± 15.0 ^{a}
Killed cells	-	90.0 ± 7.7 ^{a}

Note: Different letters indicate statistically significant ($p<0.05$). Letters from a to d indicated the membrane damaged from highest levels to the lowest ones.

Table A-3 Percent inhibition by Ag^+ on NAS 30 mM

NH_4^+-N (mg/L)	Ag^+ 0.05 mg/L	Ag^+ 0.1 mg/L	Ag^+ 0.5 mg/L	Ag^+ 5 mg/L
0.88	29.2 ± 9.9 b (g)	34.2 ± 1.2 b (h)	97.9 ± 2.3 a (a)	100.0 ± 0.0 a (a)
3.89	56.5 ± 0.3 d (d)	72.1 ± 1.1 c (ef)	98.1 ± 0.2 b (a)	99.6 ± 0.2 a (a)
9.94	23.8 ± 1.8 d (h)	77.1 ± 0.4 c (d)	92.7 ± 0.2 b (bc)	97.3 ± 0.5 a (a)
11.74	64.5 ± 0.3 d (b)	90.2 ± 0.1 c (ab)	98.6 ± 0.9 a (a)	97.1 ± 0.1 b (a)
17.46	64.3 ± 0.5 d (bc)	73.2 ± 0.7 c (de)	90.3 ± 0.6 b (d)	95.4 ± 1.6 a (bc)
27.02	34.4 ± 1.1 d (f)	75.0 ± 0.4 c (d)	90.1 ± 0.3 b (d)	99.4 ± 0.5 a (a)
31.54	68.8 ± 0.8 d (ab)	83.3 ± 1.0 c (c)	92.7 ± 0.1 b (c)	96.2 ± 1.1 a (b)
45.38	71.9 ± 2.7 c (a)	91.5 ± 1.5 b (a)	98.4 ± 0.6 a (a)	98.6 ± 1.0 a (a)
46.76	56.2 ± 0.6 c (d)	71.3 ± 0.2 b (f)	91.9 ± 0.4 a (c)	91.4 ± 4.3 a (d)
58.56	74.1 ± 2.2 b (a)	95.3 ± 0.8 a (a)	94.1 ± 4.9 a (ab)	93.7 ± 1.3 a (cd)
71.88	47.6 ± 2.7 c (e)	93.7 ± 1.9 b (a)	98.0 ± 1.2 a (a)	98.6 ± 0.9 a (a)
119.45	62.0 ± 2.6 c (c)	71.8 ± 2.1 b (f)	90.5 ± 4.7 a (cd)	93.9 ± 2.4 a (c)
174.00	56.4 ± 0.7 c (d)	78.3 ± 2.7 b (d)	96.2 ± 2.0 a (a)	96.2 ± 2.0 a (ab)
260.00	74.5 ± 1.7 c (a)	45.4 ± 8.5 b (g)	92.2 ± 4.4 a (c)	88.6 ± 2.3 a (d)
Mean	52.7 ± 2.1 c	75.3 ± 1.8 b	93.9 ± 1.9 a	96.2 ± 1.3 a

Table A-4 Percent inhibition by AgNPs on NAS 30 mM

NH_4^+-N (mg/L)	AgNPs 1 mg/L	AgNPs 10 mg/L	AgNPs 100 mg/L
0.85	49.1 ± 4.6 c (b)	66.6 ± 4.8 b (bc)	79.2 ± 0.6 a (b)
3.22	63.2 ± 7.6 b (a)	70.2 ± 5.2 b (b)	82.7 ± 2.3 a (a)
9.14	50.5 ± 0.6 b (b)	56.4 ± 5.2 b (e)	79.4 ± 5.6 b (b)
12.58	38.8 ± 5.7 c (cd)	59.6 ± 0.2 b (e)	67.2 ± 0.3 a (d)
15.83	31.2 ± 5.0 b (d)	55.1 ± 7.9 a (ef)	61.0 ± 4.0 a (e)
18.22	35.2 ± 5.1 c (d)	48.9 ± 1.8 b (f)	79.9 ± 2.1 b (ab)
21.54	45.6 ± 3.9 c (bc)	63.4 ± 4.7 b (cd)	70.4 ± 3.3 a (cd)
25.65	60.3 ± 6.4 ab (a)	65.5 ± 2.1 a (c)	68.8 ± 1.2 a (d)
28.03	17.0 ± 0.2 c (e)	63.0 ± 2.2 b (d)	82.8 ± 3.9 a (a)
53.00	49.1 ± 0.4 c (b)	60.1 ± 0.7 b (de)	82.8 ± 3.3 a (a)
72.99	62.8 ± 3.3 b (a)	78.5 ± 1.6 a (a)	80.6 ± 0.4 a (a)
110.74	51.0 ± 2.3 c (b)	57.7 ± 0.8 b (e)	74.7 ± 2.7 a (bc)
Mean	46.17 ± 13.7 c	62.1 ± 7.7 b	75.8 ± 7.2 a

Notes: Different letters indicate statistical differences ($p<0.05$). Letters in the parentheses show the statistical differences for AO respect to initial NH_4^+-N. Letters without parentheses indicate the statistical differences for ammonia oxidation respect to initial AgNPs/Ag^+ concentrations. Letters from a to f indicated the inhibition of AgNPs or Ag^+ on AO from highest levels to the lowest ones.

Table A-5 Slope of ammonia oxidation at AgNPs 0 mg/L

NH_4^+-N (mg/L)	Rep 1	Rep 2	Rep 3	Mean	SD
0	0	0	0	0	0
0.85	0.0654	0.0629	0.0642	0.0642	0.0013
3.22	0.2098	0.2381	0.2316	0.2265	0.0148
9.14	0.3616	0.3682	0.3649	0.3649	0.0033
12.58	0.3754	0.3897	0.4052	0.3901	0.0149
15.83	0.3889	0.3891	0.3890	0.3890	0.0001
18.22	0.2902	0.2837	0.2859	0.2866	0.0033
21.54	0.4477	0.4810	0.4643	0.4643	0.0167
25.65	0.3293	0.3524	0.3384	0.3400	0.0116
28.03	0.3666	0.3760	0.3861	0.3762	0.0098
53.00	0.5236	0.5217	0.5209	0.5221	0.0014
72.99	0.7296	0.7205	0.7543	0.7348	0.0175
110.74	0.6647	0.6686	0.6518	0.6617	0.0088
180.94	0.6003	0.6016	0.6521	0.6180	0.0295

Table A-6 Slope of ammonia oxidation at AgNPs 1 mg/L

NH_4^+-N (mg/L)	Rep 1	Rep 2	Rep 3	Mean	SD
0	0	0	0	0	0
1.06	0.0303	0.0349	0.0326	0.0326	0.0023
3.18	0.0919	0.0899	0.0665	0.0828	0.0141
8.63	0.1769	0.1847	0.1808	0.1808	0.0039
12.36	0.2516	0.2381	0.2251	0.2383	0.0133
17.08	0.2478	0.2872	0.2675	0.2675	0.0197
19.44	0.1732	0.1984	0.1852	0.1856	0.0126
21.25	0.2610	0.2429	0.2519	0.2519	0.0091
26.29	0.1536	0.1344	0.1157	0.1346	0.0190
27.11	0.3034	0.3127	0.3203	0.3121	0.0085
53.29	0.2689	0.2645	0.2633	0.2656	0.0029
74.70	0.2643	0.2944	0.2603	0.2730	0.0186
114.92	0.3084	0.3398	0.3243	0.3242	0.0157
191.22	0.5848	0.5526	0.5900	0.5758	0.0203

Table A-7 Slope of ammonia oxidation at AgNPs 10 mg/L

NH_4^+-N (mg/L)	Rep 1	Rep 2	Rep 3	Mean	SD
0	0	0	0	0	0
1.14	0.0250	0.0180	0.0215	0.0215	0.0035
3.41	0.0601	0.0601	0.0823	0.0675	0.0128
8.60	0.1388	0.1795	0.1591	0.1591	0.0204
13.13	0.1526	0.1576	0.1628	0.1577	0.0051
18.07	0.1441	0.2056	0.1748	0.1748	0.0308
19.04	0.1428	0.1497	0.1465	0.1463	0.0035
15.74	0.1850	0.1536	0.1693	0.1693	0.0157
25.53	0.1215	0.1166	0.1130	0.1170	0.0043
27.43	0.1282	0.1478	0.1418	0.1393	0.0100
54.28	0.2046	0.2103	0.2103	0.2084	0.0033
73.97	0.1632	0.1620	0.1477	0.1576	0.0086
114.79	0.2767	0.2810	0.2819	0.2799	0.0028
189.65	0.5145	0.5172	0.4915	0.5077	0.0141

Table A-8 Slope of ammonia oxidation at AgNPs 100 mg/L

NH_4^+-N (mg/L)	Rep 1	Rep 2	Rep 3	Mean	SD
0	0	0	0	0	0
0.61	0.0132	0.0135	0.0133	0.0133	0.0002
3.01	0.0333	0.0473	0.0372	0.0393	0.0072
8.30	0.0950	0.0552	0.0751	0.0751	0.0199
13.30	0.1224	0.1274	0.1341	0.1280	0.0059
17.66	0.1362	0.1676	0.1519	0.1519	0.0157
19.86	0.0549	0.0639	0.0539	0.0576	0.0055
16.95	0.1160	0.1562	0.1406	0.1376	0.0203
27.89	0.0985	0.1138	0.1062	0.1062	0.0077
28.45	0.0511	0.0665	0.0837	0.0671	0.0163
54.39	0.1087	0.0748	0.0862	0.0899	0.0173
75.54	0.1422	0.1371	0.1493	0.1429	0.0061
114.14	0.1512	0.1881	0.1621	0.1671	0.0190
191.74	0.4168	0.3900	0.3777	0.3948	0.0200

Table A-9. Slope of ammonia oxidation at Ag ions 0 mg/L

NH_4^+-N (mg/L)	Rep 1	Rep 2	Rep 3	Mean	SD
0	0	0	0	0	0
0.88	0.0218	0.0216	0.0221	0.0218	0.0003
3.89	0.1190	0.1189	0.1185	0.1188	0.0003
9.94	0.1597	0.1556	0.1566	0.1573	0.0021
11.74	0.1846	0.1855	0.1831	0.1844	0.0012
17.46	0.3594	0.3632	0.3519	0.3582	0.0058
27.02	0.3980	0.3977	0.3953	0.3970	0.0015
31.54	0.5327	0.5330	0.5319	0.5325	0.0006
45.38	0.3617	0.3555	0.3330	0.3501	0.0151
46.76	0.4264	0.4278	0.4418	0.4320	0.0085
58.56	0.5076	0.4967	0.5219	0.5087	0.0126
71.88	0.4835	0.4802	0.4865	0.4834	0.0032
119.45	0.4777	0.5244	0.5205	0.5075	0.0259
174.00	0.6751	0.6434	0.6000	0.6395	0.0377
260.00	0.6240	0.6000	0.6875	0.6372	0.0452

Table A-10 Slope of ammonia oxidation at Ag ions 0.05 mg/L

NH_4^+-N (mg/L)	Rep 1	Rep 2	Rep 3	Mean	SD
0	0	0	0	0	0
0.84	0.0165	0.0167	0.0131	0.0154	0.0020
3.71	0.0516	0.0514	0.0519	0.0516	0.0003
8.79	0.1185	0.1196	0.1214	0.1198	0.0015
12.10	0.0653	0.0664	0.0647	0.0655	0.0009
16.26	0.1272	0.1286	0.1277	0.1278	0.0007
26.86	0.2610	0.2653	0.2547	0.2603	0.0053
33.21	0.1687	0.1682	0.1610	0.1660	0.0043
46.61	0.0967	0.1110	0.0875	0.0984	0.0118
46.89	0.1898	0.1852	0.1932	0.1894	0.0040
60.29	0.1380	0.1346	0.1221	0.1316	0.0084
71.73	0.2432	0.2660	0.2503	0.2532	0.0117
115.82	0.1887	0.1837	0.2054	0.1926	0.0114
176.00	0.2912	0.2857	0.2596	0.2788	0.0169
254.07	0.1482	0.1629	0.1770	0.1627	0.0144

Table A-11 Slope of ammonia oxidation at Ag ions 0.10 mg/L

NH_4^+-N (mg/L)	Rep 1	Rep 2	Rep 3	Mean	SD
0	0	0	0	0	0
0.9	0.0143	0.0145	0.0143	0.0144	0.0001
4.4	0.0342	0.0338	0.0316	0.0332	0.0014
9.0	0.0359	0.0363	0.0358	0.0360	0.0003
12.3	0.0180	0.0182	0.0180	0.0181	0.0001
17.2	0.0954	0.0951	0.0971	0.0959	0.0011
24.8	0.1012	0.0977	0.0987	0.0992	0.0018
28.6	0.0921	0.0917	0.0825	0.0888	0.0054
42.9	0.0333	0.0332	0.0231	0.0299	0.0059
45.1	0.1219	0.1238	0.1260	0.1239	0.0021
61.2	0.0259	0.0257	0.0197	0.0238	0.0035
71.4	0.0403	0.0299	0.0217	0.0306	0.0093
118.6	0.1264	0.1448	0.1590	0.1434	0.0163
175.3	0.1370	0.1282	0.1485	0.1379	0.0102
264.0	0.3190	0.3859	0.3322	0.3457	0.0354

Table A-12 Slope of ammonia oxidation at Ag ions 0.50 mg/L

NH_4^+-N (mg/L)	Rep 1	Rep 2	Rep 3	Mean	SD
0	0	0	0	0	0
0.7	0.0000	0.0004	0.0010	0.0005	0.0005
4.2	0.0024	0.0024	0.0020	0.0023	0.0002
9.6	0.0120	0.0111	0.0115	0.0115	0.0005
12.1	0.0046	0.0017	0.0015	0.0026	0.0017
16.8	0.0365	0.0361	0.0315	0.0347	0.0028
26.6	0.0403	0.0380	0.0394	0.0392	0.0012
31.6	0.0391	0.0388	0.0395	0.0391	0.0004
47.3	0.0082	0.0055	0.0038	0.0058	0.0022
47.5	0.0332	0.0368	0.0349	0.0350	0.0018
60.4	0.0560	0.0275	0.0068	0.0301	0.0247
72.9	0.0058	0.0065	0.0164	0.0096	0.0059
123.0	0.0638	0.0563	0.0223	0.0475	0.0221
175.5	0.0409	0.0156	0.0168	0.0244	0.0143
259.7	0.0181	0.0552	0.0772	0.0502	0.0299

Table A-13 Slope of ammonia oxidation at Ag ions 5.00 mg/L

NH_4^+-N (mg/L)	Rep 1	Rep 2	Rep 3	Mean	SD
0	0	0	0	0	0
0.72	0	0	0	0.0000	0.0000
4.21	0.0004	0.0003	0.0008	0.0005	0.0003
9.56	0.0039	0.0037	0.005	0.0042	0.0007
12.52	0.0055	0.0054	0.0052	0.0054	0.0002
16.64	0.0198	0.0225	0.0112	0.0178	0.0059
26.14	0.006	0.0031	0.0024	0.0038	0.0019
29.73	0.0236	0.0252	0.0148	0.0212	0.0056
46.74	0.0011	0.0078	0.006	0.0050	0.0035
48.85	0.0156	0.0479	0.0484	0.0373	0.0188
61.24	0.0388	0.0316	0.026	0.0321	0.0064
73.63	0.0084	0.0007	0.0076	0.0056	0.0042
121.29	0.042	0.0265	0.0224	0.0303	0.0103
175.5	0.0409	0.0156	0.0168	0.0244	0.0143
259.69	0.0863	0.0552	0.0772	0.0729	0.0160

Appendix B Inhibitory effect of AgNPs and Ag^+ on ammonia oxidation of NAS 0.5 mM

Table B-1 Inhibitory constants (K_i) for AgNPs and Ag^+ on NAS 0.5 mM

Types of NAS	K_i (mg/L)	
	AgNPs	Ag ions
0.5 mM	3.73	0.17

Table B-2 Percent inhibition by Ag^+ on NAS 0.5 mM

NH_4^+-N (mg/L)	Ag^+ 0.05 mg/L	Ag^+ 0.10 mg/L	Ag^+ 0.50 mg/L
0.8	79.5 ± 0.7 b (e)	99.1 ± 0.5 a (a)	98.9 ± 0.5 a (a)
2.5	95.7 ± 0.8 a (b)	92.3 ± 0.3 b (b)	91.4 ± 1.9 b (e)
4.4	99.1 ± 0.8 a (a)	97.8 ± 0.7 b (a)	98.4 ± 0.7 ab (ab)
6.3	94.0 ± 0.5 c (b)	97.6 ± 1.6 b (a)	99.4 ± 0.4 a (a)
6.8	84.9 ± 0.4 c (d)	93.3 ± 0.5 b (b)	94.2 ± 0.7 a (d)
11.9	91.5 ± 0.3 c (c)	90.5 ± 0.1 b (c)	93.4 ± 0.6 a (de)
16.4	88.3 ± 0.3 bc (c)	88.1 ± 0.4 b (d)	96.7 ± 0.2 a (bc)
25.2	86.9 ± 1.2 b (cd)	92.8 ± 1.6 a (b)	83.9 ± 0.8 c (f)
34.0	74.1 ± 2.1 b (f)	64.8 ± 0.7 c (f)	95.6 ± 0.3 a (cd)
65.5	68.9 ± 2.7 c (g)	75.2 ± 2.1 b (e)	82.3 ± 4.3 a (f)
Mean	86.3 ± 0.8 b	89.1 ± 0.7 ab	93.4 ± 1.2 a

Table B-3 Percent inhibition by AgNPs on NAS 0.5 mM

NH_4^+-N (mg/L)	AgNPs 1 mg/L	AgNPs 10 mg/L	AgNPs 100 mg/L
1.06	97.1 ± 0.3 $^{c\ (ab)}$	98.8 ± 0.2 $^{b\ (a)}$	99.6 ± 0.1 $^{a\ (a)}$
3.77	99.3 ± 0.8 $^{a\ (a)}$	95.9 ± 1.9 $^{b\ (b)}$	97.6 ± 1.1 $^{ab\ (a)}$
3.94	99.1 ± 0.7 $^{a\ (a)}$	98.4 ± 2.4 $^{ab\ (a)}$	95.7 ± 1.4 $^{b\ (ab)}$
5.90	87.4 ± 1.1 $^{b\ (d)}$	83.0 ± 2.4 $^{c\ (d)}$	96.6 ± 0.5 $^{a\ (a)}$
5.89	96.0 ± 4.7 $^{a\ (b)}$	93.9 ± 4.3 $^{a\ (bc)}$	99.0 ± 0.8 $^{a\ (a)}$
9.61	96.1 ± 2.7 $^{a\ (b)}$	96.6 ± 1.5 $^{a\ (ab)}$	96.9 ± 3.7 $^{a\ (a)}$
18.04	91.5 ± 3.0 $^{a\ (c)}$	92.9 ± 0.5 $^{a\ (c)}$	89.1 ± 5.7 $^{a\ (bc)}$
24.16	93.6 ± 2.6 $^{a\ (bc)}$	93.2 ± 2.9 $^{a\ (c)}$	93.3 ± 1.4 $^{a\ (b)}$
24.82	91.3 ± 3.8 $^{a\ (cd)}$	74.3 ± 2.9 $^{b\ (e)}$	89.3 ± 2.4 $^{ab\ (b)}$
38.69	70.4 ± 1.9 $^{c\ (f)}$	90.5 ± 1.0 $^{b\ (c)}$	95.0 ± 2.2 $^{a\ (b)}$
54.14	83.1 ± 3.2 $^{b\ (e)}$	95.8 ± 1.4 $^{a\ (ab)}$	99.0 ± 0.7 $^{a\ (a)}$
81.73	81.8 ± 0.8 $^{b\ (e)}$	85.7 ± 2.3 $^{a\ (d)}$	86.9 ± 1.6 $^{a\ (c)}$
Mean	90.6 ± 8.6 ^{ab}	91.6 ± 7.2 ^{a}	94.8 ± 4.3 ^{a}

Note: Different letters indicate statistical differences ($p<0.05$). Letters in the parentheses show the statistical differences for AO respect to initial NH_4^+-N. Letters without parentheses indicate the statistical differences for ammonia oxidation respect to initial AgNPs/Ag^+ concentrations. Letters from a to f indicated the inhibition of AgNPs or Ag^+ on AO from highest levels to the lowest ones.

Table B-4 Slope of ammonia oxidation at AgNPs 0 mg/L

NH_4^+-N (mg/L)	Rep 1	Rep 2	Rep 3	Mean	SD
0	0	0	0	0	0
1.06	0.13500	0.17250	0.16860	0.1587	0.021
3.77	0.21580	0.20770	0.18850	0.2040	0.014
3.94	0.21450	0.17880	0.19440	0.1959	0.018
5.90	0.19730	0.19420	0.20110	0.1975	0.003
5.89	0.20050	0.21270	0.20790	0.2070	0.006
9.61	0.24670	0.25430	0.24260	0.2479	0.006
18.04	0.33810	0.37110	0.35490	0.3547	0.017
24.16	0.29740	0.32160	0.31730	0.3121	0.013
24.82	0.33430	0.33250	0.33260	0.3331	0.001
38.69	0.34370	0.3385	0.33750	0.3399	0.003
54.14	0.32880	0.34270	0.33250	0.3347	0.007
81.73	0.33870	0.33560	0.36680	0.3470	0.017

Table B-5 Slope of ammonia oxidation at AgNPs 1 mg/L

NH_4^+-N (mg/L)	Rep 1	Rep 2	Rep 3	Mean	SD
0	0	0	0	0	0
1.28	0.0043	0.0046	0.0048	0.0046	0.0003
3.88	0.0011	0.0000	0.0029	0.0013	0.0014
4.26	0.0024	0.0024	0.0002	0.0017	0.0013
6.48	0.0259	0.0259	0.0228	0.0249	0.0018
6.05	0.0037	0.0199	0.0017	0.0084	0.0100
9.46	0.0102	0.0028	0.0158	0.0096	0.0065
22.14	0.0398	0.0297	0.0205	0.0300	0.0097
23.52	0.0112	0.0291	0.0203	0.0202	0.0090
28.69	0.0215	0.0436	0.0219	0.0290	0.0126
37.73	0.0958	0.1069	0.0991	0.1006	0.0057
57.78	0.0607	0.0648	0.0439	0.0565	0.0111
84.69	0.0624	0.0635	0.0638	0.0632	0.0007

Table B-6 Slope of ammonia oxidation at AgNPs 10 mg/L

NH_4^+-N (mg/L)	Rep 1	Rep 2	Rep 3	Mean	SD
0	0	0	0	0	0
1.32	0.0016	0.0024	0.0017	0.0019	0.0004
3.91	0.0043	0.0105	0.0101	0.0083	0.0035
4.28	0.0009	0.0001	0.0085	0.0032	0.0046
6.64	0.0373	0.0346	0.0287	0.0335	0.0044
5.85	0.0160	0.0192	0.0024	0.0125	0.0089
8.94	0.0051	0.0128	0.0077	0.0085	0.0039
18.72	0.0223	0.0281	0.0249	0.0251	0.0029
24.87	0.0299	0.0192	0.0142	0.0211	0.0080
26.22	0.0776	0.0832	0.0961	0.0856	0.0095
38.99	0.0286	0.0340	0.0343	0.0323	0.0032
53.74	0.0185	0.0144	0.0091	0.0140	0.0047
85.39	0.0572	0.0425	0.0487	0.0495	0.0074

Table B-7 Slope of ammonia oxidation at AgNPs 100 mg/L

NH_4^+-N (mg/L)	Rep 1	Rep 2	Rep 3	Mean	SD
0	0	0	0	0	0
1.16	0.0006	0.0005	0.0006	0.0006	0.0001
3.03	0.0039	0.0035	0.0069	0.0048	0.0019
3.13	0.0058	0.0087	0.0106	0.0084	0.0024
5.97	0.0079	0.0061	0.0062	0.0067	0.0010
5.35	0.0017	0.0005	0.0038	0.0020	0.0017
7.57	0.0007	0.0044	0.0178	0.0076	0.0090
20.38	0.0588	0.0246	0.0304	0.0379	0.0183
22.51	0.0237	0.0224	0.0164	0.0208	0.0039
27.27	0.0307	0.0317	0.0449	0.0358	0.0079
36.61	0.0255	0.0100	0.0160	0.0172	0.0078
52.14	0.0022	0.0061	0.0019	0.0034	0.0023
82.16	0.0387	0.0494	0.0480	0.0454	0.0058

Table B-8 Slope of ammonia oxidation at Ag ions 0 mg/L

NH_4^+-N (mg/L)	Rep 1	Rep 2	Rep 3	Mean	SD
0	0	0	0	0	0
0.76	0.2182	0.2170	0.2188	0.2180	0.0009
2.52	0.4191	0.4161	0.4119	0.4157	0.0036
4.38	0.4763	0.4671	0.4805	0.4746	0.0069
6.31	0.5531	0.5510	0.5490	0.5510	0.0021
6.82	0.5479	0.5320	0.5548	0.5449	0.0117
11.90	0.6034	0.5944	0.5915	0.5964	0.0062
16.44	0.6743	0.6808	0.6947	0.6833	0.0104
25.24	0.7260	0.7305	0.7230	0.7265	0.0038
34.03	0.6386	0.6490	0.6457	0.6444	0.0053
65.46	0.5978	0.6017	0.6081	0.6025	0.0052

Table B-9 Slope of ammonia oxidation at AgNPs 0.05 mg/L

NH_4^+-N (mg/L)	Rep 1	Rep 2	Rep 3	Mean	SD
0	0	0	0	0	0
1.45	0.0461	0.0428	0.0450	0.0446	0.0017
3.22	0.0190	0.0143	0.0207	0.0180	0.0033
4.69	0.0078	0.0002	0.0047	0.0042	0.0038
7.35	0.0366	0.0316	0.0310	0.0331	0.0031
7.59	0.0831	0.0821	0.8180	0.3277	0.4246
11.70	0.0534	0.0494	0.0502	0.0510	0.0021
16.40	0.0775	0.0819	0.0804	0.0799	0.0022
26.02	0.0951	0.0863	0.1024	0.0946	0.0081
38.00	0.1500	0.1743	0.1758	0.1667	0.0145
62.13	0.1963	0.1944	0.1695	0.1867	0.0150

Table B-10 Slope of ammonia oxidation at AgNPs 0.10 mg/L

NH_4^+-N (mg/L)	Rep 1	Rep 2	Rep 3	Mean	SD
0	0	0	0	0	0
1.48	0.0029	0.0006	0.0021	0.0019	0.0012
3.34	0.0313	0.0317	0.0329	0.0320	0.0008
4.99	0.0140	0.0079	0.0091	0.0103	0.0032
7.16	0.0228	0.0064	0.0103	0.0132	0.0086
7.54	0.0372	0.0358	0.0374	0.0368	0.0009
12.20	0.0570	0.0572	0.0564	0.0569	0.0004
16.50	0.0819	0.0827	0.0801	0.0816	0.0013
26.38	0.0599	0.0397	0.0579	0.0525	0.0111
38.30	0.2291	0.2278	0.2229	0.2266	0.0033
66.30	0.1510	0.1601	0.1368	0.1493	0.0117

Table B-11 Slope of ammonia oxidation at AgNPs 0.50 mg/L

NH_4^+-N (mg/L)	Rep 1	Rep 2	Rep 3	Mean	SD
0	0	0	0	0	0
1.49	0.0025	0.0033	0.0012	0.0023	0.0011
3.49	0.0434	0.0380	0.0266	0.0360	0.0086
4.6	0.0041	0.0101	0.0089	0.0077	0.0032
7.15	0.0028	0.0061	0.0019	0.0036	0.0022
7.62	0.0334	0.0339	0.0278	0.0317	0.0034
12.1	0.0417	0.0411	0.0352	0.0393	0.0036
16.8	0.0219	0.0216	0.0246	0.0227	0.0017
24.21	0.1142	0.1129	0.1229	0.1167	0.0054
34.26	0.0286	0.0304	0.0264	0.0285	0.0020
62.2	0.1355	0.0903	0.0945	0.1068	0.0250

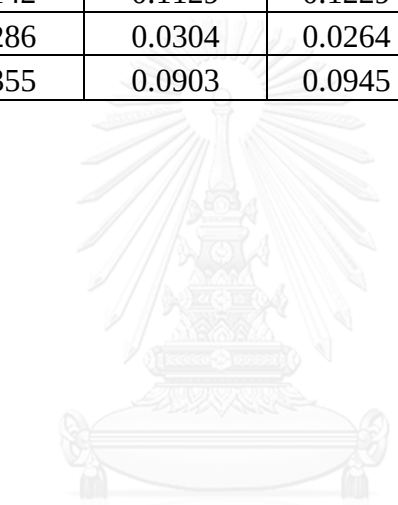

Appendix C Ammonia oxidation of entrapped cells influenced by AgNPs and Ag^+

Table C-1 Slope of AO from BA-entrapped cells influenced by AgNPs

NH_4^+-N (mg/L)	AgNPs (mg/L)	Rep1	Rep2	Rep3	Mean	SD
6.7	0	0.4208	0.4205	0.4179	0.4197	0.0016
6.7	1	0.3947	0.3948	0.3952	0.3949	0.0003
6.7	10	0.3397	0.3413	0.3425	0.3412	0.0014
6.7	100	0.3483	0.3336	0.3377	0.3399	0.0076
26.4	0	0.6808	0.6826	0.6817	0.6817	0.0009
26.4	1	0.5253	0.5253	0.5253	0.5253	0.0000
26.4	10	0.3433	0.3433	0.3432	0.3433	0.0001
26.4	100	0.4752	0.4745	0.4747	0.4748	0.0004
45.9	0	1.6406	1.6521	1.655	1.6492	0.0076
45.9	1	1.3932	1.3998	1.3834	1.3921	0.0083
45.9	10	0.9015	0.8844	0.9045	0.8968	0.0108
45.9	100	0.8441	0.841	0.8412	0.8421	0.0017
75	0	1.4427	1.4618	1.4683	1.4576	0.0133
75	1	1.2354	1.2363	1.2329	1.2349	0.0018
75	10	0.8498	0.8457	0.8448	0.8468	0.0027
75	100	0.7292	0.7389	0.7338	0.7340	0.0049
100	0	1.5114	1.4665	1.5056	1.4945	0.0244
100	1	1.2767	1.278	1.2904	1.2817	0.0076
100	10	0.8939	0.896	0.8876	0.8925	0.0044
100	100	0.79	0.7936	0.7926	0.7921	0.0019
156.5	0	1.913	1.9162	1.9107	1.9133	0.0028
156.5	1	1.5244	1.5194	1.5396	1.5278	0.0105
156.5	10	1.6254	1.6168	1.6206	1.6209	0.0043
156.5	100	1.1081	1.1204	1.1088	1.1124	0.0069

Table C-2 Slope of AO from BA-entrapped cells influenced by Ag+

$NH4_{+}$-N (mg/L)	Ag ions (mg/L)	Rep1	Rep2	Rep3	Mean	SD
6.7	0	0.4208	0.4205	0.4179	0.4197	0.0016
6.7	0.05	0.3163	0.315	0.3122	0.3145	0.0021
6.7	0.1	0.3883	0.39	0.3923	0.3902	0.0020
6.7	0.5	0.3394	0.3467	0.3479	0.3447	0.0046
26.4	0	0.6808	0.6826	0.6817	0.6817	0.0009
26.4	0.05	0.6386	0.637	0.6383	0.6380	0.0009
26.4	0.1	0.4599	0.4429	0.4516	0.4515	0.0085
26.4	0.5	0.2777	0.2784	0.278	0.2780	0.0004
45.9	0	1.6406	1.6521	1.655	1.6492	0.0076
45.9	0.05	1.1389	1.1381	1.1275	1.1348	0.0064
45.9	0.1	0.8428	0.8352	0.8237	0.8339	0.0096
45.9	0.5	0.7645	0.7599	0.7732	0.7659	0.0068
75	0	1.4427	1.4618	1.4683	1.4576	0.0133
75	0.05	1.6408	1.6411	1.6412	1.6410	0.0002
75	0.1	1.2149	1.2186	1.2293	1.2209	0.0075
75	0.5	0.8631	0.8663	0.8687	0.8660	0.0028
100	0	1.5114	1.4665	1.5056	1.4945	0.0244
100	0.05	1.5127	1.5001	1.5032	1.5053	0.0066
100	0.1	1.4824	1.481	1.4703	1.4779	0.0066
100	0.5	0.969	0.9621	0.9653	0.9655	0.0035

Table C-3 Slope of AO from PVA-entrapped cells influenced by AgNPs

NH_4^+-N (mg/L)	AgNPs (mg/L)	Rep1	Rep2	Rep3	Mean	SD
7.6	0	0.4178	0.4188	0.4164	0.4177	0.0012
7.6	1	0.3243	0.3236	0.3248	0.3242	0.0006
7.6	10	0.2943	0.2947	0.2953	0.2948	0.0005
7.6	100	0.2363	0.2367	0.237	0.2367	0.0004
24.7	0	0.6123	0.6139	0.6137	0.6133	0.0009
24.7	1	0.4782	0.4795	0.4814	0.4797	0.0016
24.7	10	0.3571	0.3564	0.3572	0.3569	0.0004
24.7	100	0.2912	0.2951	0.293	0.2931	0.0020
43.5	0	0.8993	0.9005	0.9128	0.9042	0.0075
43.5	1	0.7424	0.7474	0.7425	0.7441	0.0029
43.5	10	0.3393	0.3426	0.342	0.3413	0.0018
43.5	100	0.2305	0.2307	0.2386	0.2333	0.0046
63.2	0	1.0366	1.0348	1.0311	1.0342	0.0028
63.2	1	1.0064	1.0075	1.0082	1.0074	0.0009
63.2	10	0.2441	0.2656	0.2643	0.2580	0.0121
63.2	100	0.1685	0.1702	0.1682	0.1690	0.0011
95.5	0	1.3186	1.3248	1.3204	1.3213	0.0032
95.5	1	0.5589	0.5559	0.5613	0.5587	0.0027
95.5	10	0.4407	0.4371	0.4466	0.4415	0.0048
95.5	100	0.3445	0.3431	0.3477	0.3451	0.0024
171.6	0	1.2841	1.297	1.3014	1.2942	0.0090
171.6	1	1.0925	1.104	1.1039	1.1001	0.0066
171.6	10	0.4682	0.4801	0.4855	0.4779	0.0089
171.6	100	0.3937	0.3974	0.4031	0.3981	0.0047

Table C-4 Slope of AO from PVA-entrapped cells influenced by Ag+

NH_4^+-N (mg/L)	Ag ions (mg/L)	Rep1	Rep2	Rep3	Mean	SD
7.6	0	0.4178	0.4188	0.4164	0.4177	0.0012
7.6	0.05	0.2623	0.2619	0.2626	0.2623	0.0004
7.6	0.1	0.2455	0.246	0.2479	0.2465	0.0013
7.6	0.5	0.1587	0.159	0.1594	0.1590	0.0004
24.7	0	0.6123	0.6139	0.6137	0.6133	0.0009
24.7	0.05	0.4643	0.4651	0.4649	0.4648	0.0004
24.7	0.1	0.4268	0.4275	0.4304	0.4282	0.0019
24.7	0.5	0.3729	0.3789	0.3727	0.3748	0.0035
43.5	0	0.8993	0.9005	0.9128	0.9042	0.0075
43.5	0.05	0.7409	0.7492	0.7529	0.7477	0.0061
43.5	0.1	0.5566	0.5604	0.5614	0.5595	0.0025
43.5	0.5	0.2774	0.2789	0.2795	0.2786	0.0011
63.2	0	1.0366	1.0348	1.0311	1.0342	0.0028
63.2	0.05	0.7227	0.7259	0.7284	0.7257	0.0029
63.2	0.1	0.6367	0.6595	0.6492	0.6485	0.0114
63.2	0.5	0.4083	0.4164	0.4116	0.4121	0.0041
95.5	0	1.3186	1.3248	1.3204	1.3213	0.0032
95.5	0.05	0.7398	0.7459	0.7255	0.7371	0.0105
95.5	0.1	0.6912	0.6927	0.6937	0.6925	0.0013
95.5	0.5	0.5866	0.5865	0.5836	0.5856	0.0017
171.6	0	1.2841	1.297	1.3014	1.2942	0.0090
171.6	0.05	1.3087	1.3176	1.3029	1.3097	0.0074
171.6	0.1	1.255	1.2606	1.2643	1.2600	0.0047
171.6	0.5	0.6035	0.6311	0.5661	0.6002	0.0326

Table C-5 Slope of AO from PVA-BA entrapped cells influenced by AgNPs

NH_4^+-N (mg/L)	AgNPs (mg/L)	Rep1	Rep2	Rep3	Mean	SD
9.6	0	0.4428	0.4432	0.4424	0.4428	0.0004
9.6	1	0.4784	0.4785	0.4777	0.4782	0.0004
9.6	10	0.412	0.412	0.4123	0.4121	0.0002
9.6	100	0.332	0.333	0.3338	0.3329	0.0009
22	0	0.8545	0.8556	0.8657	0.8586	0.0062
22	1	0.8545	0.8558	0.8657	0.8587	0.0061
22	10	0.4219	0.4191	0.4245	0.4218	0.0027
22	100	0.3005	0.3041	0.3075	0.3040	0.0035
36.7	0	0.5933	0.6038	0.5977	0.5983	0.0053
36.7	1	0.6709	0.6822	0.6903	0.6811	0.0097
36.7	10	0.4592	0.4667	0.4628	0.4629	0.0038
36.7	100	0.4224	0.4226	0.436	0.4270	0.0078
74.8	0	0.8974	0.8987	0.9037	0.8999	0.0033
74.8	1	0.6781	0.6836	0.6807	0.6808	0.0028
74.8	10	0.7963	0.7953	0.7948	0.7955	0.0008
74.8	100	0.6645	0.6603	0.6658	0.6635	0.0029
97.6	0	1.0568	1.0317	1.054	1.0475	0.0138
97.6	1	0.6147	0.6229	0.632	0.6232	0.0087
97.6	10	0.5363	0.5768	0.5946	0.5692	0.0299
97.6	100	0.3137	0.3136	0.3158	0.3144	0.0012
156	0	1.0347	1.0582	1.042	1.0450	0.0120
156	1	0.9066	0.9066	0.8126	0.8753	0.0543
156	10	0.8587	0.8576	0.8661	0.8608	0.0046
156	100	0.5589	0.5647	0.553	0.5589	0.0059

Table C-6 Slope of AO from PVA-BA entrapped cells influenced by Ag^{+}

NH_4^+-N (mg/L)	Ag ions (mg/L)	Rep1	Rep2	Rep3	Mean	SD
9.6	0	0.4428	0.4432	0.4424	0.4428	0.0004
9.6	0.05	0.4616	0.4625	0.4632	0.4624	0.0008
9.6	0.1	0.4043	0.405	0.4045	0.4046	0.0004
9.6	0.5	0.1887	0.1891	0.1904	0.1894	0.0009
22	0	0.8545	0.8556	0.8657	0.8586	0.0062
22	0.05	0.6727	0.6705	0.673	0.6721	0.0014
22	0.1	0.5541	0.5425	0.5572	0.5513	0.0077
22	0.5	0.2605	0.2612	0.2644	0.2620	0.0021
36.7	0	0.5933	0.6038	0.5977	0.5983	0.0053
36.7	0.05	0.5708	0.5849	0.5906	0.5821	0.0102
36.7	0.1	0.5608	0.5804	0.568	0.5697	0.0099
36.7	0.5	0.4304	0.4584	0.4502	0.4463	0.0144
74.8	0	0.8974	0.8987	0.9037	0.8999	0.0033
74.8	0.05	0.8018	0.8066	0.8201	0.8095	0.0095
74.8	0.1	0.6121	0.6125	0.6354	0.6200	0.0133
74.8	0.5	0.5393	0.5506	0.5417	0.5439	0.0060
97.6	0	1.0568	1.0317	1.054	1.0475	0.0138
97.6	0.05	0.9666	0.9842	0.9499	0.9669	0.0172
97.6	0.1	0.486	0.546	0.5424	0.5248	0.0336
97.6	0.5	0.4331	0.4567	0.4457	0.4452	0.0118
156	0	1.0347	1.0582	1.042	1.0450	0.0120
156	0.05	1.0915	1.0921	1.0918	1.0918	0.0003
156	0.1	0.9246	0.8525	0.9103	0.8958	0.0382
156	0.5	0.8219	0.8246	0.8471	0.8312	0.0138

VITA

Nguyen Thanh Giao was born on 20 December 1982 in Can Tho, Vietnam. He attended university in 2000 and earned his Bachelor degree in Environmental Science that was awarded on 15 August 2005 by the Rector of Can Tho University, Can Tho city, Vietnam. From 2009 to 2011, he was awarded a scholarship from Scholarship Programs for Neighboring Countries to earn his master degree in the field of Environmental Management at Chulalongkorn University. He carried out the thesis entitled "Influence of silver nanoparticles on nitrification kinetics and ammonia oxidation in activated sludge" for his graduation.

After graduation, he came back and continued to work at the same place as research and teaching assistant. Then, he was assigned to work at the Delta Research And Global Observation Network (DRAGON) Institute – Mekong - Can Tho University as Project Assistant in the international project entitled "Climate Change affecting Land Use in the Mekong Delta: Adaptation of Rice-based Cropping Systems or CLUES" funded by Australian Centre for International Agricultural Research (ACIAR) for the two years (2011-2013). He received a scholarship for the period from May of 2013 to September of 2016, funded by Scholarship Program for Neighboring/ASEAN Countries from Chulalongkorn University, for his Doctoral degree in Environmental Management at International Postgraduate Program in Hazardous Substance and Environmental Management, Chulalongkorn University. He implemented his dissertation entitled "Ammonia oxidation process of entrapped and suspended cells inhibited by silver nanoparticles" to complete his doctoral degree.